

KOÇ UNIVERSITY
GRADUATE SCHOOL OF HEALTH SCIENCES

**THE ROLE OF PERICYTES IN METABOLIC
DISEASES**

YAGMUR CETIN TAS, M.D.

NEUROSCIENCE
THESIS SUBMITTED FOR THE DEGREE OF
DOCTOR OF PHILOSOPHY
ISTANBUL - 2018

KOÇ UNIVERSITY
GRADUATE SCHOOL OF HEALTH SCIENCES

**THE ROLE OF PERICYTES IN METABOLIC
DISEASES**

NEUROSCIENCE
THESIS SUBMITTED FOR THE DEGREE OF
DOCTOR OF PHILOSOPHY

YAGMUR CETIN TAS, M.D.

ADVISOR: Yasemin Gursoy Ozdemir, M.D., Ph.D.

.../.../...

This is to certify that this copy of a
Doctoral thesis by

YAGMUR CETIN TAS

has been examined and has found that it
is complete and satisfactory in all
respects, and that any and all revisions
required by the final examining
committee have been made.

Committee Members:

Signature:

Director of the Institute:

DECLARATION OF AUTHORSHIP

I hereby certify that the thesis I am submitting is entirely my own original work except where otherwise indicated. I am aware of the University's regulations concerning plagiarism, including those regulations concerning disciplinary actions that may result from plagiarism. Any use of the works of any other author, in any form, is properly acknowledged at their point of use.

Yağmur Çetin Taş

ACKNOWLEDGEMENTS

I would like to thank to my beloved advisor Prof. Dr. Yasemin Gursoy Ozdemir, for being supportive and courageous, even when the things were going all wrong. Meeting you gave me the courage to change my career and be a scientist, and in this uphill road, I learned a lot from you. Your advices and opinions on both research as well as on my career and life have been invaluable for me. I am not exaggerating when I say meeting with you changed my life and me for the better.

I would also like to thank my committee members: Firstly, to Dr. Hale Yapici Eser, for creating the opportunities when there were none, and always answering my questions with great patience and knowledge. Secondly, to Prof. Dr. Erdem Tuzun, for always listening to me with a huge interest and giving great opinions.

A bunch of many great people helped me during this period, like Dr. Sercin Karahuseyinoglu and Nesligul Senturk, who has helped me during all the imaging, even though it was quite painful sometimes. Thank you both for your unlimited patience.

I also want to thank Dr. Mujdat Zeybel, for providing awesome ideas and letting me into his project, the amount of trust was priceless. I have not met one other person who suddenly appears out of nowhere and give great ideas and disappear again (are you a magician?).

Now, the best lab mate gang ever- To Buket Yigit (cool as a cucumber, trustworthy), Ecem Ozyaprak (confused, clumsy, almost always funny), Hande Suer (always full of love and hugs), Duygu Yazici (allergy person of the team, almost always cheerful) and Burge Ulukan (has the prettiest hair and doesn't give a damn.). You people are inspiring. I learned that doing stuff with highly intelligent people is the most fun thing ever, and it was an honor to work with you.

I am deeply thankful to my mom, dad, mother-in-law, father-in-law, and my sister and two brothers for their love and support. Especially and exclusively to my father-in-law, who has genuinely expressed interest in my research and

always asked me about the results. Thanks for pushing me for the better. And the last, but actually the very first - the loveliest, the most amusing, intelligent, interesting, fascinating person I have ever met in my life, my husband, my best friend, and my irreplaceable lab mate Ali Tas. I cannot count how many sleepless nights you have spent with me trying to figure out stuff in the dark. I am not ashamed to say that this thesis would not exist without your very capable hands and mind. Nobody is as lucky as I am, because I get to live it with you.

Koç University – Seed Fund (SF.00051) of Prof. Yasemin Gursoy Ozdemir funded this research.

Institutional Animal Care and Use Committee (IACUC) of Koç University has approved all experiments and procedures, with the approval codes 2015-09 (Yasemin Gursoy Ozdemir), 2017-003 (Yasemin Gursoy Ozdemir), 2015-3 (Mujdat Zeybel).

TABLE OF CONTENTS

ACKNOWLEDGEMENTS	I
TABLE OF CONTENTS	I
LIST OF FIGURES	IV
LIST OF TABLES	VIII
LIST OF ABBREVIATIONS	IX
1. INTRODUCTION	11
1.1. General Information	11
1.1.1. Cognition, Memory and Dementia	11
1.1.2. Dementia and Metabolic Diseases	14
1.1.2.1. Type 2 Diabetes (T2DM)	16
1.1.2.2. Type 1 diabetes (T1DM)	16
1.1.2.3. Hypertension	17
1.1.3. Anxiety Disorders in Metabolic Diseases	17
1.1.4. Microcirculation in Metabolic Diseases	18
1.1.5. Pericytes in Metabolic Diseases	20
1.1.5.1. What is a pericyte?	20
1.1.5.2. The Blood Brain Barrier (BBB) and Neurovascular Unit (NVU)	21
1.1.5.3. The Molecular Mechanisms of Diabetes and Dementia	24
1.1.5.4. How to identify pericytes	30
1.1.5.5. Pericytes in Pathologic Metabolic Conditions	31
1.2. Rationale and Aims	32
2. MATERIALS AND METHODS	34
2.1. Experimental Design	34
2.1.1. Animal Models	34

2.1.1.1.	T2DM	34
2.1.1.2.	T1DM	34
2.1.1.3.	Hypertension	35
2.1.2.	Fasting Blood Glucose and Noninvasive Blood Pressure Measurements	35
2.1.3.	Intraperitoneal Glucose Tolerance Test (IPGTT)	35
2.1.4.	Behavioral Tests	37
2.1.4.1.	Open Field Test	37
2.1.4.2.	Y-Maze Test	37
2.1.4.3.	Novel Object Recognition Test	38
2.1.5.	3DISCO method for 3D Imaging	39
2.1.6.	Immunofluorescence Staining	40
2.1.7.	Measurement of biochemical parameters	41
2.1.8.	ELISA	41
2.1.9.	HOMA-IR Calculation	41
2.1.10.	Quantification of capillaries, pericytes and collagen 1 expression levels	41
2.1.10.1.	Quantification of capillaries	42
2.1.10.2.	Quantification of total numbers of pericytes and pericytes around vessels	42
2.1.10.3.	Quantification of Collagen 1 expression levels by measuring mean pixel intensity	42
2.1.10.4.	Quantification of tortuosity	43
2.1.10.5.	Quantification of pial arteriole exit point narrowing	43
2.1.11.	Statistics	43
3.	RESULTS	44
3.1.	Metabolic Outcomes of the Animal Models	44
3.1.1.	Streptozotocin-Induced T1DM Animal Model	44
3.1.2.	T2DM (HFHS animal model)	48
3.1.3.	Spontaneously Hypertensive Rats (SHRs)	55
3.2.	Cognitive Outcomes	59
3.2.1.	Open Field Tests	59
3.2.1.1.	Streptozotocin-Induced T1DM Animal Model	59
3.2.2.	T2DM (HFHS animal model)	60
3.2.2.1.	Spontaneously Hypertensive Rats (SHRs)	64
3.2.3.	Y-Maze Spontaneous Alternation Test	65
3.2.3.1.	Streptozotocin-Induced T1DM Animal Model	65
3.2.3.2.	T2DM (HFHS animal model)	66

3.2.3.3.	Spontaneously Hypertensive Rats (SHRs)	69
3.2.4.	Novel Object Recognition Test	70
3.2.4.1.	Streptozotocin-Induced T1DM Animal Model	70
3.2.4.2.	T2DM (HFHS animal model)	73
3.2.4.3.	Spontaneously Hypertensive Rats (SHRs)	79
3.3.	3D imaging and Visualization of Microcirculation	82
3.4.	Quantification of capillaries, pericytes and collagen 1 expression levels	85
3.4.1.	Quantification of capillaries	85
3.4.2.	Quantification of total numbers of pericytes and pericytes around vessels	90
3.4.3.	Quantification of Collagen 1 expression levels by measuring mean pixel intensity	93
3.4.4.	Quantification of tortuosity	99
3.4.5.	Quantification of pial arteriole exit point narrowing	101
4.	DISCUSSION	104
5.	CONCLUSION AND FUTURE PERSPECTIVES	112
6.	REFERENCES	116

LIST OF FIGURES

Figure 1. Memory Types	12
Figure 2. Dementia Types	14
Figure 3. Dementia Risk Factors	15
Figure 4. (A) Cellular elements of the blood–brain barrier (BBB) are displayed. There is a dynamic interaction of astrocyte end-feet, pericytes, and endothelial cells. (B) Structure of tight (TJ) and adherence junctions (AJ) are schematized (Gursoy-Ozdemir & Cetin Tas, 2017).	22
Figure 5. Schematic representation of transport systems located on BBB-forming endothelial cells (Gursoy-Ozdemir & Cetin Tas, 2017).	23
Figure 6. Effects of hyperinsulinemia	30
Figure 7. Novel and familiar objects that are used in these experiments.	38
Figure 8. Spatial cues and camera setup used in these experiments.	39
Figure 9. Brain tissues in 3DISCO procedure. The picture on the right is after overnight 4% PFA incubation. The picture in the middle is after THF gradient. The last picture is after DBE incubation.	40
Figure 10. Insulin and blood glucose levels of T1DM and control group CD1 mice.	46
Figure 11. Blood biochemical parameters of T1DM and control group CD1 mice.	47
Figure 12. Insulin levels of HFHS, Low-fat and Normal chow fed mice on Week 11 and Week 16	50
Figure 13. Blood glucose levels of HFHS, Low-fat and Normal chow fed mice on Week 11 and Week 16	51
Figure 14. HOMA-IR values of HFHS, Low-fat and Normal chow fed mice. Numbers inside parentheses indicate sample size.	52
Figure 15. Blood biochemical parameters of HFHS & NC fed mice on Week 11	53
Figure 16. Blood biochemical parameters of HFHS, LF and Normal chow fed mice on Week 16	55
Figure 17. Blood pressure measurements in spontaneously hypertensive rats (mean \pm SEM)	56
Figure 18. Biochemical parameters of SHR and control group Wistar rats	58
Figure 19. Time spent in central area in Streptozotocin-induced type 1 diabetic mice (mean \pm SEM)	59
Figure 20. Total distance traveled in Streptozotocin-induced type 1 diabetic mice (mean \pm SEM)	59
Figure 21. Time spent in central area in animals fed with high-fat high sucrose diet (mean \pm SEM)	60
Figure 22. Total distance traveled in animals fed with high-fat high sucrose diet at weeks 11 and 16 (mean \pm SEM)	61
Figure 23. Total distance travelled of the same animals between week 11 and 16 (mean \pm SEM)	62
Figure 24. Percentage of time spent in the central area of the same animals between week 11 and 16 (mean \pm SEM)	63

Figure 25. Time spent in central area in spontaneously hypertensive rats (mean \pm SEM)	64
Figure 26. Total distance traveled in spontaneously hypertensive rats and control group Wistar rats at weeks 23, 27 and 31(mean \pm SEM)	65
Figure 27. Spontaneous alternation in Streptozotocin-induced type 1 diabetic mice (mean \pm SEM)	66
Figure 28. Spontaneous alternation rates in animals fed with high-fat high sucrose diet (mean \pm SEM)	67
Figure 29. Spontaneous alternation rates of same animals between week 11 and 16 (mean \pm SEM)	68
Figure 30. Spontaneous alternation in spontaneously hypertensive rats in week 23, 27 and 31 (mean \pm SEM)	69
Figure 31. Spontaneous alternation in spontaneously hypertensive rats, age effect excluded (mean \pm SEM)	70
Figure 32. Trend analysis of spontaneous alternation rates in SHR and Wistar rats from week 23 to 31.	70
Figure 33. Novel object recognition score in Streptozotocin-induced type 1 diabetic mice (mean \pm SEM)	71
Figure 34. The percentage of time spent exploring the novel object in T1DM and control group.	72
Figure 35. Total object exploration time in Streptozotocin-induced type 1 diabetic mice (mean \pm SEM)	72
Figure 36. Novel object recognition scores in animals fed with high-fat high sucrose diet (mean \pm SEM)	73
Figure 37. Novel object recognition scores of the same animals in HFHS animal group between week 11 and 16 (mean \pm SEM)	74
Figure 38. Percentage of time spent exploring the novel object in HFHS, LF and NC fed mice in week 11 and 16.	75
Figure 39. Percentage of time spent exploring the novel object of the same animals between week 11 and 16.	76
Figure 40. Total object exploration time in animals fed with high-fat high sucrose diet (mean \pm SEM)	77
Figure 41. Total exploration time of the same animals in HFHS animal group between week 11 and 16 (mean \pm SEM)	78
Figure 42. Novel object recognition score in spontaneously hypertensive rats (mean \pm SEM)	79
Figure 43. Percentage of time spent exploring novel object of SHR and their Wistar control groups in weeks 23, 27, and 31.	80
Figure 44. Trend analysis for the percentage of time spent exploring novel object of SHR and	

Wistar control group rats from week 23 to 31.	80
Figure 45. Trend analysis for novel object recognition test scores of SHRs and Wistar control group rats from week 23 to 31.	81
Figure 46. Total object exploration time in spontaneously hypertensive rats (mean \pm SEM)	81
Figure 47. Trend analysis for total exploration time of SHRs and Wistar control group rats from week 23 to 31.	82
Figure 48. T1DM animal group maximum projection and 3D reconstruction 3DISCO images, respectively. Images A and B show the microcirculation of STZ induced T1DM animal, while images C and D show microcirculation of a control group animal.	83
Figure 49. 16-week HFHS animal group maximum projection and 3D reconstruction 3DISCO images, respectively. Images A and B show the microcirculation of a HFHS fed animal; images C and D show the microcirculation of a LF fed animal, and images E and F show the microcirculation of a NC fed control group animal.	85
Figure 50. Percentage of isolectin positive areas in parietotemporal cortex and hippocampus for T1DM and control group.	85
Figure 51. Isolectin B4 immunofluorescence staining of parietotemporal cortex in (A) control and (B) T1DM animals.	86
Figure 52. Percentage of isolectin positive areas in parietotemporal cortex and hippocampus for HFHS, LF, and NC fed groups at week 11 and week 16.	87
Figure 53. Isolectin B4 immunofluorescence staining of parietotemporal cortex in (A) NC fed and (B) HFHS fed animals.	87
Figure 54. Percentage of isolectin positive areas in parietotemporal cortex and hippocampus for SHRs and Wistar control groups at weeks 23, 27, and 31.	88
Figure 55. Trend analysis of isolectin positive area percentage in SHRs and Wistar rats from week 23 to 31.	89
Figure 56. Isolectin B4 immunofluorescence staining of parietotemporal cortex in 23-week-old (A) Wistar control group and (B) SHR animals.	89
Figure 57. Two-way ANOVA results of isolectin percentages in SHR and Wistar rats.	90
Figure 58. Pericyte count and location in T1DM and control group.	91
Figure 59. Double immunofluorescent staining showing PDGFR β and isolectin B4 expression in parietotemporal cortex of (A) control (B) T1DM animal group.	91
Figure 60. Pericyte count and location in HFHS, LF, and NC fed groups at weeks 11 and 16.	92
Figure 61. Pericyte count and location in SHRs and Wistar control groups at weeks 23, 27 and 31.	93
Figure 62. Collagen 1 (Col1) average pixel intensity in T1DM and control groups.	94
Figure 63. Percentage of collagen 1 positive area in T1DM animals and their control group	95

Figure 64. Collagen 1 (Col1) average pixel intensity in HFHS, LF, and NC fed animals in week 11 and 16.	96
Figure 65. Percentage of collagen 1 positive area in HFHS, LF, and NC fed animals in week 11 and 16	96
Figure 66. Collagen 1 (Col1) average pixel intensity in SHRs and Wistar control groups at weeks 23, 27 and 31.	97
Figure 67. Trend analysis of Col1 Average Pixel Intensity in SHRs and Wistar rats from week 23 to 31.	98
Figure 68. Percentage of collagen 1 positive area in SHRs and Wistar control groups in week 23, 27 and 31.	98
Figure 69. Immunofluorescence staining of Col1 and isolectin in the parietotemporal cortex of T1DM (A-D), SHR (E-H), HFHS fed animals (I-L) and control group (M-P) is shown above. Images D, H, L, and P are zoomed from the previous images.	99
Figure 70. Number of tortuous vessels in T1DM mice and control group	100
Figure 71. Number of tortuous vessels in HFHS, low-fat and normal chow fed animals	101
Figure 72. Number of obstructed vessels in T1DM mice and control group	102
Figure 73. Maximum projection 3DISCO images of (A) T1DM (B) control group. Arrow indicates pial arteriole exit point obstruction point, while arrowheads indicate tortuous vessels.	102
Figure 74. Number of obstructed vessels in HFHS, low-fat and normal chow fed animals	103

LIST OF TABLES

Table 1. Summary of animal models and applied tests.	36
Table 2. Body weight measurements in Streptozotocin-induced type 1 diabetic animals (mean \pm SEM) (* denotes $p < 0.0001$)	44
Table 3. Fasting blood glucose measurements in Streptozotocin-induced type 1 diabetic animals (mean \pm SEM) (* denotes $p < 0.0001$)	45
Table 4. Blood pressure measurements in streptozotocin-induced type 1 diabetic animals (mean \pm SEM)	48
Table 5. Body weight measurements in animals fed with high-fat high sucrose diet and normal chow at week 11 (mean \pm SEM) (*denotes $p < 0.0001$)	48
Table 6. Body weight measurements in animals fed with high-fat high sucrose diet, low-fat diet, and normal chow at week 16 (mean \pm SEM) (*denotes $p = 0.0001$)	49
Table 7. Blood pressure measurements in animals fed with high-fat high sucrose diet (mean \pm SEM)	49

LIST OF ABBREVIATIONS

‰: percent

α -SMA: alpha-smooth muscle actin

μ g: microgram

μ L: microliter

μ m: micrometer

μ M: micromolar

AD: Alzheimer's Disease

APP: Amyloid Precursor Protein

BBB: Blood Brain Barrier

CNS: Central Nervous System

CSF: Cerebrospinal Fluid

DLB: Dementia with Lewy Bodies

DLPFC: Dorsolateral Prefrontal Cortex

DR: Diabetic Retinopathy

FAD: Familial Alzheimer's Disease

FITC: fluorescein isothiocyanate

FTD: Frontotemporal Dementia

IGF-1: Insulin like growth factor-1

IGF-2: Insulin like growth factor-2

IR: Insulin Receptors

LTM: Long Term Memory

LTP: Long Term Potentiation

MetS: Metabolic Syndrome

NORT: Novel Object Recognition Test

NORT-FP: Novel Object Recognition Test- Familiarization Phase

OFT: Open Field Test

PSEN1: Presenilin 1

PSEN2: Presenilin 2

rCBF: regional Cerebral Blood Flow

SHRs: Spontaneously Hypertensive Rats

SMC: Smooth Muscle Cell

STM: Short-term Memory

T1DM: Type 1 Diabetes Mellitus

T1DMACD: T1DM Associated Cognitive Decline

T2DM: Type 2 Diabetes Mellitus

VaD: Vascular Dementia

W/V: weight/volume

WMHs: White Matter Hyperintensities



1. INTRODUCTION

1.1. General Information

1.1.1. Cognition, Memory and Dementia

Cognition can be described as the mind process by which we became aware of a stimulant by perception, think about it, decide the nature of the stimulant via using our memories and emotions (“cognition | Definition of cognition in English by Oxford Dictionaries,” n.d.). These cognitive skills, such as consciousness, orientation, attention, registration and short-term memory, long-term memory, constructional and visuospatial memory, abstraction and conceptualization, executive functions and language are what make us human, and enable us to survive and enjoy the everyday life (Monsell, 1981). Memory is a cognitive system that enables us to organize and alter the information and experiences to a form that can be used by the brain (encoding), holding on to it for some period of time (storing) and recalling it (retrieving) if needed. There are mainly 3 kinds of memory: working memory, short-term memory and long-term memory (Cowan, 2008). Human mind has the ability to hold a limited amount of information briefly in a very accessible state, and this is named ‘short-term memory (STM)’. When a person is trying to keep a phone number in their head until they write it down or remember where they parked their car last night, they are using their short-term memory. While working memory (WM) may not be so distinguishable from the short-term memory, it refers to the theoretical framework of the brain areas that are temporarily used in processing sensory data. In other words, working memory is like brain’s own scratchpad, and it helps the brain to temporarily store and process the data. For example, when someone is calculating their shopping bill, deciding which groceries to buy, mentally arranging their office area to fit another desk for a coworker, they are using their working memory. WM is mainly associated with multiple areas of prefrontal cortex. If the information is transferred to the next stage and consolidated with long term potentiation (LTP), the information can be remembered for much longer, and this is called ‘long term memory (LTM)’. Somebody remembering their mother’s maiden

name or their childhood memories on a vacation are examples of LTM. LTM can mainly be divided into 2 groups, declarative and non-declarative (procedural). The information of driving a car or riding a bike can be defined as non-declarative, while remembering the date of French Revolution or your wedding anniversary is declarative. Progressive functional loss of the aforementioned memory mechanisms is the main clinical symptom of dementia (Cowan, 2008; Kandel, Dudai, & Mayford, 2014).

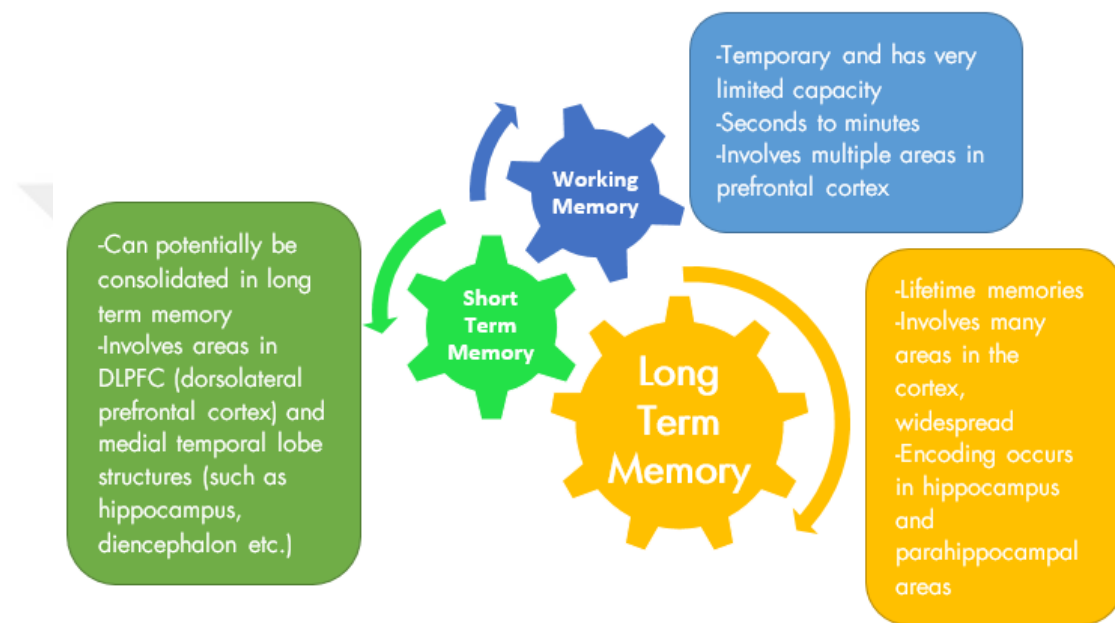


Figure 1. Memory Types

Dementia means ‘out of one’s mind’ in Latin (“dementia | Definition of dementia in English by Oxford Dictionaries,” n.d.). Dementia as used today is a chronic and progressive deterioration of the cognitive skills such as intellect, memory and personality without the impairment of consciousness. This cognitive decline can be observed clinically as memory loss, impaired judgement, difficulty of abstract thinking, loss of communication skills, time and place disorientation, neglect of personal care, gait, motor, and balance problems, inappropriate behaviors and even hallucinations and paranoia. At the structural level, there is significant loss of neurons in cortex and hippocampus, resulting with grey matter atrophy that leads to fronto-temporo-parietal cortical thinning and atrophy in hippocampal, parahippocampal and

subcortical areas (Mak et al., 2017).

Dementia is a disease with vast amount of etiologies (Figure 2). Most common form of dementia is Alzheimer's disease (AD). AD is characterized with neuronal loss; formation of amyloid plaques and neurofibrillary tangles and major clinical manifestation of the disease is progressive memory loss. There is also vascular dementia (VaD), which was previously known as multi-infarct dementia and is associated with vascular risk factors such as hypertension, diabetes mellitus, and smoking. VaD has a very heterogeneous clinical symptom palette, as patients show symptoms depending on the specific brain areas where the blood flow is compromised. Another type of dementia is Frontotemporal Dementia (FTD), which was previously known as "Pick's Disease". FTD is characterized by significant frontotemporal atrophy, and the prominent clinical symptom is changes in behavior and personality, while the memory skills remain intact. The last type of dementia is dementia with Lewy bodies (DLB), which manifests with fluctuating changes in alertness and attention, and visual hallucinations.

Although dementia is most common in elderly people, it can also be seen at younger people. Alzheimer's dementia that is seen at a younger person often indicates a genetic predisposition, which is called 'Familial Alzheimer's Disease (FAD)' and typically has an early onset, which is before age 65. Risk factors of FAD include inheritable mutations in the genes of presenilin 1 (PSEN1), presenilin 2 (PSEN2) and/or amyloid precursor protein (APP). FAD has much aggressive course, and a relatively shorter survival time when compared to sporadic AD.

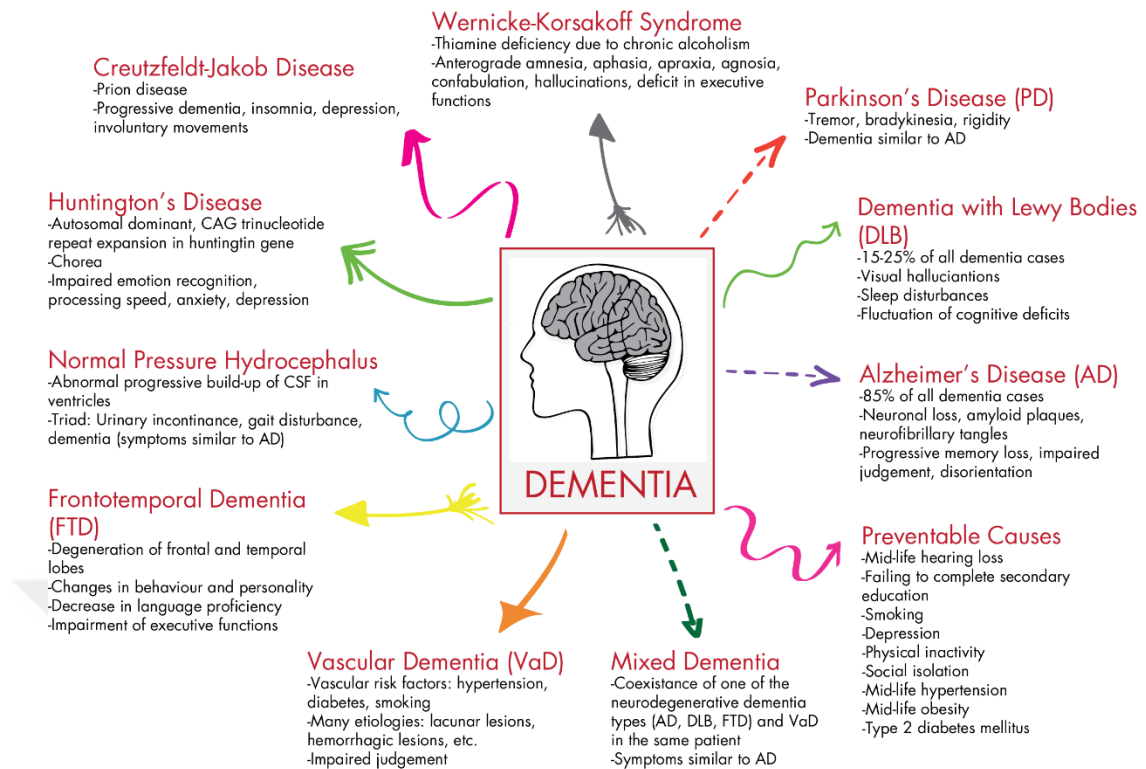


Figure 2. Dementia Types

1.1.2. Dementia and Metabolic Diseases

Dementia became a major healthcare problem, as the mean life span of humans got higher in the last decade. In year 2016, more than 46 million people were diagnosed with dementia worldwide, and the number is expected to triple in 2050 (Prince et al., 2015). A new meta-analysis shows that 7-13% of dementia in patients above age 60 is associated with T2DM. Moreover, people with T2DM have more risk of developing any type of dementia, and they are also 2 times more likely to have Alzheimer's disease at an older age (Chatterjee et al., 2016). Approximately 80% of Alzheimer's disease patients have a glucose metabolism disorder. These numbers are expected to rise, as the prevalence of T2DM itself is expected to increase and the lifespan of humans are continually rising every year (Prince et al., 2013; Roser, 2018). Aside from T2DM, other modifiable factors such as physical inactivity, midlife obesity and hypertension, depression, smoking, low education levels have also been associated with dementia progression (Barnes & Yaffe, 2011;

Norton, Matthews, Barnes, Yaffe, & Brayne, 2014). The association between hypertension and cognitive decline has been widely researched, and it seems to differ according to age. While midlife hypertension is found to be a relative risk factor of AD and dementia, late onset hypertension had no significant association. On the contrast, hypotension in late life is significantly associated with the risk of cognitive decline and dementia, particularly in elderly people who are using antihypertensive drugs (Kennelly, Lawlor, & Kenny, 2009; Kloppenborg, van der Berg, Kappelle, & Biessels, 2008; Purnell & Gao, 2009) (Figure 3).

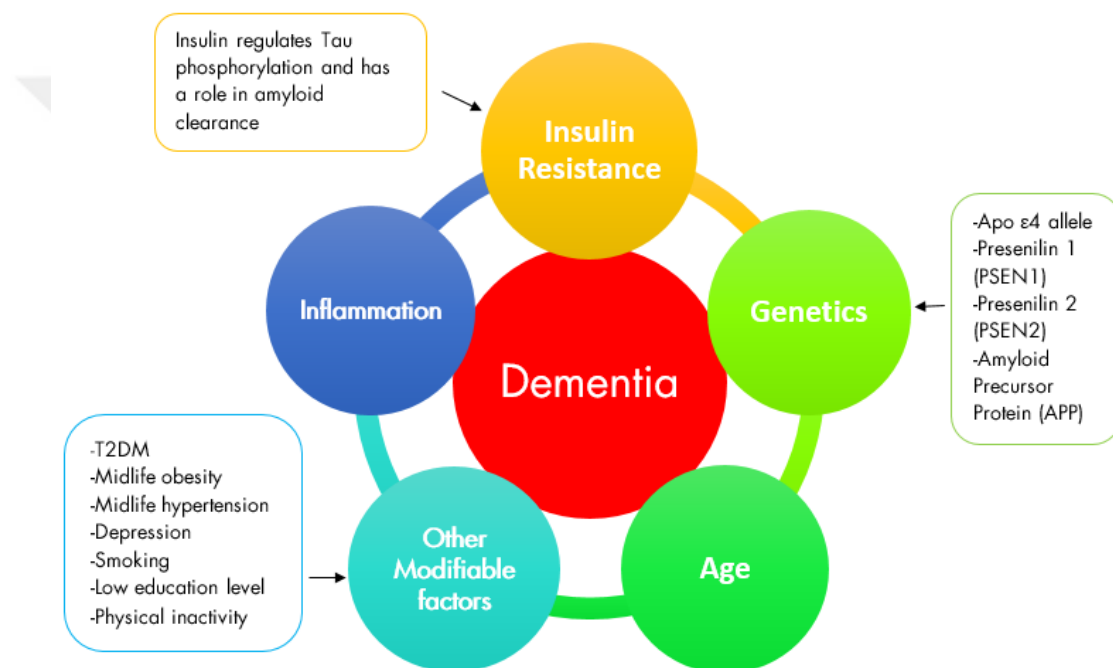


Figure 3. Dementia Risk Factors

Whether T1DM is a risk factor for cognitive decline and dementia is still a controversial subject. Early onset T1DM has been shown to be associated with several brain structural changes (Ferguson et al., 2003; Marzelli et al., 2014), and there are many studies that show impaired cognitive functions in children and young adults (Li, Huang, & Gao, 2017).

Three major metabolic diseases investigated in this study are, type 2 diabetes (T2DM), type 1 diabetes (T1DM) and hypertension. These diseases and their relationship with cognitive decline are described below.

1.1.2.1. Type 2 Diabetes (T2DM)

T2DM is the most common subtype of diabetes and it is mainly characterized with hyperglycemia and hyperinsulinemia via peripheral insulin resistance. T2DM is a part of a complex syndrome, named 'metabolic syndrome', which is the combination of several risk factors of cognitive decline. At least three of the following conditions characterizes metabolic syndrome: abdominal obesity, high blood pressure, high blood sugar, high serum triglycerides and low high-density lipoprotein (HDL) levels. High blood sugar levels in this description relate to T2DM. Unlike T1DM, which is characterized by the deficiency of insulin, T2DM is primarily caused by insensitivity of peripheral insulin receptors (Luchsinger, 2012; Roy et al., 2015; Tiehuis et al., 2008; Yates, Sweat, Yau, Turchiano, & Convit, 2012). Many studies have linked T2DM and insulin resistance (IR) to cognitive decline, vascular dementia and Alzheimer's disease (Biessels, Staekenborg, Brunner, Brayne, & Scheltens, 2006; Kong, Park, Lee, Cho, & Moon, 2018; Lutski, Weinstein, Goldbourt, & Tanne, 2017). Cognitive decline in diabetic patients might be the result of hyperglycemia and hyperinsulinemia itself, but it can also be the result of diabetes related disorders, such as increased levels of triglycerides, LDL, decreased levels of HDL, hypertension, cerebrovascular disease, ischemic heart disease and depression (Strachan, Deary, Ewing, & Frier, 1997). However, the pathophysiology of this cognitive decline that happens in IR and T2DM patients and the effects of these diseases on cerebral microcirculation are not yet fully understood.

1.1.2.2. Type 1 diabetes (T1DM)

T1DM is a medical condition characterized by apoptosis of pancreatic β cells that in normal conditions secrete insulin. Their apoptosis leads to a little or no insulin at the periphery, leading to high levels of blood glucose. Unlike T2DM and hypertension, T1DM usually manifests in younger patients, typically related to some microvascular complications (Kodl et al., 2008; K. Nunley et al., 2015). Cognitive impairment and microvascular complications in T1DM patients might be the result of chronic hyperglycemia and episodes of

hypoglycemia (K. A. Nunley et al., 2015). Tonoli and al. suggested that T1DM-associated cognitive decline (T1DMACD) is more severe in adults than children, indicating the duration of the disease and its resulting metabolic conditions might have an importance (Tonoli et al., 2014). T1DM is a potential source of chronic microvascular disease and its effects on cerebral microcirculation should be further investigated.

1.1.2.3. Hypertension

Hypertension is a medical condition where the blood pressure is persistently elevated. High blood pressure is known to be a very important risk factor of stroke and therefore, vascular dementia. It is also the second cause of death worldwide and known to be one of the major causes of long term disability (Lawes, Bennett, Feigin, & Rodgers, 2004). Also, hypertension is the systemic disease most related to WMHs and cognitive decline in elderly patients (de Leeuw et al., 2002). It is known that the neuronal tissue loss in stroke patients leads to cognitive decline and eventually results with vascular dementia (Ivan et al., 2004; Kokmen, Whisnant, O'Fallon, Chu, & Beard, 1996; Mies & Paschen, 1984; Pohjasvaara, Erkinjuntti, Vataja, & Kaste, 1997; Tatemichi et al., 1994). In a clinical study that consists of 453 stroke patients, 26% was found to be demented 3 months after stroke (Desmond et al., 2000). The effects of hypertension in intracranial microcirculation are not fully examined. However, research has shown that hypertension increases actin levels and consequently the contractile properties of the pericytes in the retina (Mitchell et al., 2007; Wallow, Bindley, Reboussin, Gange, & Fisher, 1993). The effects of hypertension on cerebral microcirculation and pericytes should be further investigated.

1.1.3. Anxiety Disorders in Metabolic Diseases

The diagnosis of T1DM is associated with psychological distress and increased anxiety symptoms due to changes and limitations in the lifestyle of pediatric patients (Reynolds & Helgeson, 2011). However, whether the accompanying anxiety is due to physiological mechanisms or external social factors is still not clear.

Similarly, in T2DM patients, depression and anxiety disorders were observed in several studies (Ali, Stone, Peters, Davies, & Khunti, 2006; Collins, Corcoran, & Perry, 2009; Fisher et al., 2008; Kahl et al., 2015). While there is a higher risk of anxiety disorders in T2DM patients, whether this is the reason or the result of the disease is still debated (Carroll et al., 2009; Skilton, Moulin, Terra, & Bonnet, 2007).

Anxiety disorders are also concomitant with hypertension in humans. A recent meta-analysis showed that anxiety and hypertension is significantly correlated in cross sectional studies, and directly associated with each other in prospective studies (Pan et al., 2015). Scalco et al. showed that both hypotension and hypertension increases the risk of depression and anxiety, and anxiety and depression increases the risk of hypertension as well (Scalco, Scalco, Azul, & Lotufo Neto, 2005). On the other hand, another meta-analysis done in elderly hypertensive patients did not find hypertension as a possible risk factor for depression (Long et al., 2015).

Although anxiety disorders seen in these three major metabolic diseases are widely researched, the results have been inconsistent. As there is an increased prevalence of these diseases, their effects on the brain should be further investigated to increase quality of life of these patients.

1.1.4. Microcirculation in Metabolic Diseases

Microcirculation can be defined as vessels lacking the muscular layer and it is composed of a complex, branching network of vessels. It consists of small arterioles, precapillary arterioles, capillaries, postcapillary venules, and small venules. Microcirculatory vessels are responsible for regulation of tissue perfusion. In arterioles, smooth muscle cells surrounding vessels control vessel diameter via sympathetic innervation and these vessels are around 10-100um diameter. In precapillary sphincters, the contractile smooth muscle cells and pericytes mainly respond to local factors. On the other hand, capillaries (vessel diameter of 5-10 um) consist of only tunica intima, a thin wall which is appropriate for exchange of nutrients and metabolites. Venules have a diameter of 10-200 um, and they have less surrounding smooth muscle

cells than arterioles.

The common microvascular complications of T2DM comprise diabetic retinopathy (DR), nephropathy, and neuropathy. In a 10--year follow-up study of 5102 patients it has been shown that early diagnosis of diabetes and a good control of blood glucose afterwards is associated with reduced risk of developing microvascular complications (Holman, Paul, Bethel, Matthews, & Neil, 2008). DR is one of the earliest observable complication of T2DM, and also a cause of blindness in advanced stages (N. Cheung, Mitchell, & Wong, 2010). The easily and noninvasively accessible retina is also important for following-up other microvascular complications in T2DM patients. A new study including T2DM patients with DR shows that there is a decline in regional cerebral blood flow (rCBF) at frontal, parietal and occipital lobes and at cerebral cortices when compared to T2DM patients without DR using SPECT (Zherdiova et al., 2018).

Arterioles respond to increased blood pressure by reducing the blood flow via constriction. Chronic hypertension eventually causes endothelial damage, which leads to atherosclerosis and narrowing points in the arterioles. If the rise in the blood pressure is gradual and slow, the arteries adapt to change by thickening the tunica media that contains smooth muscle cells, which result with an increased media/lumen ratio and therefore limit the blood flow to the retina. The hypertrophy of the smooth muscle cells in tunica media is accompanied by accumulation of extracellular matrix proteins such as fibronectin and collagen. This is called the hypertrophic remodeling and it causes arterial stiffening, which is a good predictor of cognitive decline and silent brain lesions in hypertensive patients (Faraco & Iadecola, 2013). This suggests the microvascular events that happen in the chronic hypertensive patients might also be occurring in their cerebral microcirculation systems.

Hypertension also is a risk factor for small vessel disease (SVD), whose main pathological feature is arteriolosclerosis. As the name points out, it mainly effects small vessels, such as small arterioles and venules, and capillaries. Arteriolosclerosis is characterized by the loss of smooth muscle cells, thickening of the vessel wall and deposits of fibro-hyaline material (Pantoni,

2010). As the arteriosclerosis thickens and stiffens the vessel walls, there becomes an energy demand-supply mismatch, and that leads to hypoxia in tissue level.

1.1.5. Pericytes in Metabolic Diseases

1.1.5.1. *What is a pericyte?*

Pericytes are mural cells located at the abluminal faces of the precapillary arterioles, capillaries and in the postcapillary venules. Although they exist throughout the body's microvessels, in the brain they have more specialized functions. Pericytes in the brain protect the vessel's integrity and therefore protect the functions of blood tissue barriers such as the blood-brain barrier (BBB) and the blood-retinal barrier (BRB), guide angiogenesis, regulate the blood flow by contracting, and prevent toxicity by phagocytosis of some toxic molecules (Attwell, Mishra, Hall, Farrell, & Dalkara, 2016; Trost et al., 2016). Pericytes are also necessary for proper and healthy development of neuronal structures as they help with clearing the cellular toxic byproducts around neurons (Bell et al., 2010). Pericytes are proven to have multipotent stem cell activity in vitro (Tian, Brookes, & Battaglia, 2017). However, researchers are challenging the idea of pericytes as tissue-specific progenitors in vivo (de Souza, Malta, Kashima Haddad, & Covas, 2016; Guimarães-Camboa et al., 2017). The morphology of pericytes varies depending on their location. Their processes are circumferential at the arteriolar sides of the precapillary arterioles and longitudinal at capillaries. Furthermore, they appear to be more stellate shaped as they get closer to the postcapillary venules (Attwell et al., 2016). Platelet-derived growth factor B (PDGF-B) is secreted from the endothelial cells and binds to the platelet-derived growth factor receptor beta (PDGFR β) on pericytes. This binding initiates the recruitment of pericytes to the vessel walls, and plays an important role in proliferation and migration of pericytes (Armulik, Abramsson, & Betsholtz, 2005). As they have many different functions and morphology, pericytes are versatile cells and this makes them difficult to study. A great deal of our knowledge about the physiology of microvascular brain pericytes comes from the developmental

studies that were done with pericyte deficient transgenic mice with an interrupted PDGF-B/PDGFR β signaling (Lindahl, Johansson, Levéen, & Betsholtz, 1997; Lindblom et al., 2003). Targeted deletion of PDGF-B or PDGFR β in mice results in defective pericyte recruitment. In addition, the deletion of either of these two genes is lethal. The embryos die during late gestation due to edema, widespread capillary hemorrhage and cardiac failure (M Hellström, Kalén, Lindahl, Abramsson, & Betsholtz, 1999; Lindahl et al., 1997). By the histological examination of these embryos, Hellstrom et al. proved that they showed vascular defects such as endothelial hyperplasia, abnormal endothelial cell morphology and increased capillary diameter (Mats Hellström et al., 2001). Pericytes are remarkable cells that have many functions and play a crucial role in homeostasis and pathophysiology of many diseases. However, they are not fully understood.

1.1.5.2. *The Blood Brain Barrier (BBB) and Neurovascular Unit (NVU)*

The blood brain barrier is a structural barrier, and the major component of this barrier is endothelial cells. These endothelial cells are tightly lined upon a basal lamina (basement membrane), and between these specialized endothelial cells, there are many adherent and tight junctions, which effects the overall permeability of these vessels. On top of the basal lamina, astrocytic end-feet cover most of the capillary walls. These astrocytes communicate with other astrocytes and neurons close by, and play a great role in maintaining the homeostasis of the microenvironment surrounding these cells. Pericytes also reside around these capillary walls, and they communicate with endothelial cells via contact points. Ramified microglia are also found in this environment, just to detect neuronal injury or intervene if any infection occurs. These cells all together form the BBB, and via controlling the permeability, they keep the CNS healthy (Gursoy-Ozdemir & Cetin Tas, 2017).

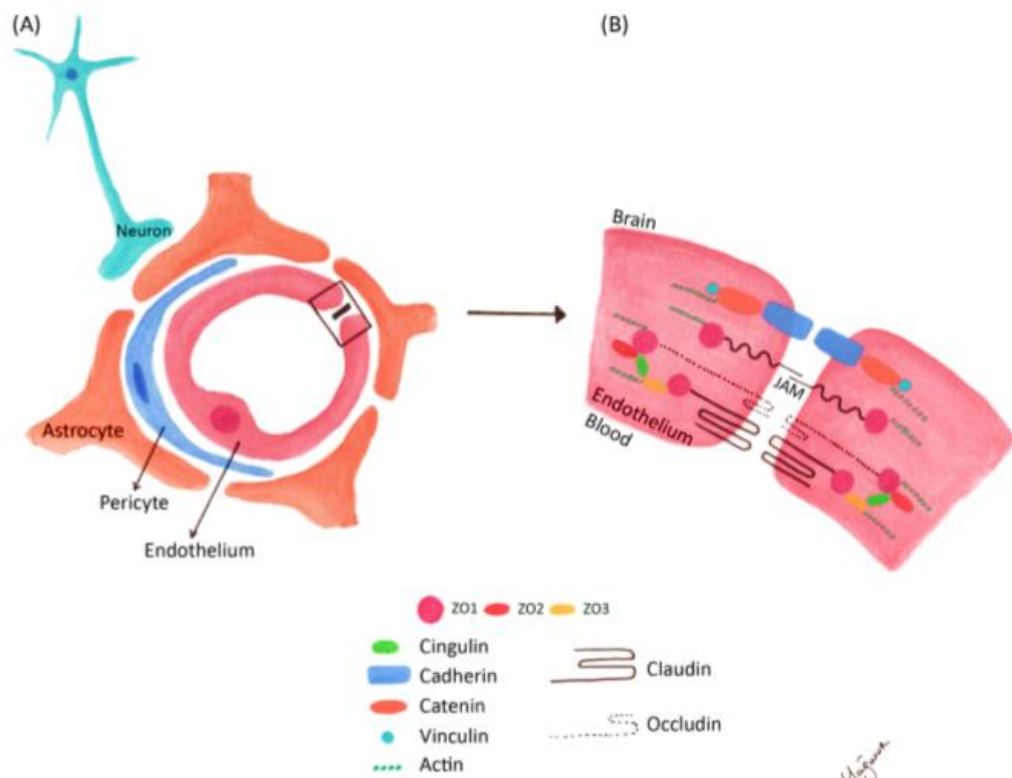


Figure 4. (A) Cellular elements of the blood–brain barrier (BBB) are displayed. There is a dynamic interaction of astrocyte end-feet, pericytes, and endothelial cells. (B) Structure of tight (TJ) and adherence junctions (AJ) are schematized (Gursoy-Ozdemir & Cetin Tas, 2017).

When neuronal activity occurs, the demand for oxygen and nutrients increases. To meet this demand, hyperemia occurs in that specific area, which is called neurovascular coupling where smaller vessels dilate or constrict due to tissues' metabolic needs. The occurrence of neurovascular coupling depends on a close group of cells called the neurovascular unit (NVU). Neurovascular unit is composed of neurons, astrocytes, endothelial cells, and pericytes. Under physiological conditions, the NVU restricts the passage of microorganisms, ions, large molecules and many of the small molecules from the blood to the brain. However, the brain cannot survive without nutrients, oxygen, and a system to remove the metabolites, so some modifications were made in this strict barrier. For example, water-soluble agents pass through

paracellular hydrophilic diffusion, small gaseous molecules like oxygen and carbon dioxide and small lipophilic molecules can pass via transcellular lipophilic diffusion. Glucose, amino acids, and nucleosides use solute carrier systems; insulin and transferrin are carried by receptor-mediated transcytosis; albumin and other serum proteins are carried by adsorptive transcytosis. There is also a system for waste products, as they have to leave brain via active efflux transporters (Keaney & Campbell, 2015).

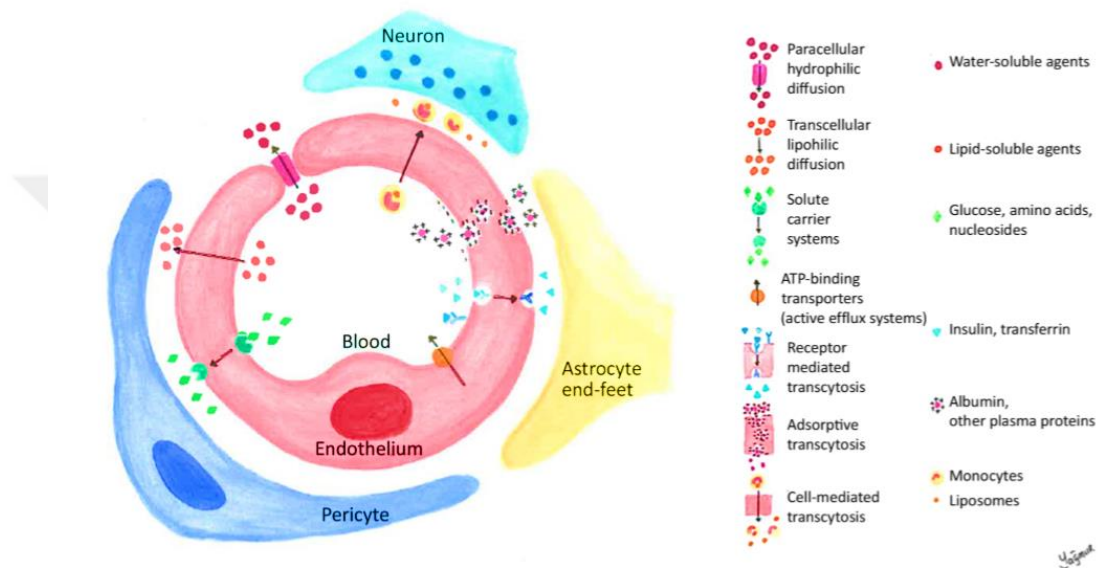


Figure 5. Schematic representation of transport systems located on BBB-forming endothelial cells (Gursoy-Ozdemir & Cetin Tas, 2017).

Whether pericytes at the capillary level or smooth muscle cells (SMCs) in the upstream arterioles control the blood flow in the microcirculatory area was a controversial issue until very recently. Many in vivo studies showed the contractile properties of microcirculatory pericytes in brain and retina (Fernandez-Klett, Offenhauser, Dirnagl, Priller, & Lindauer, 2010; Hall et al., 2014; Kornfield & Newman, 2014; Peppiatt, Howarth, Mobbs, & Attwell, 2006). Nevertheless, when it came to demonstrating contractility in molecular level, the scientists hit a brick wall, as the contractile abilities of these cells were attributed to alpha-smooth muscle actin (α -SMA) expression and they could not prove that capillary pericytes were expressing α -SMA. A recent paper rejected the idea of pericytes being contractile cells via classifying

microcirculatory α -SMA positive cells as SMCs and claimed arteriolar smooth muscle cells were controlling the blood flow, not pericytes (Hill et al., 2015). This idea was dismissed by a more recent study that suggested the method used in classic fixation methods with 4% PFA resulted with degrading of α -SMA before it was even detected and created a new fixation method with ice-cold methanol and phalloidin for α -SMA detection. Using this method, they proved that capillary pericytes produced α -SMA and brought this discussion to an end (Alarcon-Martinez et al., 2018).

1.1.5.3. *The Molecular Mechanisms of Diabetes and Dementia*

Two major types of glucose transporter families control glucose transport through BBB. The most common ones are sodium independent bidirectional transporters that belong to solute carrier 2 (SLC2) family and they have 14 isoforms (GLUTs 1-14). The other family is sodium dependent unidirectional transporters and they have 12 isoforms (SGLTs 1-12). Under physiological circumstances, the major glucose transporter in the BBB is GLUT1. Once in the extracellular space of the brain parenchyma, it is uptaken by passive diffusion by numerous cells, like neurons, astrocytes, and microglia. The distribution of these isoforms differs among the cells and is dependent on physiological conditions. For example, GLUT1 (55 kDa form) is abundant in endothelial cells of the BBB, while GLUT1 (45 kDa form) is abundant in astrocytes. GLUT3 is abundant in neurons and GLUT5 is the major glucose transporter of the microglial cells. GLUT1 is located at both luminal and abluminal sides of the endothelial cells, but the distribution is highly asymmetrical and approximately 40% of the transporters are sequestered in cell cytoplasm. Expression of GLUT1 in endothelial cells is regulated by circulating concentrations of glucose and it changes during neural development as energy demands of the brain shows variations. GLUT4 and GLUT8 are also found in NVU in lesser amounts, and they are important because of their insulin responding properties. The primary role of insulin is to regulate glucose uptake into cells (Leney & Tavaré, 2009). Insulin triggers the translocation of GLUT4 from cytosol to plasma membrane and GLUT8 to rough endoplasmic reticulum; both mechanisms exist to increase intracellular

glucose concentration. SGLT1 (sodium-dependent glucose transporter 1) exists in both endothelial cells and neurons, while SGLT2 has only been detected in endothelial cells (Augustin, 2010; Carruthers, DeZutter, Ganguly, & Devaskar, 2009; Patching, 2017).

Glycemic imbalance, both hypoglycemia and hyperglycemia have effects on expression and distribution of these glucose transporters at the BBB. Before the presence of the alerting symptoms of the dementia itself, the reduction in the function of the glucose transporters of the BBB is observed and discussed as a causative effect of the vascular pathophysiology of Alzheimer's disease (Patching, 2017). Both hypoglycemia and hyperglycemia can be present in diabetics. Although hyperglycemia is mainly part of the disease pathophysiology, hypoglycemia mostly happens because of the anti-diabetic drugs or insulin treatment, and its effects on brain is as important as hyperglycemia regarding the cognitive and structural changes seen in these patients. Blood glucose levels lower than 65 mg/dl can be defined as hypoglycemia. Experiments done in rat models of insulin induced chronic hypoglycemia showed an increase of 50% in the mRNA and protein levels of GLUT1 (Kumagai, Kang, Boado, & Pardridge, 1995). Another experiment in the same model showed 23% increase in total GLUT1 and a 52 % increase in luminal GLUT1 in isolated rat brain microvessels (Simpson et al., 1999). These studies suggest glucose is important for maintaining brains normal functions, as it adapts itself to uptake more glucose from the bloodstream when it is scarce.

Hyperglycemia mostly results from untreated or ineffectively treated diabetic conditions. It can be defined as blood sugar levels higher than 126 mg/dl while fasting or blood sugar levels higher than 200 mg/dl 2 hours after a meal. Although Duelli et al. demonstrated chronic hyperglycemia results with decreased average GLUT 1 density in rat brains (Duelli et al., 2000), there are other studies that showed no change in expression or activity of glucose transporters (Simpson et al., 1999). At the cellular level, vascular endothelial cells show the earliest pathological responses, as they are the first ones to encounter the high glucose levels. Advanced glycation end-product exposure

to retinal endothelial cells causes increased nitric oxide synthase (NOS) and vascular endothelial growth factor (VEGF) expression (Murata et al., 1997). Retinal pericytes are also affected by hyperglycemia, as hyperglycemia associated inflammation, oxidative stress and glycation is shown to induce the apoptosis of retinal pericytes (Ejaz, Chekarova, Ejaz, Sohail, & Lim, 2007; Timothy J Lyons & Lyons, 2013). Losing pericytes result with the loss of contractile properties of microcirculatory vessels. Another prominent histopathological feature that is associated with the diminished contractile properties is the thickening of the capillary basement membrane, which is not only seen in retina, but in glomeruli, skin, and other organs as well. Hyperglycemia also causes increased formation of reactive oxygen species, which results with increased oxidative stress (Murata et al., 1997), which is a part of disease pathophysiology. If we look at DR in a more macroscopic level, we can see changes in vascular diameter. Both retinal arteriolar narrowing (Wong et al., 2002; Wong, Shankar, Klein, Klein, & Hubbard, 2005) and retinal venular widening (Ikram et al., 2006) has found to be associated with diabetes. Vessel tortuosity is a debated subject, as the Singapore Malay Eye Study (SiMES) showed that people with diabetes had straighter arterioles (less tortuous) (C. Y.-L. Cheung et al., 2012), whereas Sasongko et al. found out that diabetic patients had more tortuous retinal arterioles (Sasongko et al., 2011). The duration of diabetes and higher HbA1c levels have also been associated with retinal vascular network changes in younger type 1 diabetic patients without DR, such as increased tortuosity, changes in arteriolar and venular diameter and larger arteriolar branching angle (Sasongko et al., 2010). This suggests retinal changes may be early indications of microvessel injury in these patients. The effects of hypertension in the retina has also been investigated in numerous studies, and it mainly results with retinal arteriolar narrowing, increased wall/lumen ratio and rarefaction of retinal vasculature (C. Y. -I. Cheung, Ikram, Sabanayagam, & Wong, 2012; Ding et al., 2014; Sun, Wang, Mackey, & Wong, 2009). The effects of these diseases on the retinal microvasculature should be thoroughly reviewed as they are postulated to be very similar to the pathophysiology in the cerebral microvasculature.

Insulin is an anabolic hormone that belongs to receptor tyrosine kinase superfamily. The same family includes insulin like growth factors-1 (IGF-1) and -2 (IGF-2) and relaxin (Schulingkamp, Pagano, Hung, & Raffa, 2000). Although insulin is considered a mainly peripheral hormone, it also exists in brain tissue and cerebrospinal fluid (CSF). The amount of insulin varies among developmental stages. In rabbits, the highest amount of insulin in the brain was measured in late fetal and early neonatal periods, while lesser amounts were measured in adults. Though brain insulin levels in vivo is a controversial subject, the insulin amount is found to be 10 to 100 fold higher than plasma levels (Schechter et al., 1992). The insulin found in adult CNS mainly comes from the peripheral sources (pancreatic β -cells) and crosses the BBB via protein transporters. Just like insulin, peripheral IGF-1 can also pass the BBB via transporters. However, this is not the only way for the insulin to pass to CNS; it can also use the leaky vessels around area postrema. While an acute increase in peripheral insulin levels lead to increased CSF insulin, a chronic peripheral insulinemia doesn't have the same results because of the downregulation of insulin receptors (IRs) at the BBB (Moreira, Duarte, Santos, Rego, & Oliveira, 2009). Moreover, evidence shows that there is de-novo synthesis of insulin in some brain regions including hippocampus, prefrontal cortex, entorhinal cortex, and olfactory bulb, mainly in pyramidal neurons, and it is released upon Ca^{+} and K^{+} induced membrane depolarization, which suggests release upon increased neuronal activity (Clarke, Mudd, Boyd, Fields, & Raizada, 2006; Hoyer, 2003).

Some brain areas are rich in IRs, such as olfactory bulb, hypothalamus, cerebral cortex, cerebellum, hippocampus, and striatum (Burns et al., 2007). In a cellular approach, IRs are abundant in neural cells, while they are limited in glial cells (Baskin, Sipols, Schwartz, & White, 1993; Unger, Moss, & Livingston, 1991). IGF-1 and insulin can bind to each other's receptors, while they have higher affinity for their own receptors (Conejo & Lorenzo, 2001). Once bound to its receptor, insulin phosphorylates tyrosine residues, and this activates 2 major signaling cascades, one being PI3K/Akt/glycogen synthase kinase-3 β (GSK-3 β) signaling cascade, and the other one being Ras/Raf-

1/extracellular signal-regulated kinases (ERK1 and ERK2, ERK1/2) (Moloney et al., 2010; van der Heide, Ramakers, & Smidt, 2006; Wada, Yokoo, Yanagita, & Kobayashi, 2005). The activation of PI3K/Akt/glycogen synthase kinase-3 β (GSK-3 β) signaling cascade leads to pro-apoptotic Bad, caspase-9, and GSK-3 phosphorylation which results with the inhibition of apoptosis. The same signaling pathway inactivates GSK-3 β , which also has an anti-apoptotic effect (Crowder & Freeman, 2000; Pap & Cooper, 1998; Sanchez et al., 2003). Besides the two signaling mechanisms that are described before, insulin also activates MAPK and this contributes to the anti-apoptotic effects of the other signaling mechanisms, it is also shown to stimulate glucose transport and antioxidant related gene expression (Geiger, Wright, Han, & Holloszy, 2005; Konrad et al., 2001).

Mullins et al. suggests insulin playing a role in Tau phosphorylation and amyloid clearance (Mullins, Diehl, Chia, & Kapogiannis, 2017). They hypothesized that insulin resistance is an important link in both amyloid beta and Tau pathologies (de la Monte, 2012; Steen et al., 2005). Indeed, Watson et al. showed that high levels of insulin inhibit the degradation of A β via competing as a target for IDE (Insulin Degrading Enzyme) leading to decreased IDE activity and an increase in A β levels (Watson et al., 2003). Furthermore, it has been shown that brain IR promotes A β fibrillogenesis in presynaptic membranes (Yamamoto et al., 2012).

Another key pathological element in AD is the tau protein, which is from a protein family known as microtubule-associated proteins (MAPs). While the tau protein is normally soluble, hyperphosphorylation of tau proteins can lead to aggregates of tau proteins and neurodegeneration. Short-term hyperinsulinemia is shown to lead to a rapid hyperphosphorylation of tau proteins (<2 mins), but the long term exposure to insulin causes decreased phosphorylation (Lesort & Johnson, 2000; Lesort, Jope, & Johnson, 1999). Hyperinsulinemia causes a downregulation of IRs in BBB, which leads to lesser amounts of glucose transported through BBB. Downregulation of IRs in hippocampus is shown to impair spatial learning, synaptic plasticity, and the occurrence long term potentiation in mice (Grillo et al., 2015). Moreover, the

downregulation of IRs in hypothalamus is shown to cause depression-like behavior in rats via reduced BDNF levels (Grillo et al., 2011).

Hyperinsulinemia can also be seen in metabolic disorders such as metabolic syndrome, type-2 diabetes and obesity which are known to be associated with increased oxidative stress (Tangvarasittichai, 2015). This oxidative stress also increases tau phosphorylation and accumulation of A β (Chen, Xu, Lahousse, Caggiano, & de la Monte, 2003) (Figure 6).

Pericytes have a significant role in the regulation of endothelial cell proliferation, differentiation, contractility, and permeability. In angiogenesis, after the formation of nascent microvessels, the most important step is pericyte recruitment to these newly formed microvessels. Pericytes in turn, have a stabilization effect on these microvessels as they inhibit endothelial proliferation (Armulik et al., 2005; Carmeliet & Jain, 2011). Endothelial cells are quiescent and they are protected by autocrine signals (vascular endothelial growth factor (VEGF), angiopoietin-1 (ANG-1), fibroblast growth factors (FGFs), and Notch signaling) and paracrine signals from pericytes, which mainly inhibits endothelial proliferation (Escudero et al., 2017). First description of IRs on human pericytes were made in the 80s and it showed insulin had a proliferative effect on pericytes (King et al., 1983). Pericytes have a major role in regulating angiogenesis, and pericyte loss and dysfunction has been a prominent sign in the early phase of DR (Richards, Raines, & Attie, 2010). The effects of insulin on endothelial cell proliferation however, are still an issue of discussion. While some studies showed proliferation (Jiang et al., 2003; Stout, 1991), some other ones established no difference (King et al., 1983; Liu, Petreaca, & Martins-Green, 2009; Shrader, Bailey, Konat, Cilento, & Reilly, 2009; Yamagishi et al., 1999). King et al. has also suggested that macrovascular and microvascular endothelia might be responding to insulin differently. Experiments done with calf retina microvascular endothelium showed a dose dependent increase in endothelial cell proliferation as response to insulin treatment while endothelia isolated from calf aorta did not show any differences (King et al., 1983).

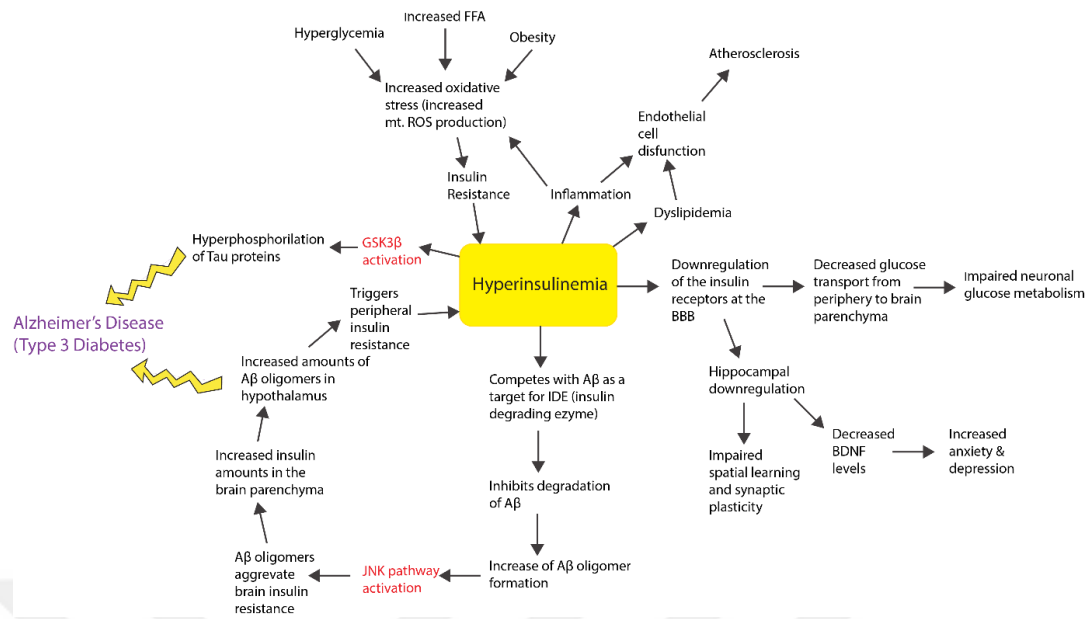


Figure 6. Effects of hyperinsulinemia

1.1.5.4. How to identify pericytes

Kumar et al. recently proved that mural cells, such as smooth muscle cells (SMCs) that surround the bigger vessels like arterioles and venules, and pericytes (PCs) that surround smaller vessels like precapillary arterioles, capillaries, and postcapillary venules, originate from the same mesenchymal progenitor called mesenchymoangioblast (MB) (Kumar et al., 2017). SMCs are primarily identified by their α -SMA expression. However, this protein is not specific to SMCs. It is also abundant in some types of pericytes and fibroblasts. High expression levels of this protein are positively correlated with a higher ability to contract. Most common pericytes markers are alpha-smooth muscle actin (α -SMA), NG2, alkaline phosphatase (ALP), PDGFR- β . Some less common markers that are associated with pericytes are desmin, vimentin, CD13, CD133, and CD146 (Armulik et al., 2005; Armulik, Genové, & Betsholtz, 2011; Díaz-Flores et al., 2009). Developmental pericytes are recruited by endothelial cells and they express CD134, but as soon as the recruitment process finishes, they stop expressing CD134. Adult pericytes are NG2 positive, but NG2 is also not specific to pericytes since oligodendrocytes also express NG2. Pericytes also express desmin. However, desmin is

abundant in skeletal, cardiac, and smooth muscles as well, so it is not a valid marker for pericytes in skeletal tissues. CD13 is a valid pericyte marker in PDGFR- β deficient transgenic animal studies. Yet, vascular SMCs, endothelial cells of tumors and inflamed tissue, and kidney epithelial cells also express CD13. Using cDNA microarray, Bondjers et al. proved that the most downregulated gene in the brains of PDGF-B and PDGFR- β null animals was RGS5 (regulator of G-protein signaling 5) gene (Bondjers et al., 2003). RGS5 gene is upregulated during wound healing, ovulation and angiogenic switch in carcinogenesis (Berger, Bergers, Arnold, Hämmerling, & Ganss, 2005). In contrast, the gene downregulates in regressing tumors under therapy (Ganss, Ryschich, Klar, Arnold, & Hammerling, 2002). This suggests RGS5 is involved in vessel modelling during neovascularization. Due to the lack of a good antibody, RGS5 is not widely used. The most reliable marker of adult pericytes is PDGFR- β , but it is also slightly expressed in some other cells, such as mesenchymal stem cells, smooth muscle cells, myofibroblasts, and some neurons and neuronal progenitors in CNS (Armulik et al., 2011). Also, Rubin et al. showed pronounced expression of PDGFR- β in pericytes of inflamed tissues when compared to pericytes of healthy tissues (Rubin et al., 1988). This information challenges the idea of safe and reliable labeling of pericytes.

1.1.5.5. Pericytes in Pathologic Metabolic Conditions

Healthy pericytes are mandatory for healthy cerebral microcirculation. It is known that pericyte loss leads to vascular damage in mainly two mechanisms. The first mechanism is the reduction in brain microcirculatory vessels. This decrease on capillary networks results in reduced brain capillary perfusion and therefore, hypoxia in those brain areas. Hypoxia on the long term leads to secondary neurodegenerative changes. These secondary neurodegenerative changes and microvascular reductions are related to cognitive decline, and even to Alzheimer's disease. The second mechanism is associated with the breakdown of the BBB. This insufficient barrier cannot prevent the accumulation of serum proteins and some other blood-derived products that are potentially toxic to the brain. (Armulik et al., 2010; Bell et al., 2010; Winkler, Bell, & Zlokovic, 2011; Zlokovic, 2011) Healthy pericytes are crucial for the

healthy brain microcirculation.

1.2. Rationale and Aims

In the last decade, many studies attempted to show the link between cognitive decline and metabolic diseases. Vascular dementia is concomitant with many metabolic changes such as the increase in total cholesterol, LDL and triglyceride levels, and impaired glucose metabolism. However, the mechanism of how these metabolic changes lead to dementia is still unknown. Previous studies have shown that T2DM is linked to accelerated cognitive decline; and is positively correlated with dementia and several structural brain abnormalities, such as atrophy, WMHs, and lacunar infarcts (Luchsinger, 2012; Manschot et al., 2006; Reijmer et al., 2013; van Harten, Oosterman, Muslimovic, et al., 2007; van Harten, Oosterman, Potter van Loon, Scheltens, & Weinstein, 2007). T1DM also leads to microvascular complications in the retina, kidney, and peripheral and autonomic nerves, primarily by chronic hyperglycemia (Ferguson et al., 2003; Kodl et al., 2008; Weinger et al., 2008; Wessels et al., 2007). Hypertension is a very common systemic disease in the elderly population and it has been associated with the presence of structural changes in the brain as well as cognitive decline (de Leeuw et al., 2002; Liao et al., 1996; van Dijk et al., 2004; van Swieten et al., 1991). With the increasing prevalence of diabetes and hypertension, it is expected that the related vascular complications will soon be an important socioeconomical issue.

Understanding the roles of pericytes in these pathologies can potentially prevent or alleviate the vascular and cognitive effects of these metabolic diseases. In this project, we aimed to show the changes that happen in cerebral microcirculation in three major metabolic diseases. We also aimed to investigate the pericytes role in the pathological conditions we see, and to lighten up the cognitive outcomes of these diseases. Metabolic conditions such as hyperglycemia, hyperinsulinemia, or high blood pressure change the protein expression levels of pericytes. By this change in protein levels, these conditions turn beneficial physiological states to malicious, lesion forming states that eventually lead to cognitive decline and dementia and this was one of the foundations of our hypothesis.

To sum up, our hypotheses are stated below:

Hypothesis 1: To show the changes in cerebral microcirculation in metabolic diseases.

Hypothesis 2: To show the effects on cerebral microcirculatory pericytes in metabolic diseases.



2. MATERIALS AND METHODS

In all experiments and procedures, we have applied the protocols and criteria approved by the Institutional Animal Care and Use Committee (IACUC) of Koç University.

2.1. Experimental Design

2.1.1. Animal Models

We used three animal models to establish previously described metabolic derangements. The methods used are described below:

2.1.1.1. T2DM

We have fed C57 mice with high fat, high sucrose diet (HFHSD, Research Diet Inc., D11092103) for 16 weeks. As control groups, we used two types of chow. We have fed the first group with a low-fat diet (LFD, Research Diet Inc., D11092101) and the second group with normal chow (NCD, SDS- VRF1-P) for the same period (Yang, Miyahara, Takeo, & Katayama, 2012; Zhou et al., 2013). LFD diet contained 11% fat-derived calories (9% corn oil and 2.5% butter) and 67.7% carbohydrate-derived calories without sugar. HFHSD contained 36% fat derived-calories (9% corn oil and 27% butter), and 43.2% carbohydrate-derived calories with sucrose (30% sucrose-derived calories).

2.1.1.2. T1DM

We induced T1DM in CD1 mice through the application of low dose intraperitoneal streptozotocin (STZ) for five consecutive days. We fasted male mice, aged 20 to 22 weeks, for approximately 4 hours before intraperitoneally injecting them with a freshly prepared Streptozotocin solution of 7.5 mg/ml concentration. The final dosage of each mouse was 50 mg/kg. Later, we supplied the mice with 10% sucrose water to avoid sudden post-injection hypoglycemia. After consecutive injections, we measured their fasting blood glucose levels and weights at least once a week. We injected the control group only with the vehicle, the Na-citrate solution, for 5 consecutive days (Furman, 2015).

2.1.1.3. Hypertension

To imitate essential hypertension, we obtained spontaneously hypertensive rats (SHR) from Charles River Laboratories. We have used Wistar albino rats of the same age as control group. We fed Wistar albino rats and SHRs weighing 250–400 g with a standard laboratory rat chow ad libitum and housed them in Plexiglas cages with 12-h light/dark cycle in a temperature-controlled room (20 ± 3 °C). SHRs are established to have a high systolic blood pressure after 5-6 weeks of age, which generally rises to 180-200 mmHg. We have specifically chosen SHRs for this study because they tend to have a higher risk of hypertensive end-organ damage but do not necessarily have a higher incidence rate of atherosclerosis, vascular thrombosis, or stroke. We sacrificed SHRs and Wistar control groups of the same age at week 23, 27, and 31 and obtained their brain tissues to observe the progress of the lesions.

2.1.2. Fasting Blood Glucose and Noninvasive Blood Pressure Measurements

In T1DM animal model, we measured fasting blood glucose levels every week after 16 hours of fasting with an ACCUCHEK glucometer, 12 weeks after STZ injections. In HFHS animal model, we measured fasting blood glucose levels after 11 weeks and 16 weeks of diet feeding. We measured blood pressure of each animal with CODA MONITOR system. In T1DM animal model, we measured BP 12 weeks after STZ injections, whereas in HFHS animal model, we measured BP after 11 weeks and 16 weeks of diet feeding. Hypertensive rats and their Wistar control groups BP's were measured at 23 weeks, 27 weeks, and 31 weeks. All animals were habituated to the restrainer for 3 weeks and twice a week, 5 minutes per session before the actual measurements were done. No anesthesia was used during measurements. All the measurements were done at dark cycle. At least three measurements were done and their mean value was accepted as the final BP value.

2.1.3. Intraperitoneal Glucose Tolerance Test (IPGTT)

In HFHS animal group, IPGTT was done after 11 weeks and 16 weeks of diet

feeding, as described before. In T1DM animal group, animals were kept alive for 12 weeks after the STZ injections and their fasting glucose levels were measured once a week just to ensure their blood glucose levels were still high. One animal from STZ injected group had normal fasting blood glucose levels after week 7 and excluded from the study. Food was withdrawn at 5 PM, and fast was performed overnight (lasted for 16 hours) until the test started at 9 AM. Baseline body weight and blood glucose were measured for each animal. 10% and 20% D-glucose (Sigma Aldrich, catalog number: G8270) solutions in PBS were prepared and filtered with 0.2 um filter for sterilizing purposes. We injected the animals with 2 mg glucose/g intraperitoneally and the baseline weight data was used for the calculation. For animals with body weight greater than 30 g, we used 20% glucose solution. Fasting blood glucose was measured at 15, 30, 60, 90, 120 minutes with an ACCUCHEK glucometer. For insulin measurements, 50-80 µl blood was collected at each time point, including baseline. Blood was immediately centrifuged, and the serum was separated and stored at -80°C until insulin was measured.

Animal Model	Species	Applied Tests
Streptozotocin induced T1DM model	CD1 mice	Weekly weight measurements Weekly fasting blood glucose measurements Noninvasive blood pressure measurements IPGTT
HFHS diet induced T2DM model	C57BL/6 mice	Weekly weight measurements Noninvasive blood pressure measurements IPGTT
Hypertension model	Spontaneously Hypertensive Rats / Wistar rats	Weekly weight measurements Noninvasive blood pressure measurements

Table 1. Summary of animal models and applied tests.

2.1.4. Behavioral Tests

All apparatus utilized in the behavioral tests were constructed out of matte acrylic sheets, in black and white colors. We chose the color of the apparatus to contrast the colors of the animals in the groups. The experimenter handled the animals at least twice a week for at least 2 weeks before the onset of behavioral experiments, to habituate the animals to the experimenter. A single experimenter performed all behavioral tests, in the same room and lighting conditions. All the behavioral experiments were performed in the dark cycle and were recorded via a video camera. The experimenter did not stay in the room while the behavioral experiment was in progress and we scored all the experiments from the recordings. We cleaned the mazes with 70% ethanol and let them dry after each experiment.

2.1.4.1. *Open Field Test*

We subjected all animal groups to the open field test, to exclude the effects of anxiety on the outcome of the spatial and temporal memory tests. The dimensions of the arenas were 40x40x40 cm for mice, and 60x60x60 cm for rats. We placed each animal in a clean cage to habituate the animal to the room and the lighting conditions for 10 minutes before the experiment. During the experiment, we always handled the animals by the base of their tails. At the beginning of the experiment, we put the mice and rats directly to the center of the maze and allowed them to explore the maze for 6 and 10 minutes, respectively (Sweatt, 2010). We measured total distance travelled and thigmotaxis levels as a measurement of locomotion and anxiety.

2.1.4.2. *Y-Maze Test*

We used the Y-Maze test to measure the impairment of spatial working memory in all three animal models. The maze had three arms with the same dimensions, placed at 120° angles. The dimensions of the arms of the maze were 20x40x10 cm for mice and 20x40x10 cm for rats. We have placed physical cues on the 4 exterior sides of the maze. We have chosen an arm as the starter arm and placed all animals on the same arm at the beginning of the experiment. The animal could explore and pass from one arm to the other

(transition in between arms) freely without any cues inside the maze itself (Hughes, 2004). We manually did the scoring and calculation of maximum spontaneous transition chance.

2.1.4.3. Novel Object Recognition Test

We have used novel object recognition test to understand the effects of the metabolic diseases on the visual recognition memory. First, we habituated the animals to the open field arena for 6 minutes. The animals were subjected to two identical items for 10 minutes in the same open arena 24 hours later, where they could explore the objects. We have excluded the animals that explored the objects for less than 20 seconds at this stage from the study. Later, we took the animals back to their cage for a defined time interval (6 hours for mice and 24 hours for rats (Antunes & Biala, 2012; Leger et al., 2013)). Then, we changed one of the two identical items with a novel object randomly. Following this change, we placed the animals back in the arena for 5 minutes (Antunes & Biala, 2012; Bevins & Besheer, 2006; Freret et al., 2012; Leger et al., 2013; Şik, Van Nieuwehuyzen, Prickaerts, & Blokland, 2003). We defined object exploration as sniffing, licking, and touching an object while facing towards it in the 2 cm perimeter of the object. We did not accept whisker contact, climbing and touching the object while facing away from the object or towards the ceiling as an act of exploration (Leger et al., 2013). We have scored the exploration times of the old and new objects using Ethovision XT video tracking software on the recordings. The score of each animal was calculated by dividing the time spent exploring the novel object to the total exploration time of both objects (Antunes & Biala, 2012).



Figure 7. Novel and familiar objects that are used in these experiments.



Figure 8. Spatial cues and camera setup used in these experiments.

2.1.5. 3DISCO method for 3D Imaging

For visualization of the microcirculatory changes in three-dimensional perspective, we used 3DISCO procedure, which is a fast tissue clearing procedure. We have anesthetized the animals with isoflurane and transcardially perfused with ice-cold heparin-saline solution (50IU/L), 4% PFA, and 2% gelatin-albumin-FITC solution. Immediately after perfusion, we buried the animals in ice with their head directed at the bottom of the container to solidify the albumin-FITC and gelatin mixture. 10 minutes later, we dissected the brain tissues and kept at 4% PFA overnight at 4°C. We sliced the tissues according to need and went through the 3DISCO protocol. We placed the slices in a 10% tetrahydrofuran (THF) solution. Then, we placed them into a horizontal shaker at 300 rpm at room temperature for 1 hour. We have repeated the same process with 30%, 60%, 80%, and 100% THF solutions. Afterwards, we placed the tissues in dibenzyl ether (DBE) and spent 12 hours at a horizontal shaker at 300 rpm, at room temperature. We have kept the cleared tissues in DBE in a dark place at room temperature and imaged in DBE solution with multiphoton microscopy (Ertürk et al., 2012; Lugo-Hernandez et al., 2017).



Figure 9. Brain tissues in 3DISCO procedure. The picture on the right is after overnight 4% PFA incubation. The picture in the middle is after THF gradient. The last picture is after DBE incubation.

Clarified brain tissues were imaged using Leica DM6 Confocal Scanning Microscope using 20x magnification. The collected images were processed using LasX. For each comparison, we used the experimental groups and their own control groups. In order to compare fluorescence intensities between groups reliably, all images in the same group were collected with the same laser intensity, gain, and offset settings using identical confocal aperture settings on the same day. Post capture image manipulation for contrast and background noise was applied identically.

2.1.6. Immunofluorescence Staining

To demonstrate the relationship of pericytes with microcirculation, we used immunofluorescence-staining method. We have anesthetized the animals with isoflurane and transcardially perfused them with ice-cold heparin-saline solution (10IU/L), 4% PFA, and kept their brains in 4% PFA overnight at +4C. Later, we dehydrated the brains by a gradient of sucrose in 0.1 M Phosphate buffer at +4C (10%, 20%, and 30%). Then we embedded them in cryomatrix and sliced at a thickness of 40 μ m. Later, we incubated the slices with both anti-PDGFR β (ab32570) and Isolectin GS-IB4- Alexa Fluor 488 conjugate (I21411) antibodies in 1:100 dilution to stain the endothelial cells and pericytes at the same time. Isolectin staining marked the endothelial cells, while

PDGFR- β staining indicated pericytes' locations at the microvasculature. After incubating with primary antibodies, sections were incubated with appropriate secondary antibodies conjugated with Alexa Fluor 594 in 1:200 dilution for 2 hours in 37°C. Immunofluorescence labeling of the brain tissues were observed using Leica DMI8 SP8 Confocal Scanning Microscope.

2.1.7. Measurement of biochemical parameters

At the end of the experimental period, each animal was given overdose isoflurane anesthesia. Blood was obtained by cardiac puncture by means of a 5 ml hypodermic syringe. Blood was immediately centrifuged for 10 minutes at 800x g and 10 minutes at 2000x g, respectively. Serum was separated and stored at -80°C until needed. Blood lipid panel (HDL, LDL, triglyceride, and total cholesterol) was measured using colorimetric assays, and ALT, AST levels were measured via IFCC without pyridoxal phosphate.

2.1.8. ELISA

Plasma insulin concentrations were determined by commercially available ELISA kit (Ultra-Sensitive Mouse Insulin ELISA Kit- Crystal Chem, catalog #90080). As previously described, serum samples obtained from IPGTT were used in this assay.

2.1.9. HOMA-IR Calculation

To assess insulin resistance of the HFHS animal group, HOMA-IR scores were calculated via using the formula below:

$$\text{HOMA-IR} = 26 \times \text{fasting insulin level (ng/ml)} \times \text{fasting glucose level (mg/dl)} / 405$$

(Murakami et al., 2014).

2.1.10. Quantification of capillaries, pericytes and collagen 1 expression levels

Immunofluorescence labeling of the brain tissues were observed using Leica DMI8 SP8 Confocal Scanning Microscope. The collected images were processed using LasX. For each comparison, we used the experimental groups and their own control groups. To compare fluorescence intensities

between groups reliably, all images in the same group were collected with the same laser intensity, gain, and offset settings using identical confocal aperture settings on the same day. Post capture image manipulation for contrast and background noise was applied identically. Differences in between experimental and control groups were analyzed from matched areas for statistical significance by Student's t-test by GraphPad PRISM Software. A two tailed 'p' value of <0.05 was considered as significant.

2.1.10.1. Quantification of capillaries

Images used at isolectin quantification were obtained at 20x magnification. Later, ImageJ was used to segment isolectin positive areas of the acquired images via thresholding. Identical thresholding adjustments were made for each image for reliable comparison. The ratio of isolectin positive area to the total imaging area was calculated with ImageJ.

2.1.10.2. Quantification of total numbers of pericytes and pericytes around vessels

Brain slices of 40 μm thickness were stained as previously described in the methodology section with anti-PDGFR β and isolectinB4 antibodies. The samples were then imaged with Leica DMI8 SP8 Confocal Scanning Microscope using 63x magnification. To compare fluorescence intensities between groups reliably, all images in the same group were collected with the same laser intensity, gain, and offset settings using identical confocal aperture settings on the same day. The experimenter manually counted PDGFR β positive cells and PDGFR β positive cells around the vessels.

2.1.10.3. Quantification of Collagen 1 expression levels by measuring mean pixel intensity

Brain slices of 40 μm thickness were stained as previously described in the methodology section with anti-collagen 1 and isolectinB4 antibodies. The samples were then imaged with Leica DMI8 SP8 Confocal Scanning Microscope using 63x magnification. To compare fluorescence intensities between groups reliably, all images in the same group were collected with the

same laser intensity, gain, and offset settings using identical confocal aperture settings on the same day. ImageJ was used to measure average pixel intensity of acquired images.

2.1.10.4. Quantification of tortuosity

Whether tortuous vessel numbers differ or not is also a controversial issue, so we counted the numbers of tortuous vessels in previously obtained 3DISCO images manually.

2.1.10.5. Quantification of pial arteriole exit point narrowing

We also observed narrowings in pial arterioles at the exit points from the arteries, so we counted narrowings from the previously obtained 3DISCO images manually.

2.1.11. Statistics

All results were expressed as mean \pm SEM. Student's t-tests were used when comparing two groups, and ANOVA was used when comparing more than two groups. Tukey test was used for comparing means after a one-way ANOVA, and Holm-Sidak test was used for comparing means after two-way ANOVA tests. A p value less than 0.05 was considered statistically significant.

3. RESULTS

3.1. Metabolic Outcomes of the Animal Models

We measured several parameters such as weight and fasting blood glucose periodically to establish solid and reliable animal models of metabolic diseases.

3.1.1. Streptozotocin-Induced T1DM Animal Model

Experiment group and control group did not exhibit any significant weight differences at the beginning of the study. The diabetic group showed significant weight loss 7 weeks and 12 weeks after the injections when compared to their same-aged control groups ($p < 0.0001$) (Table 2).

Group	Day 1, before injection	7 weeks post injection	12 weeks post injection
	Weight, g	Weight, g	Weight, g
<i>Diabetic</i>	42.28 ± 1.03 (17)	*34.36 ± 0.63 (17)	*33.42 ± 0.79 (17)
<i>Control</i>	43.04 ± 0.89 (11)	42.05 ± 0.7 (11)	40.85 ± 1.1 (11)
<i>TTEST</i>	p = 0.2901	p <0.0001	p <0.0001

Table 2. Body weight measurements in Streptozotocin-induced type 1 diabetic animals (mean ± SEM) (* denotes $p < 0.0001$)¹

Fasting blood glucose measurements were also significantly higher in diabetic group when compared to their same-aged control group both in 7 weeks and 12 weeks after injection ($p < 0.0001$) (Table 3). Fasting blood sugar levels of the animals in both groups were measured once a week after approximately 6 hours of fasting and always at the same time of the day. One animal did not exhibit high fasting blood sugar levels after week 7 and it was excluded from the study.

¹ Numbers in parentheses indicate sample size

Group	7 weeks after injection	12 weeks after injection
	glucose (mg/dL)	glucose (mg/dL)
<i>Diabetic</i>	*471.35 ± 18.42 (17)	*349.15 ± 26.7 (17)
<i>Non-diabetic</i>	101.45 ± 5.12 (11)	116.64 ± 5.16 (11)
<i>TTEST</i>	p <0.0001	p <0.0001

Table 3. Fasting blood glucose measurements in Streptozotocin-induced type 1 diabetic animals (mean ± SEM) (* denotes p < 0.0001) ²

To validate the diabetic model further, we have used intraperitoneal glucose tolerance tests (IPGTT). We have measured blood glucose and serum insulin levels at 0, 15, 30, 60, 90, 120 minutes after intraperitoneal injections of glucose. Insulin levels of the control group were significantly higher at each time point (p < 0.0001 at every time point, Holm-Sidak's multiple comparisons test), and serum insulin was nearly nonexistent in T1DM mice (Figure 10). Blood glucose levels on T1DM mice were significantly higher during the test (p < 0.0001, two-way ANOVA).

² Numbers in parentheses indicate sample size

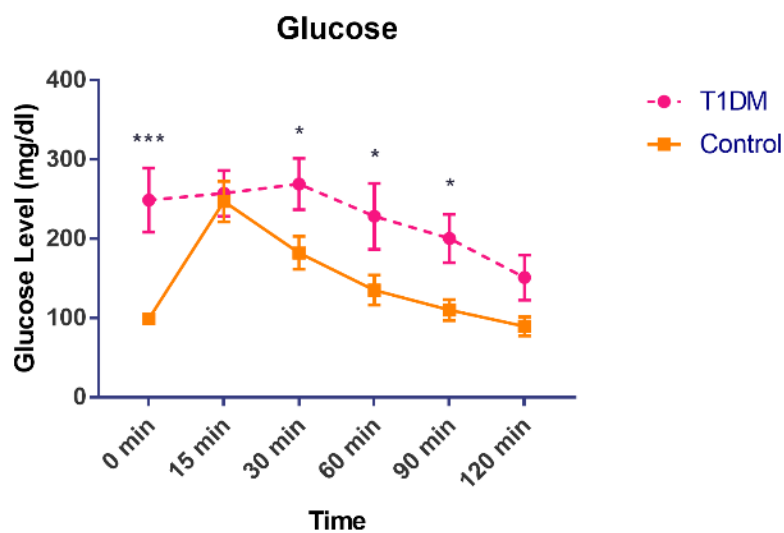
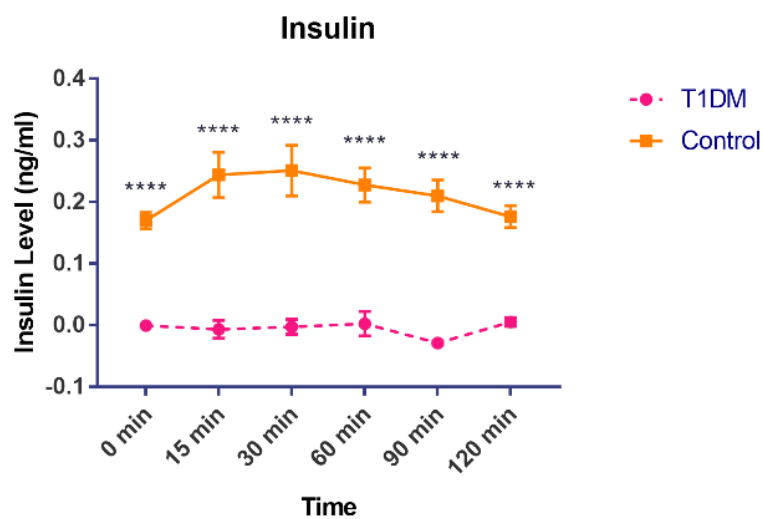


Figure 10. Insulin and blood glucose levels of T1DM and control group CD1 mice.

We have also measured biochemical parameters of both groups and found that only ALT levels were significantly elevated in the T1DM group ($p = 0.0120$, two-tailed Student's t-test), while there were no significant changes in other parameters (Figure 11).

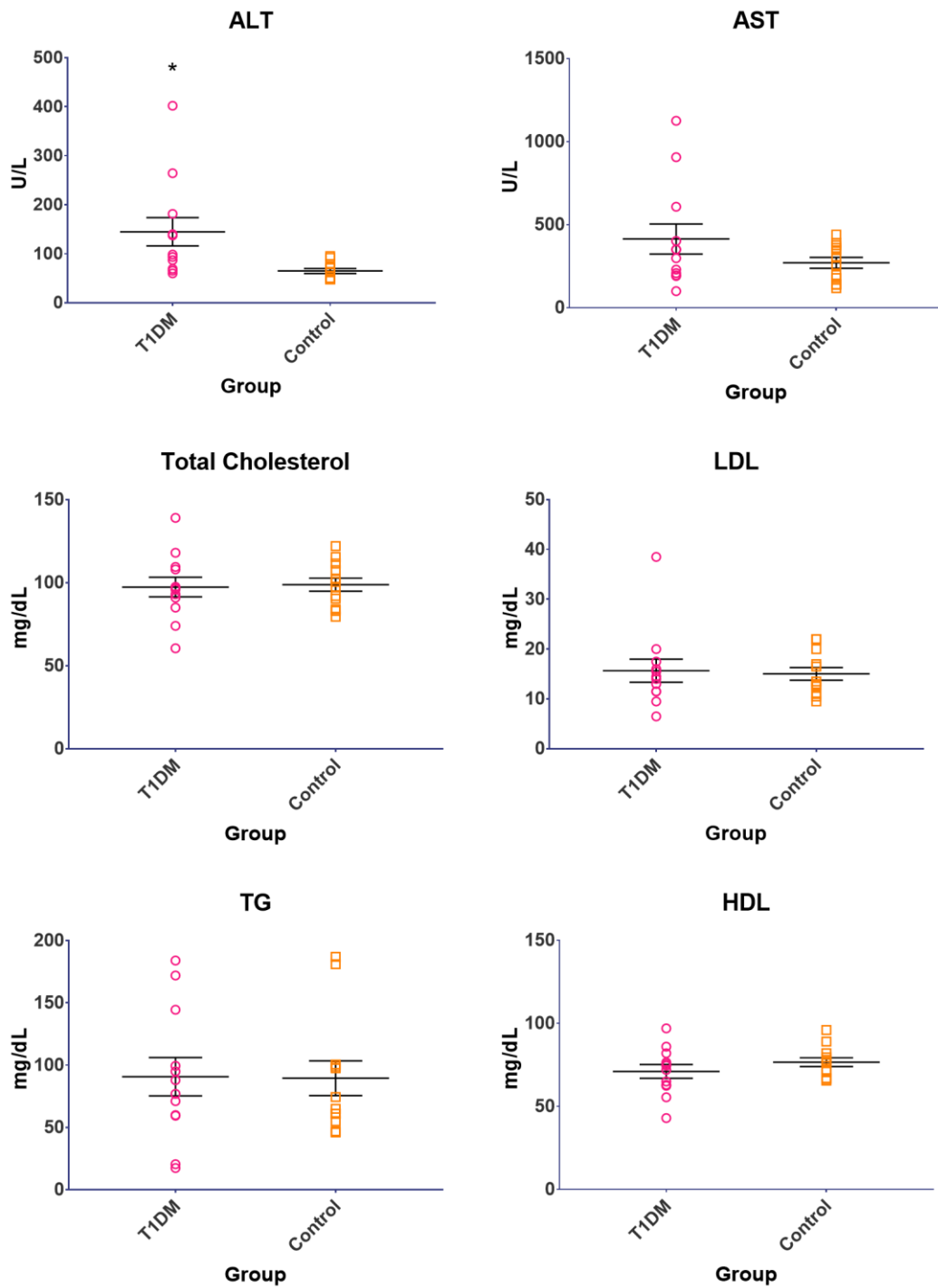


Figure 11. Blood biochemical parameters of T1DM and control group CD1 mice.

We measured animals' blood pressure with CODA noninvasive blood pressure measurement device, 12 weeks after injection to eliminate the

possibility of high blood pressure. The differences in systolic, diastolic, and mean blood pressures were not significant between the diabetic group and their same-aged control group (Student's t-test, $p > 0.05$) (Table 4).

Group

	Systolic BP, mmHg	Diastolic BP, mmHg	Mean BP, mmHg
<i>Diabetic</i>	112.6 ± 6.22 (4)	82.4 ± 8.77 (4)	92.1 ± 7.45 (4)
<i>Non-diabetic</i>	125.6 ± 4.2 (4)	101.1 ± 4.63 (4)	108.9 ± 4.44 (4)
<i>TTEST</i>	$p = 0.1407$	$p = 0.1247$	$p = 0.1111$

Table 4. Blood pressure measurements in streptozotocin-induced type 1 diabetic animals (mean ± SEM)

3.1.2. T2DM (HFHS animal model)

The HFHS group weighted significantly higher when compared to same-aged normal chow and low-fat fed animals at week 11 ($p < 0.0001$, Student's t-test) (Table 5), and in week 16 ($p = 0.0001$, Tukey's multiple comparisons test) (Table 6).

Group	Weight, g	Age
<i>HFHS</i>	*43.39 ± 1.315, n=8	24 weeks
<i>Normal Chow</i>	24.04 ± 0.5686, n=8	24 weeks

Table 5. Body weight measurements in animals fed with high-fat high sucrose diet and normal chow at week 11 (mean ± SEM) (*denotes $p < 0.0001$)

Group	Weight, g	Age
<i>HFHS</i>	*42.49 ± 1.292, n=8	29 weeks
<i>Low Fat</i>	31.94 ± 1.413, n=5	29 weeks
<i>Normal Chow</i>	29.77 ± 2.262, n=6	29 weeks
<i>ANOVA & Tukey's multiple comparisons test</i>	<p>p < 0.0001 for ANOVA</p> <p>p = 0.0001 for HFHS vs. Normal Chow</p> <p>p = 0.6798 for Low Fat vs. Normal Chow</p>	

Table 6. Body weight measurements in animals fed with high-fat high sucrose diet, low-fat diet, and normal chow at week 16 (mean ± SEM) (*denotes p = 0.0001)

We have measured and analyzed the systolic, diastolic, and mean blood pressures of the animals with one-way ANOVA. The HFHS, LF, and normal chow groups did not exhibit any significant changes in any of the parameters (Table 7).

Group	Systolic BP, mmHg	Diastolic BP, mmHg	Mean BP, mmHg
<i>HFHS</i>	123.5 ± 6.66, n=8	93.12 ± 6.26, n=8	102.9 ± 6.37, n=8
<i>LF</i>	114.3 ± 2.40, n=5	87.07 ± 2.47, n=5	95.77 ± 2.41, n=5
<i>Normal Chow</i>	115.1 ± 5.82, n=6	90.67 ± 5.74, n=6	98.43 ± 5.71, n=6
<i>ANOVA</i>	p = 0.4744	p = 0.7652	p = 0.4001

Table 7. Blood pressure measurements in animals fed with high-fat high sucrose diet (mean ± SEM)

Serum insulin levels of the HFHS group was significantly higher than normal chow and low-fat fed groups on both week 11 and week 16 (p < 0.0001 at both weeks, 2-way ANOVA & Holm-Sidak's multiple comparisons test, significance levels indicated at time points are between HFHS and normal chow groups) (Figure 12).

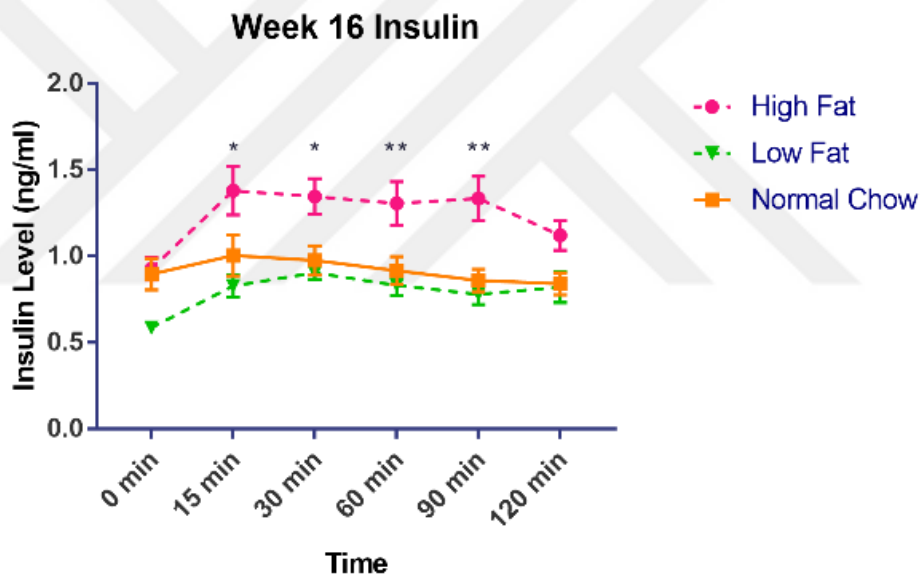
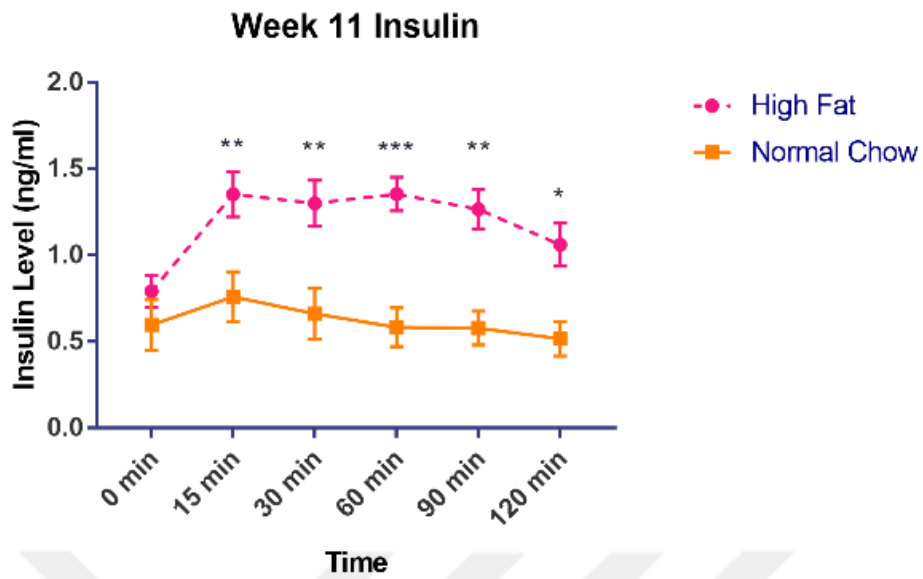


Figure 12. Insulin levels of HFHS, Low-fat and Normal chow fed mice on Week 11 and Week 16

Similarly, blood glucose levels of the HFHS group was significantly higher than normal chow and low-fat fed groups on both week 11 ($p < 0.0001$, 2-way ANOVA) and week 16 ($p < 0.0001$, 2-way ANOVA & Holm-Sidak's multiple comparisons test, significance levels indicated at time points are between HFHS and normal chow groups) (Figure 13).

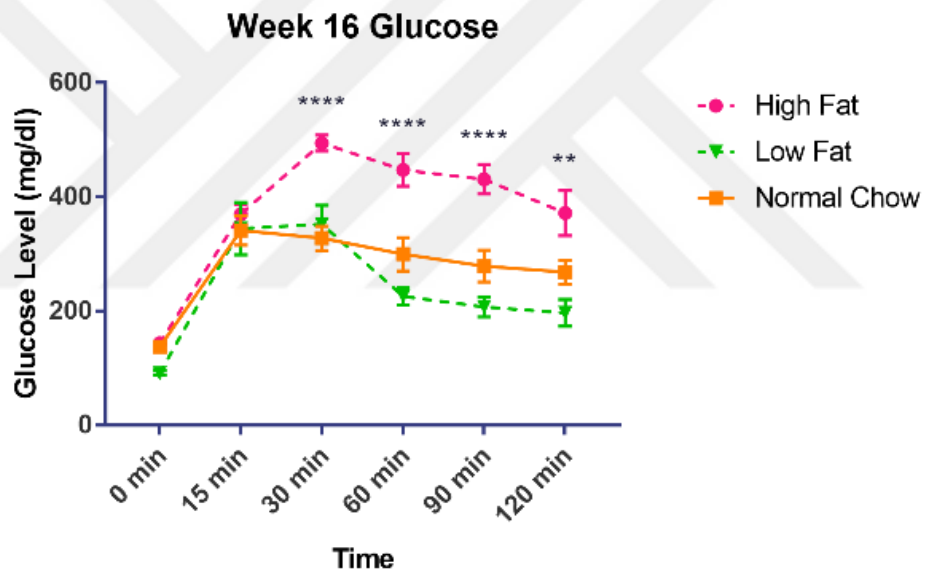


Figure 13. Blood glucose levels of HFHS, Low-fat and Normal chow fed mice on Week 11 and Week 16

We have also calculated insulin resistance (HOMA-IR) values for each group, and the values for HFHS fed group were significantly higher than both normal chow and low fat fed groups. ($p = 0.0328$, $p = 0.0023$ respectively, one-way ANOVA & Tukey multiple comparisons test) but there was no significant difference between normal chow and normal fed group ($p = 0.1114$, one-way ANOVA & Tukey multiple comparisons test) (Figure 14).

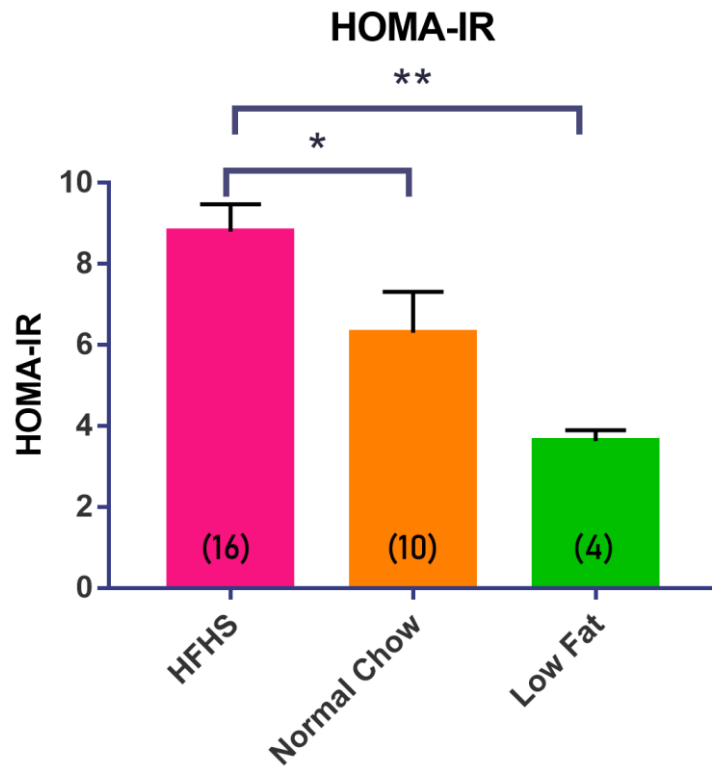


Figure 14. HOMA-IR values of HFHS, Low-fat and Normal chow fed mice. Numbers inside parentheses indicate sample size.

Total cholesterol, LDL and HDL levels were significantly higher in the HFHS group compared to normal chow group on week 11 ($p = 0.0293, 0.0260, 0.0194$ respectively, two tailed Student's t-test) (Figure 15).

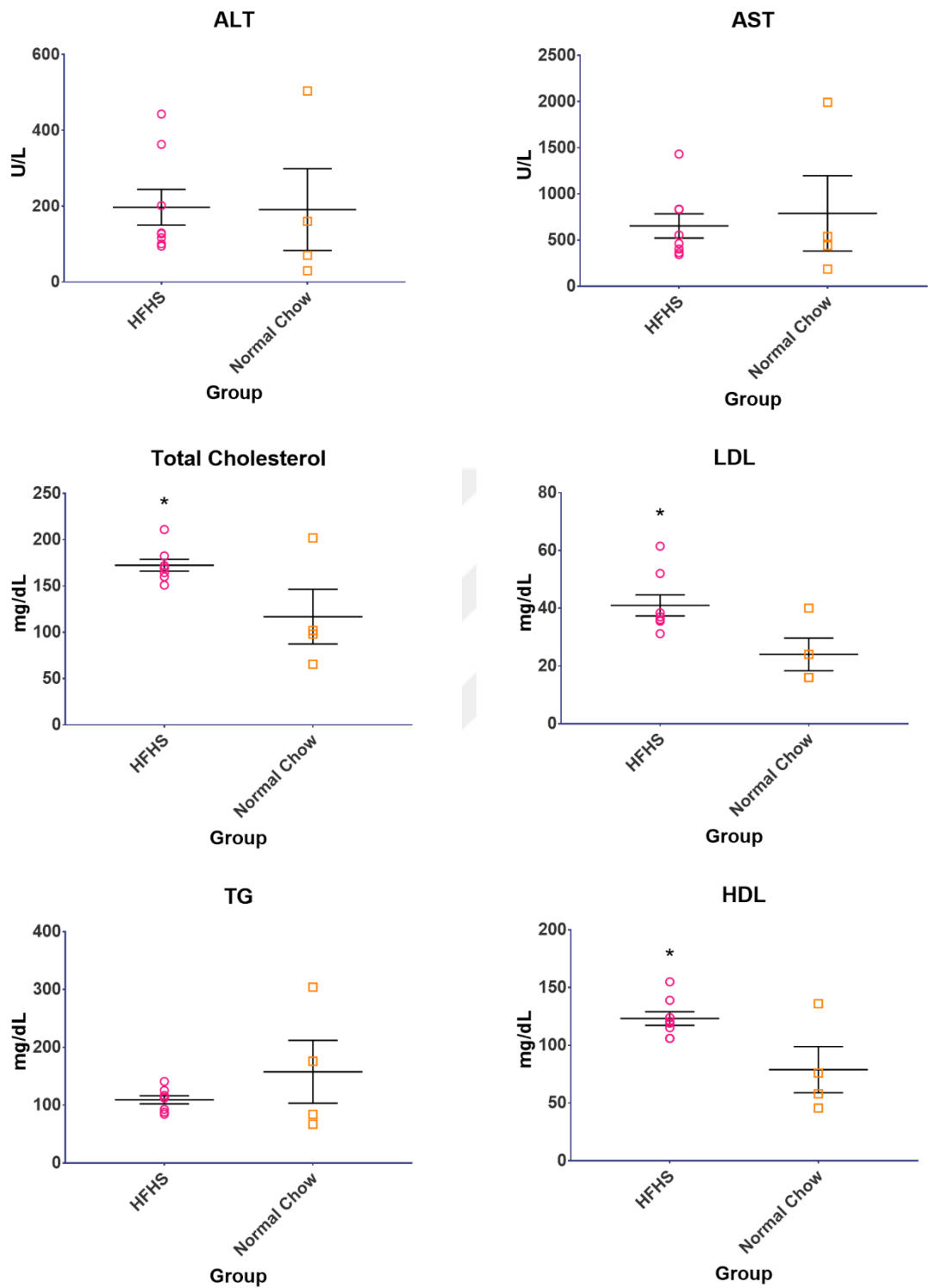


Figure 15. Blood biochemical parameters of HFHS & NC fed mice on Week 11

Whereas on the 16th week; ALT, AST, total cholesterol, LDL and HDL levels

were significantly elevated in HFHS fed mice when compared to the normal chow group ($p = 0.0043, 0.0026, <0.0001, 0.0001, <0.0001$ respectively, Tukey's multiple comparisons test following one-way ANOVA) (Figure 16). Additionally, total cholesterol and HDL levels were also significantly higher in low-fat fed group when compared to normal chow fed mice ($p = 0.0146, 0.0027$ respectively, Tukey's multiple comparisons test following one-way ANOVA).



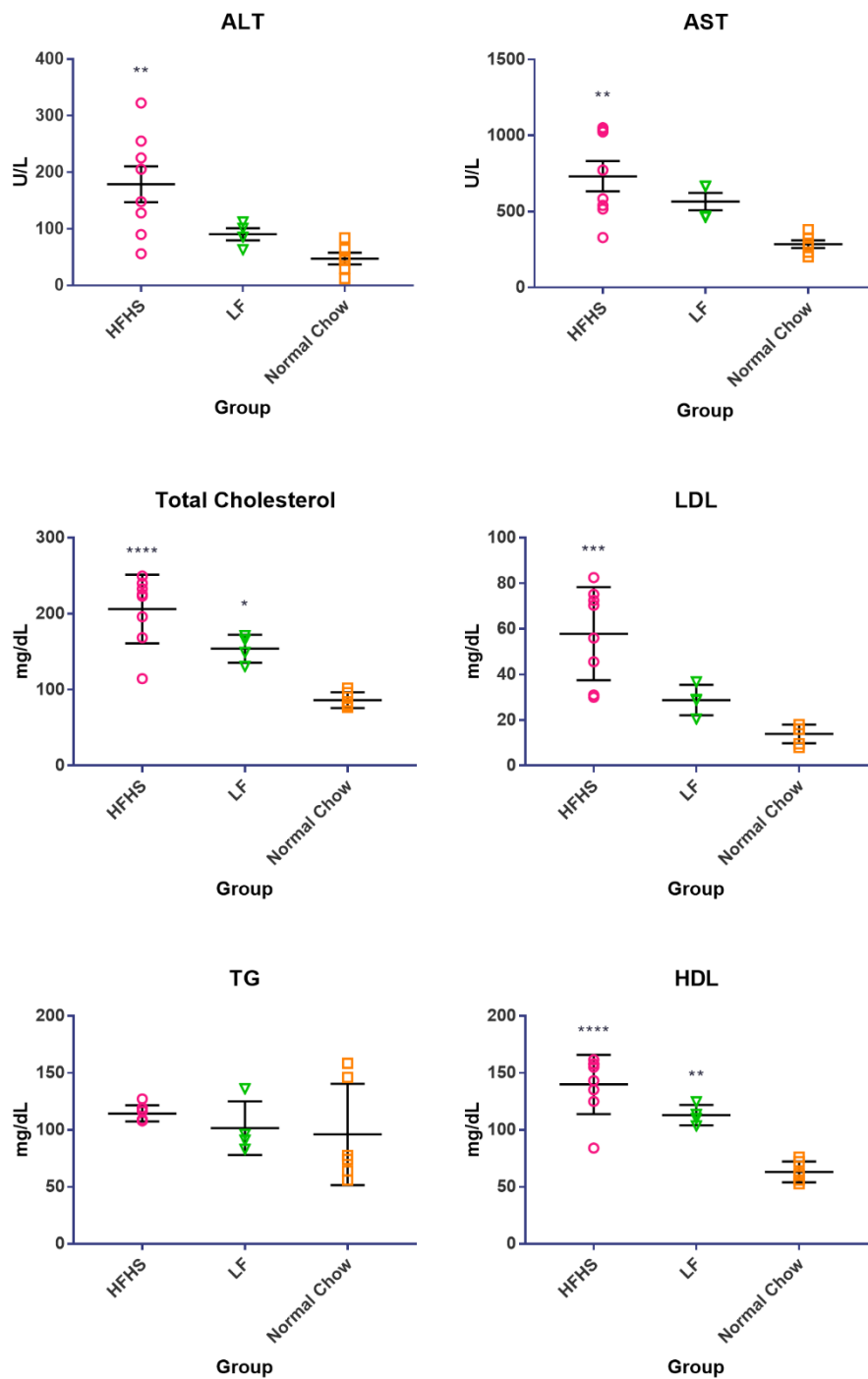


Figure 16. Blood biochemical parameters of HFHS, LF and Normal chow fed mice on Week 16

3.1.3. Spontaneously Hypertensive Rats (SHRs)

We have purchased the SHRs from Charles River Laboratories. We measured

their blood pressure with CODA noninvasive blood pressure measurement system to verify the blood pressure difference between their same-aged Wistar control groups. All three groups of SHRs (23, 27, 31 weeks old) showed a significant increase in systolic, diastolic, and mean blood pressures in comparison to their control groups (Figure 17).

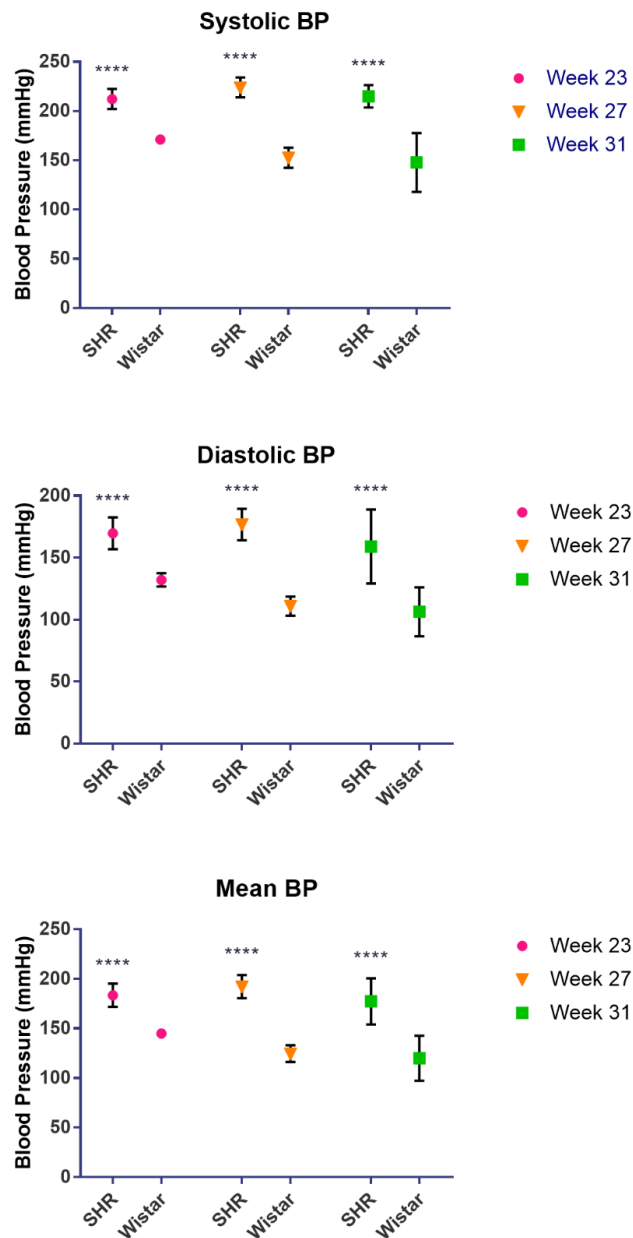


Figure 17. Blood pressure measurements in spontaneously hypertensive rats (mean \pm SEM)

When measured, the ALT, AST levels of the SHR mice were significantly higher than control group Wistar rats at every week ($p < 0.0001$ for ALT at every week, $p = 0.02, 0.002, 0.02$ at week 23, 27, 31 respectively for AST, Holm-Sidak's multiple comparisons test) (Figure 18). Furthermore, SHR had higher triglyceride ($p = 0.0068$, Holm-Sidak's multiple comparisons test) and HDL ($p = 0.0037$, Holm-Sidak's multiple comparisons test) levels on week 23 and higher total cholesterol ($p = 0.313$, Holm-Sidak's multiple comparisons test), LDL ($p < 0.0001$, Holm-Sidak's multiple comparisons test) and triglyceride ($p = 0.0005$) levels on week 27 when compared to Wistar control groups.



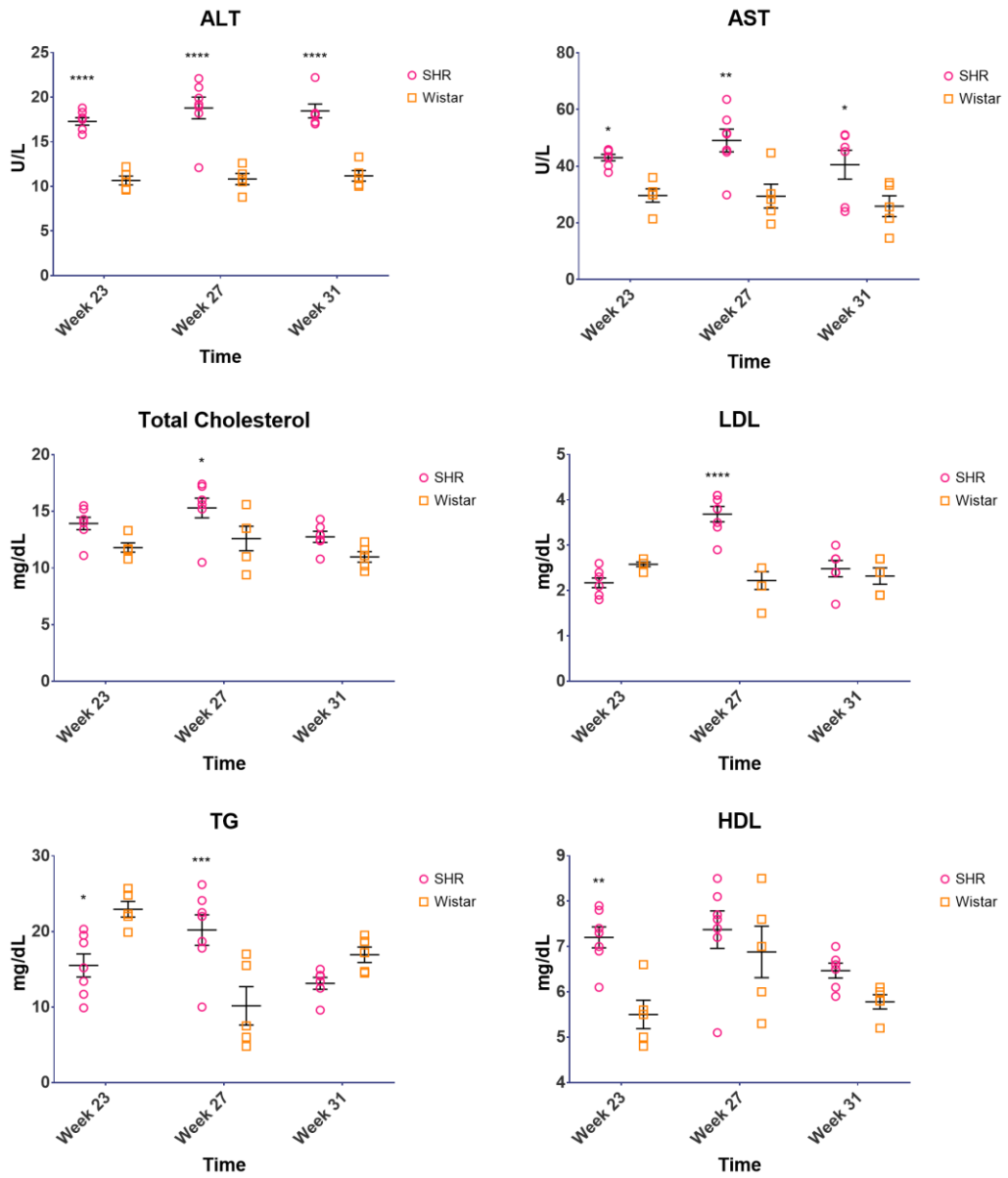


Figure 18. Biochemical parameters of SHR and control group Wistar rats

3.2. Cognitive Outcomes

3.2.1. Open Field Tests

3.2.1.1. *Streptozotocin-Induced T1DM Animal Model*

In diabetic mice, time spent in central area was less than the control group, though the difference between the groups were statistically insignificant ($p = 0.9185$, two-tailed t-test) (Figure 19). However, total distance traveled by the diabetic mice was significantly less than the control group ($p = 0.0036$, two-tailed t-test) (Figure 20).

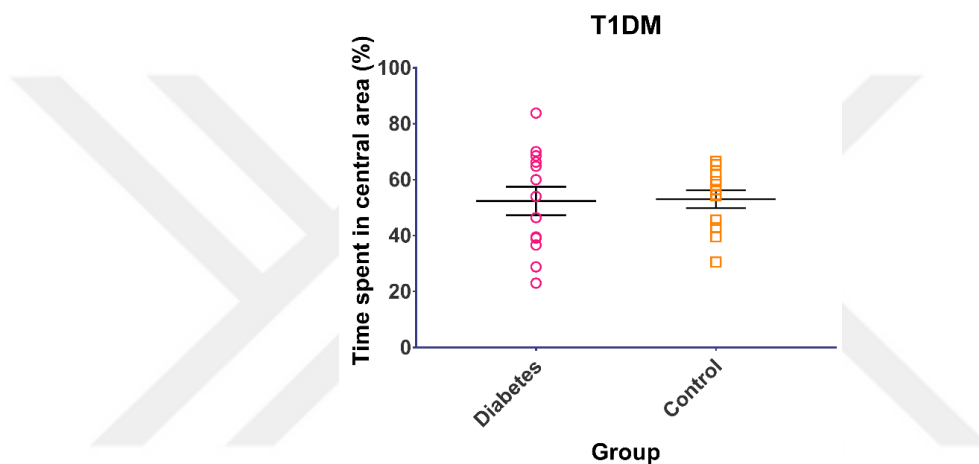


Figure 19. Time spent in central area in Streptozotocin-induced type 1 diabetic mice (mean \pm SEM)

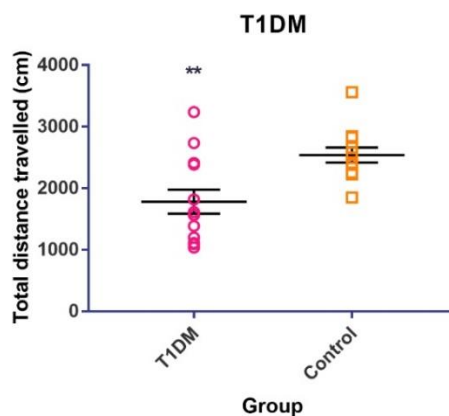


Figure 20. Total distance traveled in Streptozotocin-induced type 1 diabetic mice (mean \pm SEM)

3.2.2. T2DM (HFHS animal model)

On both 11th and 16th weeks, mice fed with high fat high sucrose chow spent more time in the central area compared to mice fed with normal chow ($p = 0.02$, $p = 0.0012$ respectively, Holm-Sidak's multiple comparisons test), suggesting a decline of anxiety in these animals (Figure 21). Interestingly, there has also been an increase in time spent in the central area in animals fed with low fat on week 11 ($p = 0.02$, Holm-Sidak's multiple comparisons test), but not on week 16 ($p = 0.1017$, Holm-Sidak's multiple comparisons test).

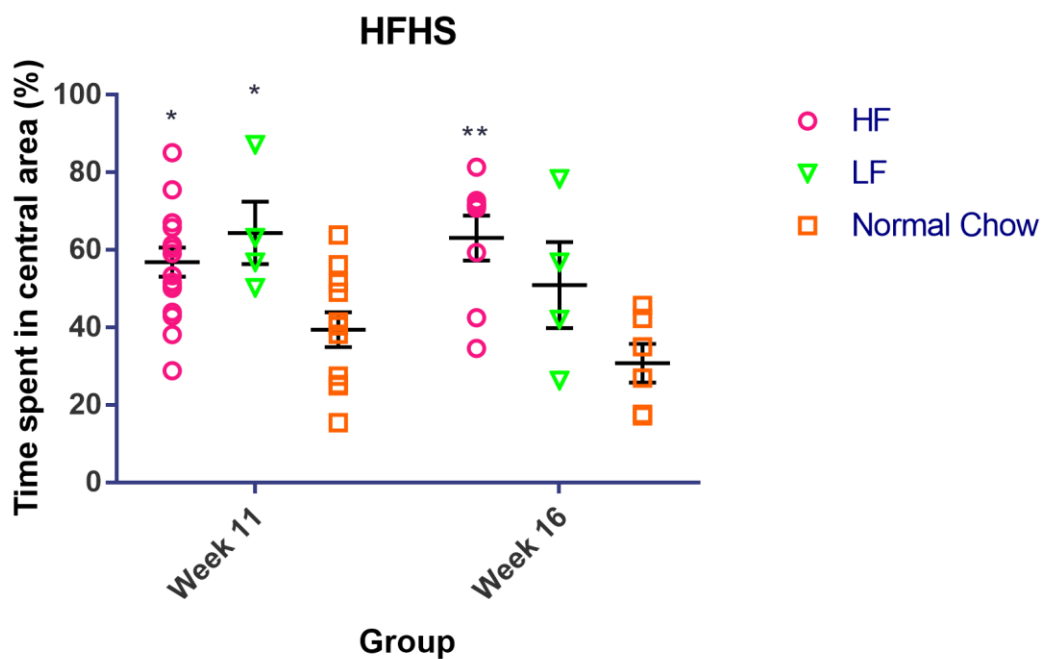


Figure 21. Time spent in central area in animals fed with high-fat high sucrose diet (mean \pm SEM)

While there was no significant difference in total distance traveled on the 16th week between groups, on the 11th week, animals fed by both high fat, high sucrose diet, and with low fat diet traveled less than animals fed with normal chow ($p < 0.0001$, Holm-Sidak's multiple comparisons test) (Figure 22).

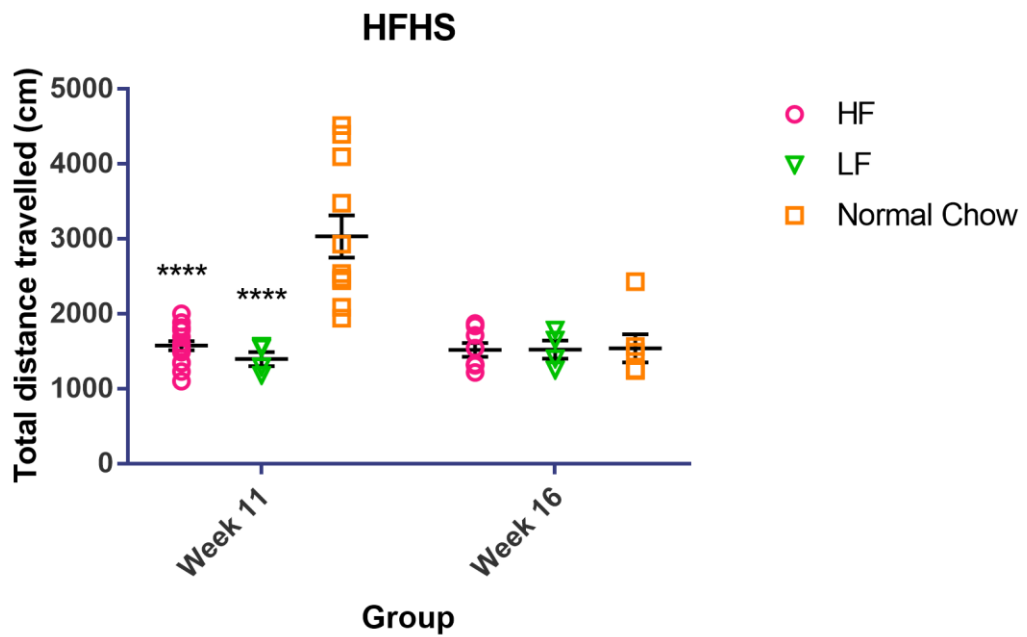


Figure 22. Total distance traveled in animals fed with high-fat high sucrose diet at weeks 11 and 16 (mean ± SEM)

Comparison of total distance travelled of the same animals between week 11 and 16 was only significant in NC fed group ($p = 0.0007$, two tailed paired t-test).

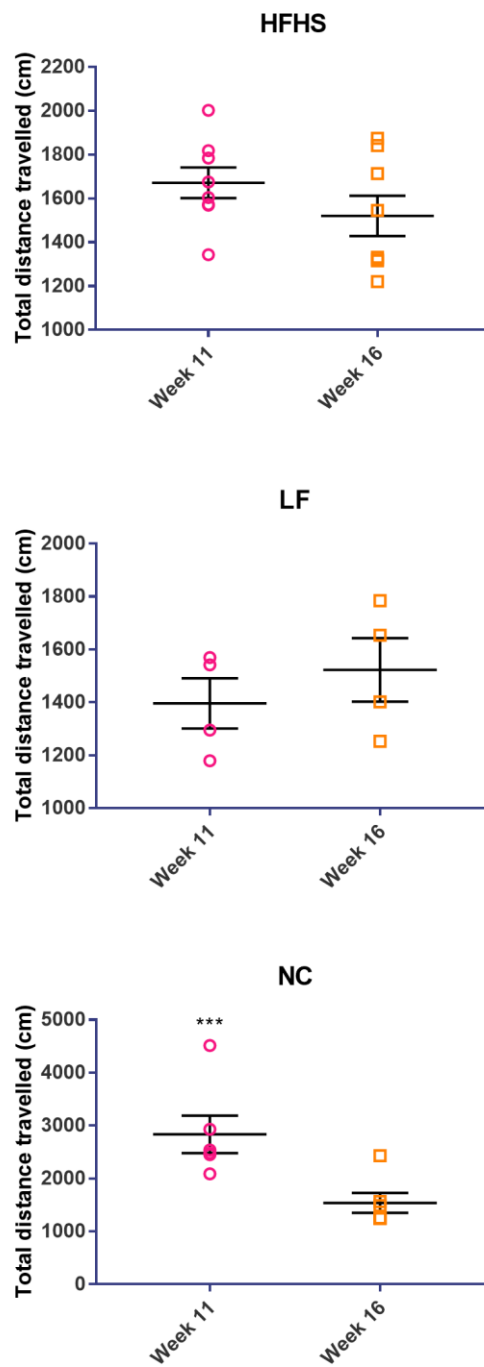


Figure 23. Total distance travelled of the same animals between week 11 and 16 (mean \pm SEM)

The comparison of the percentage of time spent in central area for the same animals between week 11 and 16 were not significant (Figure 24).

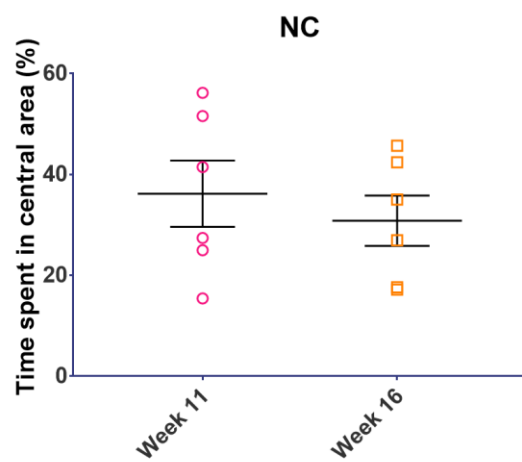
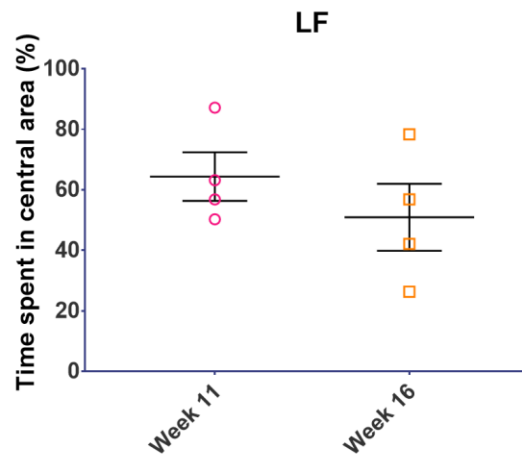
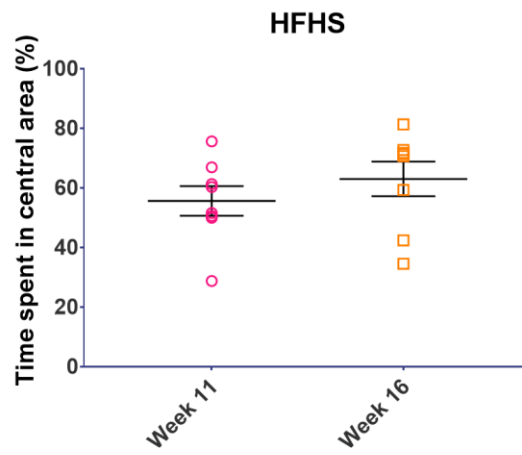


Figure 24. Percentage of time spent in the central area of the same animals between week 11 and 16 (mean \pm SEM)

3.2.2.1. Spontaneously Hypertensive Rats (SHRs)

On both 27th and 31st weeks, spontaneously hypertensive rats spent more time in the central area compared to Wistar control group ($p < 0.0001$, $p = 0.0021$ respectively, Holm-Sidak's multiple comparisons test), suggesting a decline of anxiety in these animals (Figure 25). Furthermore, a two-way ANOVA test suggested an overall increase in time spent in the central area in spontaneously hypertensive rats ($p < 0.0001$), further supporting the decline of anxiety.

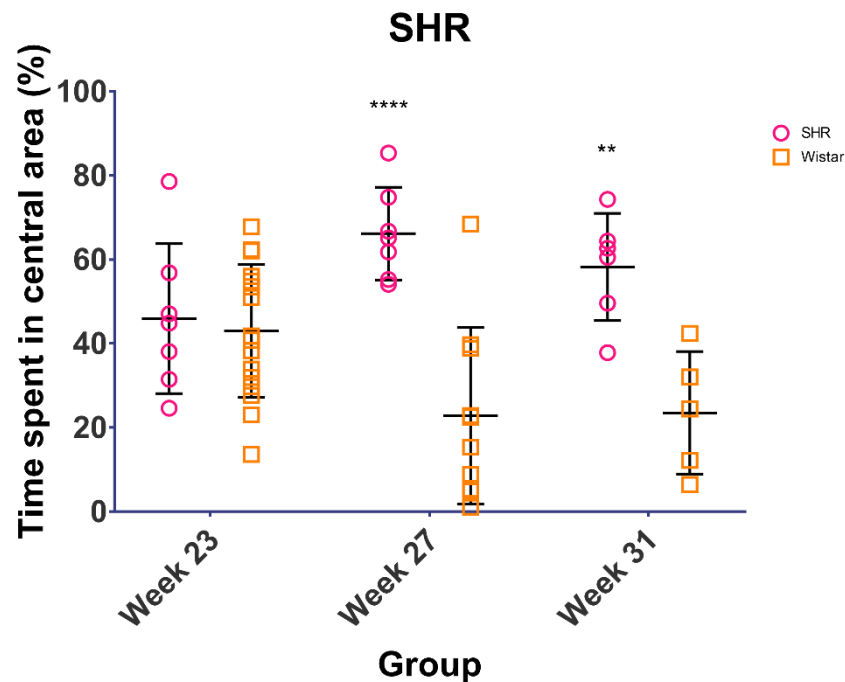


Figure 25. Time spent in central area in spontaneously hypertensive rats (mean \pm SEM)

While there was no significant difference in total distance traveled on any single week, when all three weeks are compared, spontaneously hypertensive rats traveled more distance than the control group. ($p = 0.0453$, two-way ANOVA) (Figure 26).

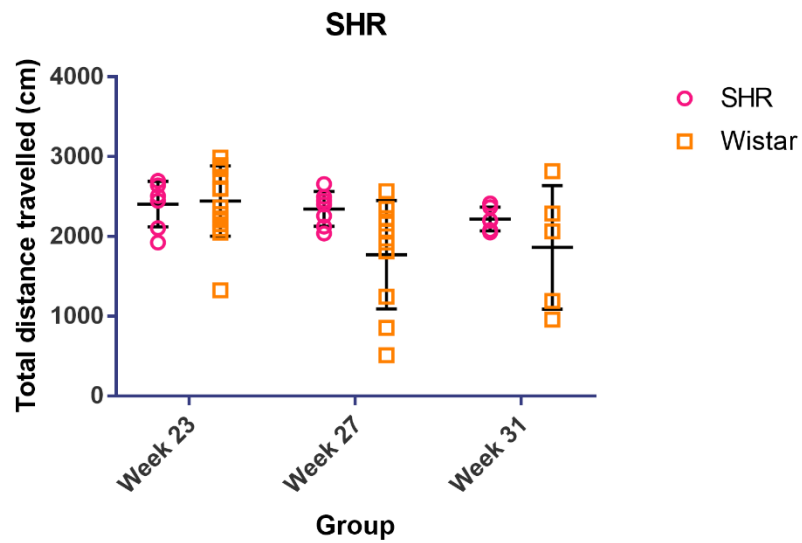


Figure 26. Total distance traveled in spontaneously hypertensive rats and control group Wistar rats at weeks 23, 27 and 31(mean ± SEM)

3.2.3. Y-Maze Spontaneous Alternation Test

3.2.3.1. *Streptozotocin-Induced T1DM Animal Model*

Spontaneous alternation rates were similar and the difference was not significant ($p = 0.9630$, two-tailed t-test) for streptozotocin-induced type 1 diabetic mice in the Y-maze (Figure 27), and there was no significant correlation between spontaneous alternation rates and total distance traveled or time spent in central area in both groups.

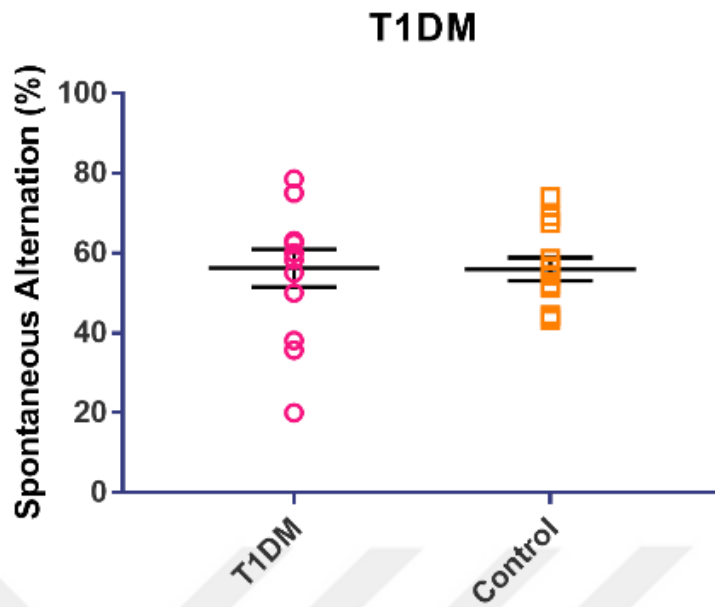


Figure 27. Spontaneous alternation in Streptozotocin-induced type 1 diabetic mice (mean \pm SEM)

3.2.3.2. T2DM (HFHS animal model)

Spontaneous alternation rates of animals fed with high-fat high-sucrose diet were surprisingly higher when compared to animals fed with a normal chow diet ($p = 0.0140$, two-way ANOVA), but there was no significant increase on individual weeks ($p = 0.1451$, $p = 0.0593$, Holm-Sidak's multiple comparisons test) (Figure 28).

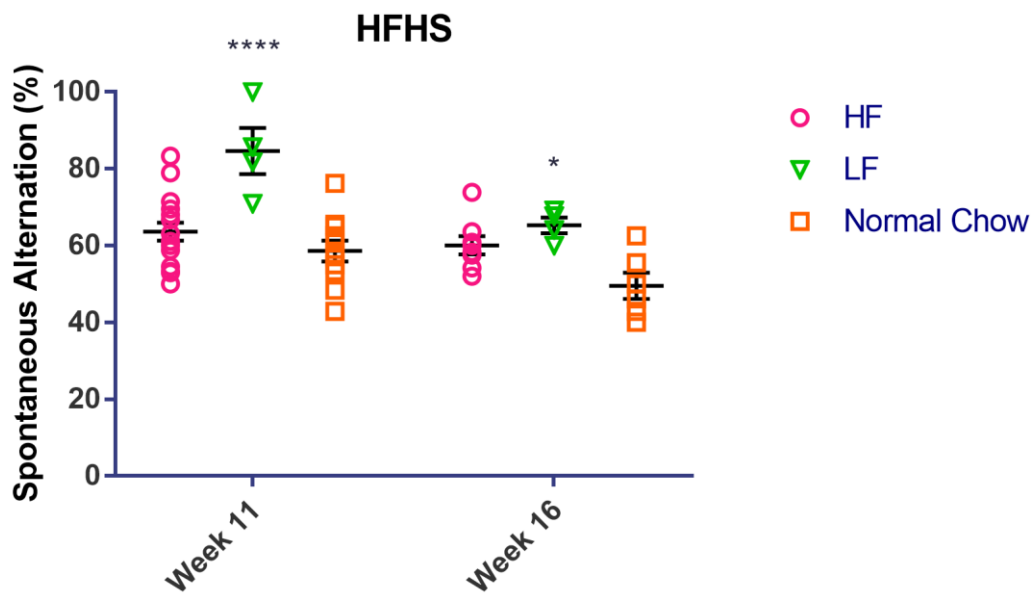


Figure 28. Spontaneous alternation rates in animals fed with high-fat high sucrose diet (mean \pm SEM)

Spontaneous alternation rates were even higher in animals fed with low-fat chow on both weeks ($p < 0.0001$ on week 11 and $p = 0.0226$ on week 16 when compared with normal chow diet, Holm-Sidak's multiple comparisons test). While the rate for the all group decreased on the 16th week, the only significant decrease was in the low-fat group ($p = 0.0091$, Holm-Sidak's multiple comparisons test).

Regression analysis showed no significant correlation between spontaneous alternation rates and total distance traveled or time spent in central area in any of the groups on both weeks.

The comparison of spontaneous alternation rates for same animals between week 11 and 16 was only significant for LF fed group ($p = 0.0219$, two-tailed paired t-test) (Figure 29).

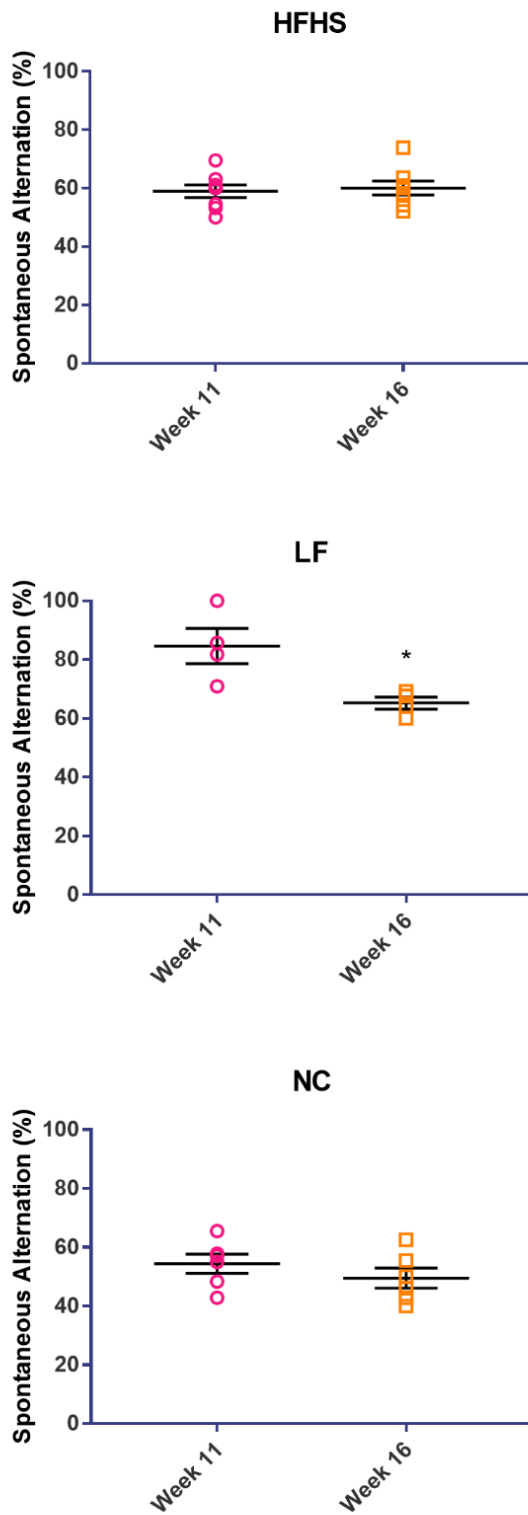


Figure 29. Spontaneous alternation rates of same animals between week 11 and 16 (mean \pm SEM)

3.2.3.3. Spontaneously Hypertensive Rats (SHRs)

Spontaneous alternation rates for SHRs were lower than the control group at weeks 23, 27 and 31 (Figure 30), however, the difference was not statistically significant ($p = 0.4626, 0.4626, 0.3257$, respectively, Holm-Sidak's multiple comparisons test).

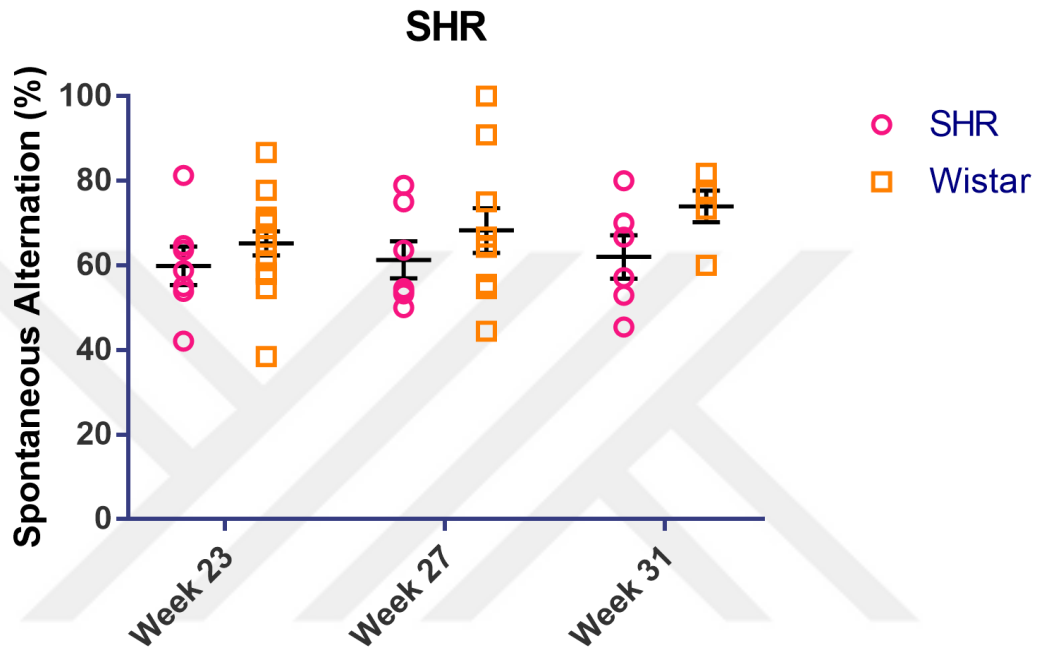


Figure 30. Spontaneous alternation in spontaneously hypertensive rats in week 23, 27 and 31 (mean \pm SEM)

However, a 2-way ANOVA of the data revealed a statistically significant difference between SHRs and the Wistar control group ($p = 0.0387$) (Figure 31).

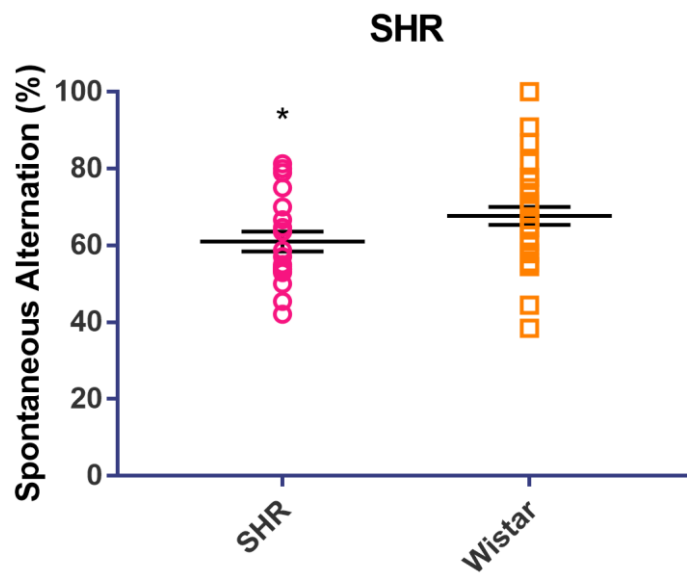


Figure 31. Spontaneous alternation in spontaneously hypertensive rats, age effect excluded (mean \pm SEM)

To assess if there is a trend in spontaneously alternation rates between weeks, trend analysis was performed, and there were no significant changes in SHR or Wistar group (Figure 32).

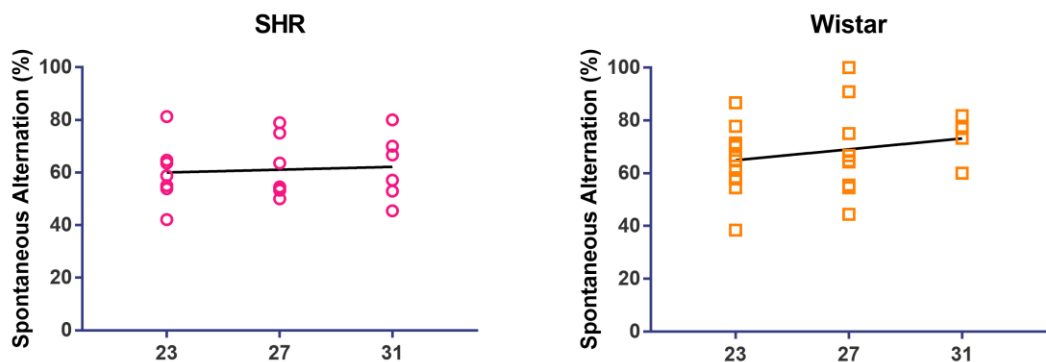


Figure 32. Trend analysis of spontaneous alternation rates in SHRs and Wistar rats from week 23 to 31.

3.2.4. Novel Object Recognition Test

3.2.4.1. Streptozotocin-Induced T1DM Animal Model

Novel object recognition scores (calculated by dividing the time spent

exploring the novel object to the total exploration time of both objects) were similar and the difference was not significant ($p = 0.8404$, two-tailed Student's t-test) for streptozotocin-induced type 1 diabetic mice in the novel object recognition test (Figure 33).

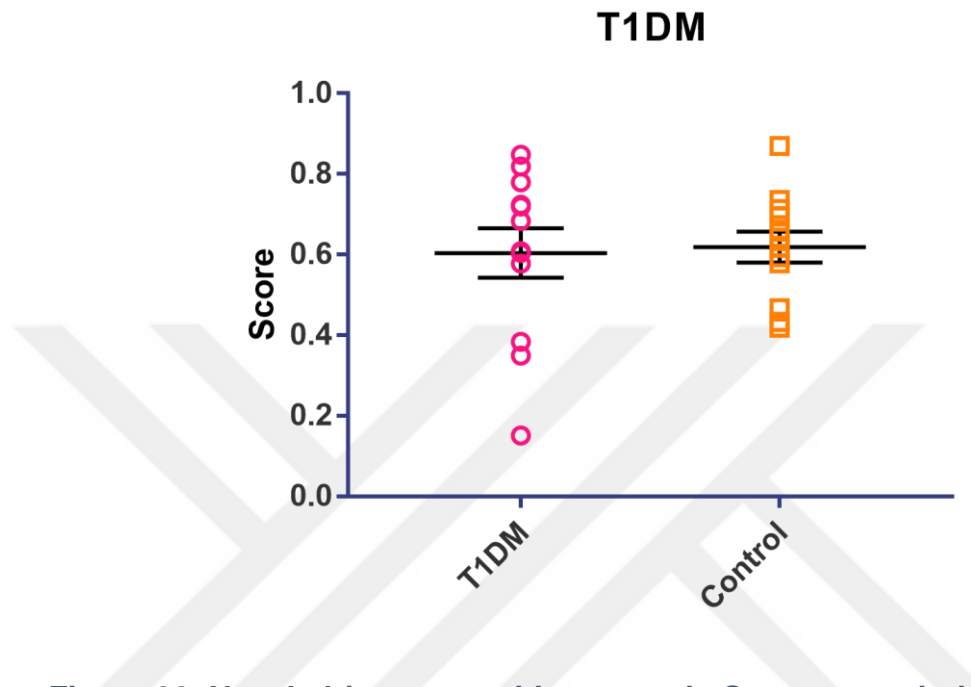


Figure 33. Novel object recognition score in Streptozotocin-induced type 1 diabetic mice (mean \pm SEM)

The percentage of time spent exploring the novel object is also calculated, but there was no significant difference between T1DM and control group (Figure 34).

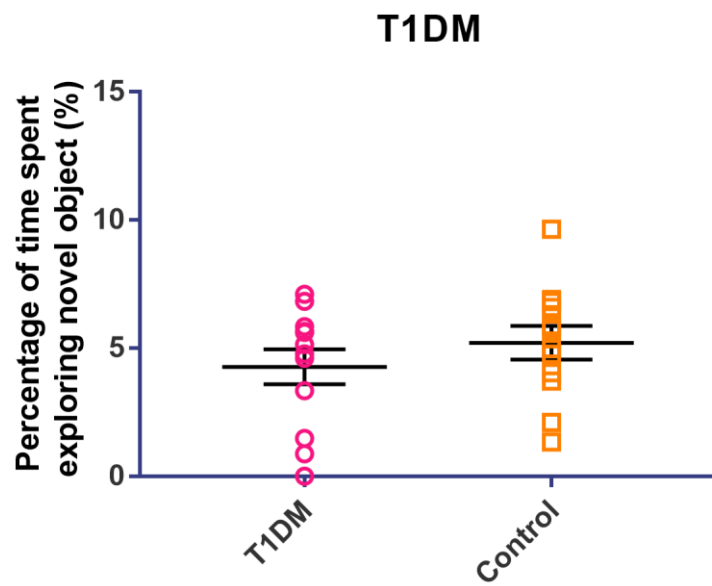


Figure 34. The percentage of time spent exploring the novel object in T1DM and control group.

Additionally, the total exploration time for these groups were also similar ($p = 0.8404$, two-tailed Student's t-test) (Figure 35).

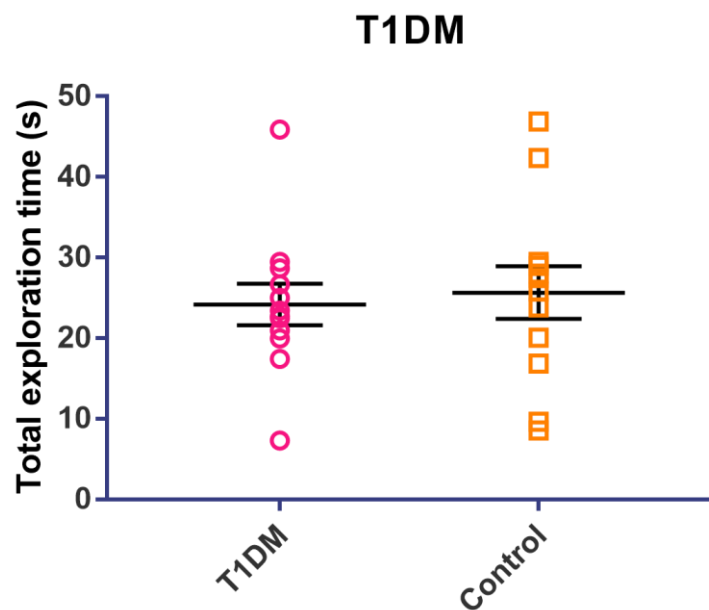


Figure 35. Total object exploration time in Streptozotocin-induced type 1 diabetic mice (mean \pm SEM)

3.2.4.2. T2DM (HFHS animal model)

Novel object recognition scores were similar and the difference was neither significant at 11th ($p = 0.4847$, one-way ANOVA) or 16th weeks ($p = 0.2837$, one-way ANOVA), nor was it significant in the overall ($p = 0.3204$, two-way ANOVA test) (Figure 36).

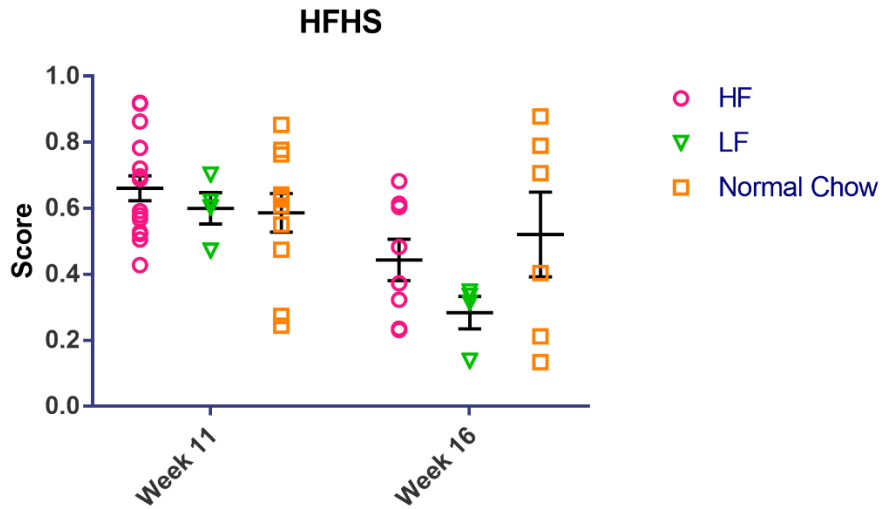


Figure 36. Novel object recognition scores in animals fed with high-fat high sucrose diet (mean \pm SEM)

Comparison of novel object recognition scores of the same animals between week 11 and 16 showed significant decrease in both HFHS and LF fed animals, while NC group established no significant difference ($p = 0.0299$ in HFHS group, $p = 0.0004$ in LF group, two tailed paired t-test) (Figure 37).

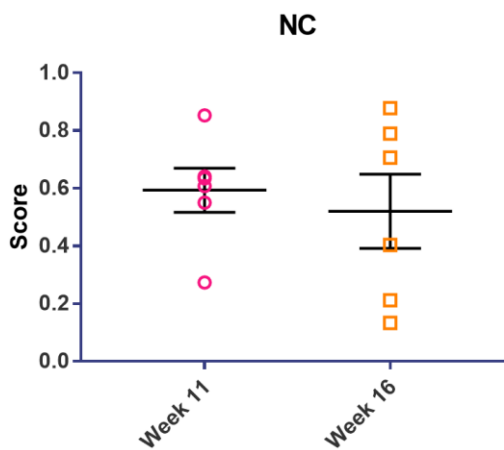
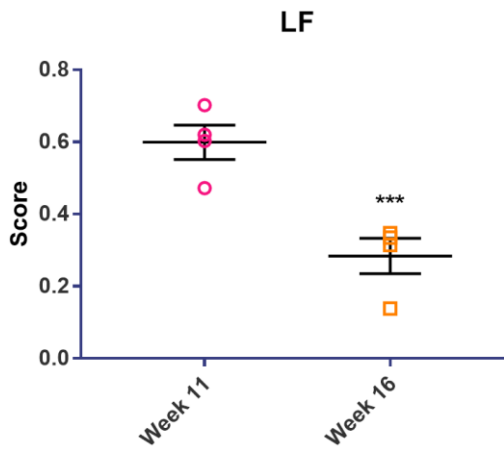
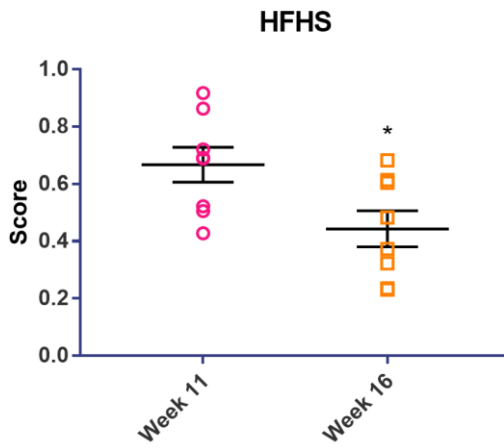


Figure 37. Novel object recognition scores of the same animals in HFHS animal group between week 11 and 16 (mean \pm SEM)

However, if the percentage of time spent exploring the novel object is calculated, LF group has significantly higher score in week 11 when compared to same age NC fed group ($p= 0.0114$, Holm-Sidak's multiple comparisons test) (Figure 38).

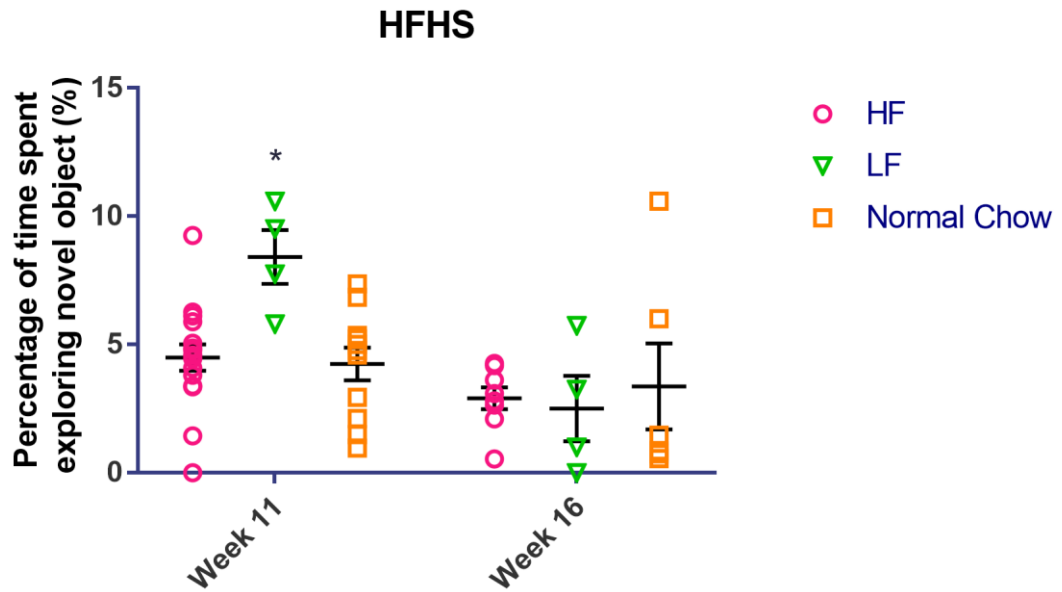


Figure 38. Percentage of time spent exploring the novel object in HFHS, LF and NC fed mice in week 11 and 16.

When the percentage of time spent exploring the novel object data of the same animals is compared between weeks 11 and 16, LF fed group has a significant decrease ($p=0.0161$, paired t-test), while HFHS and NC fed animals have no statistically significant difference (Figure 39).

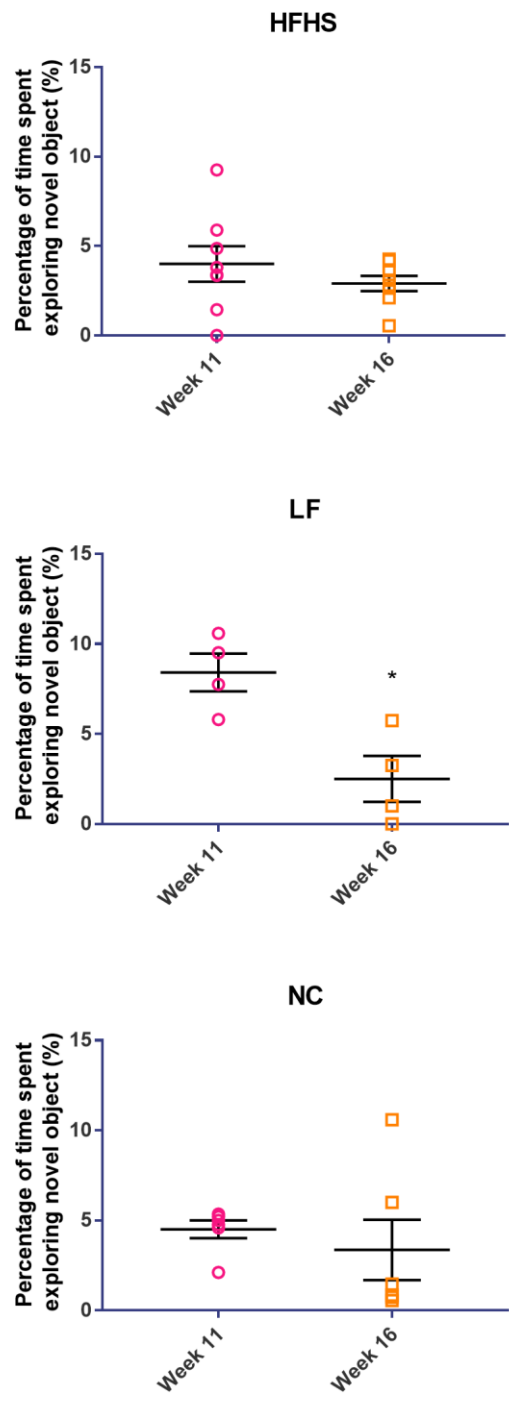


Figure 39. Percentage of time spent exploring the novel object of the same animals between week 11 and 16.

However, the total exploration time for the low-fat group was significantly higher on both week 11 ($p = 0.0275$, Holm-Sidak's multiple comparisons test) and week 16 ($p = 0.0444$, Holm-Sidak's multiple comparisons test) (Figure 40).

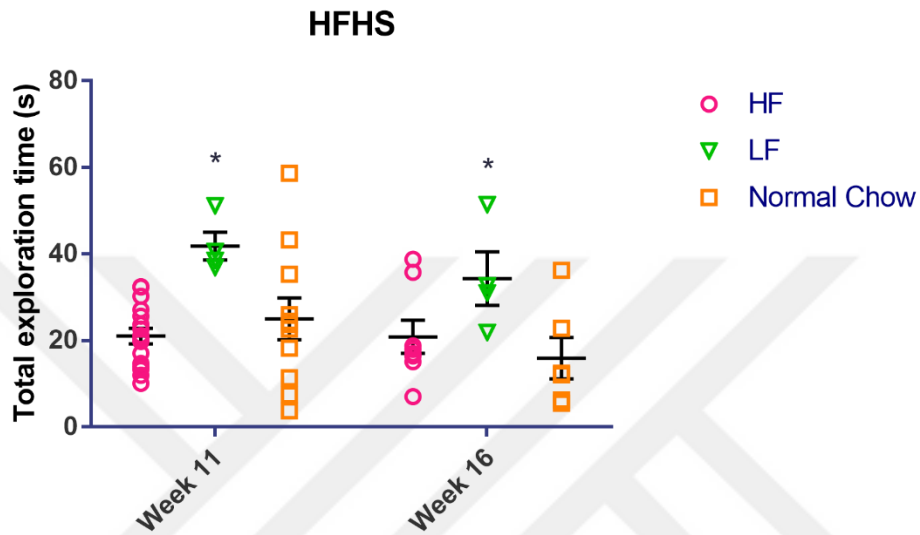


Figure 40. Total object exploration time in animals fed with high-fat high sucrose diet (mean \pm SEM)

Total exploration time of the same animals between week 11 and 16 showed no significant difference (Figure 41).

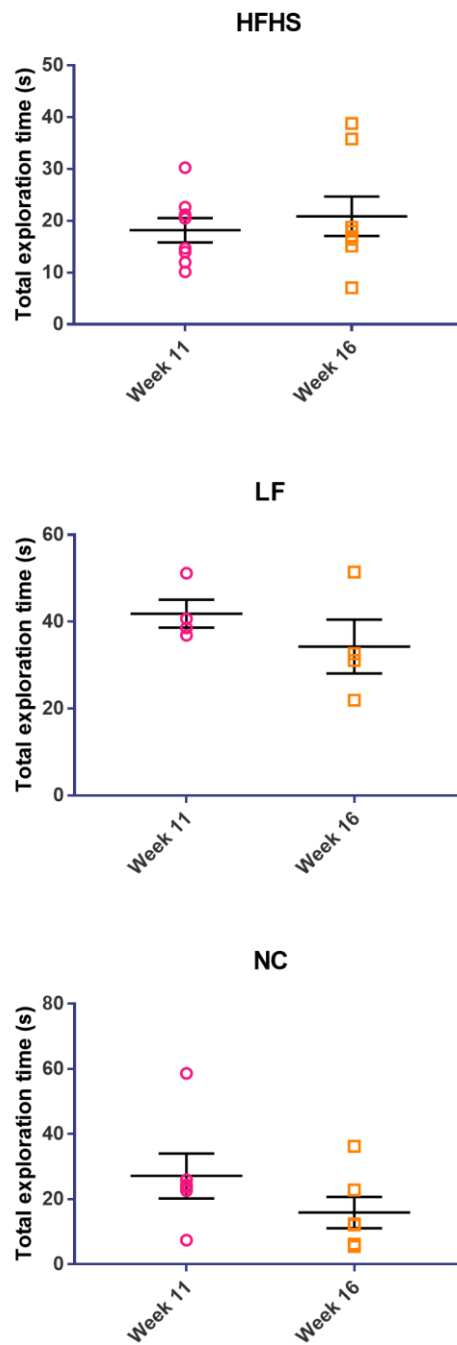


Figure 41. Total exploration time of the same animals in HFHS animal group between week 11 and 16 (mean \pm SEM)

3.2.4.3. Spontaneously Hypertensive Rats (SHRs)

Novel object recognition scores were similar and the difference was neither significant at any week, and $p = 0.9573, 0.4953, 0.9573$ for weeks 23, 27 and 31, Holm-Sidak's multiple comparisons test) nor was it significant in the overall ($p = 0.3242$, two-way ANOVA test) (Figure 42).

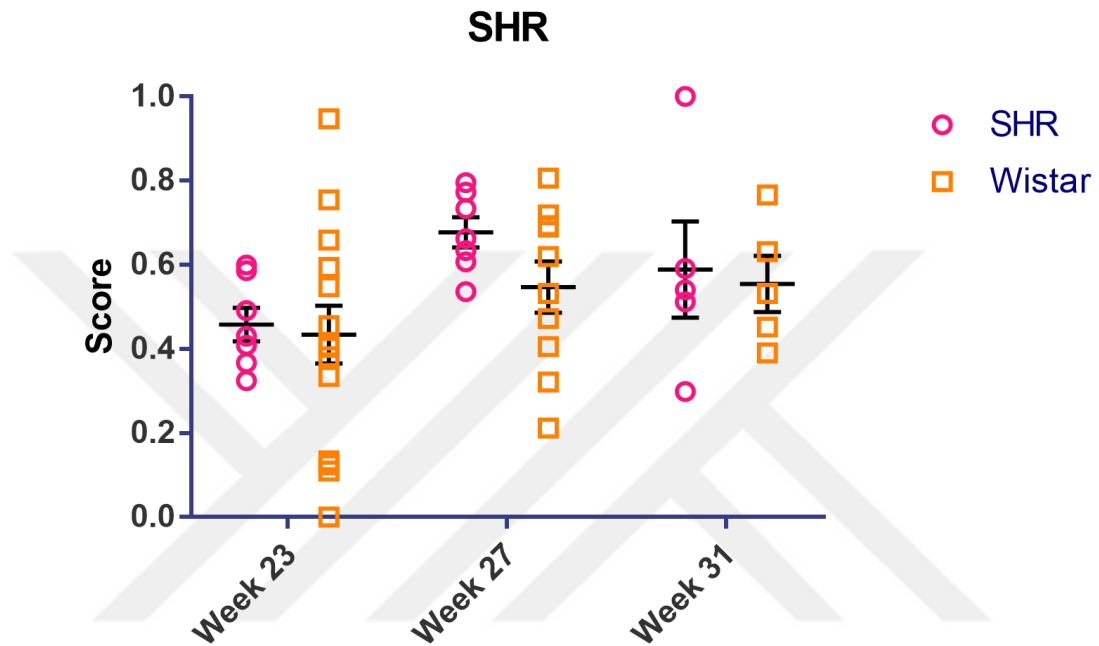


Figure 42. Novel object recognition score in spontaneously hypertensive rats (mean \pm SEM)

However, if the percentage of time spent exploring the novel object is calculated, SHR group in week 27 has significantly higher scores when compared to same age Wistar rat group ($p = 0.0073$, Holm-Sidak's multiple comparisons test). The data on other two time points are statistically insignificant (Figure 43).

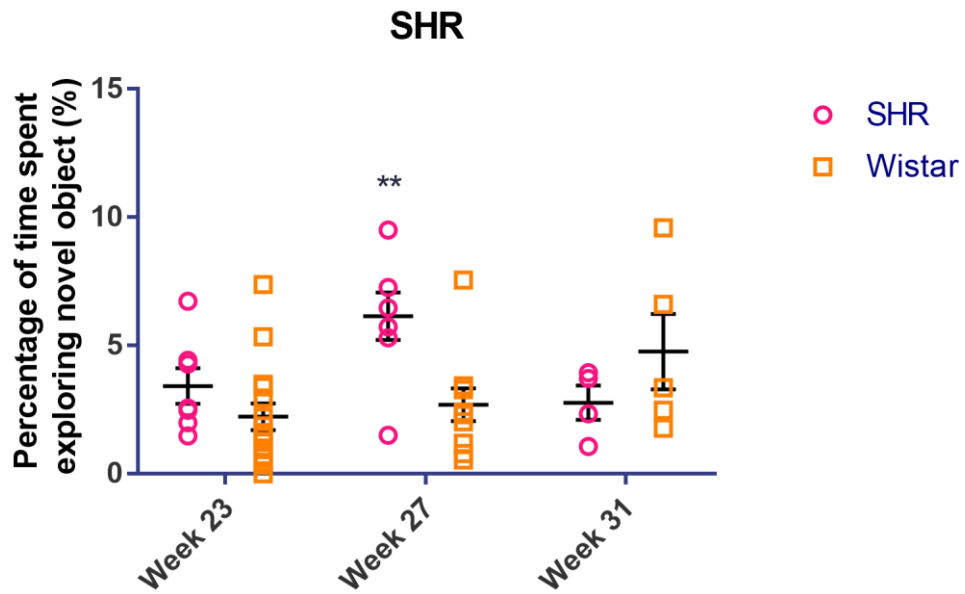


Figure 43. Percentage of time spent exploring novel object of SHRs and their Wistar control groups in weeks 23, 27, and 31.

When trend analysis is performed, there is a significant increase in the percentage of time spent exploring novel object in Wistar control group from week 23 to 31 ($p=0.0377$, trend analysis following one-way ANOVA) (Figure 44). The trend analysis for Novel Object Recognition Test Scores showed no statistically significant difference (Figure 45).

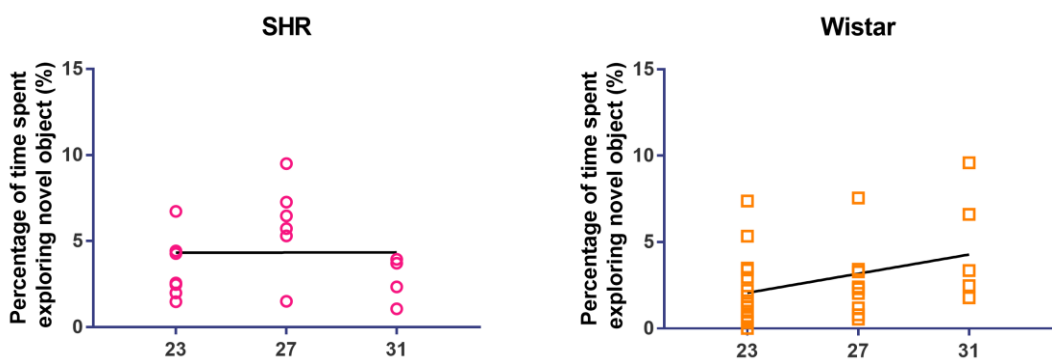


Figure 44. Trend analysis for the percentage of time spent exploring novel object of SHRs and Wistar control group rats from week 23 to 31.

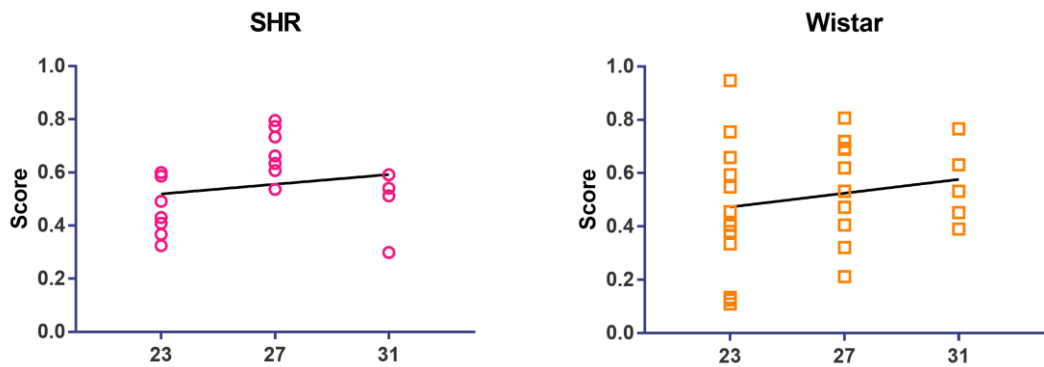


Figure 45. Trend analysis for novel object recognition test scores of SHRs and Wistar control group rats from week 23 to 31.

However, the total exploration time for the SHR group was significantly higher than Wistar control group on week 27 ($p = 0.0040$, Holm-Sidak's multiple comparisons test), but there were no significant differences on week 23 ($p = 0.1199$) or week 31 ($p = 0.1199$) (Figure 46).

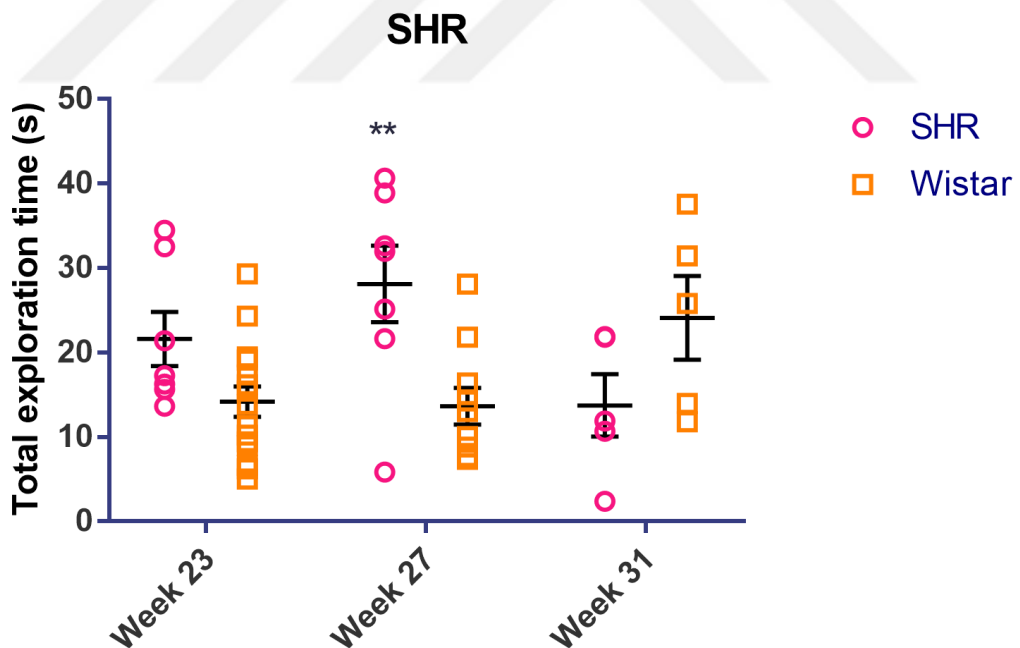


Figure 46. Total object exploration time in spontaneously hypertensive rats (mean ± SEM)

When trend analysis is performed, there is a significant increase in the total

exploration time in Wistar control group from week 23 to 31 ($p= 0.0187$, trend analysis following one-way ANOVA)

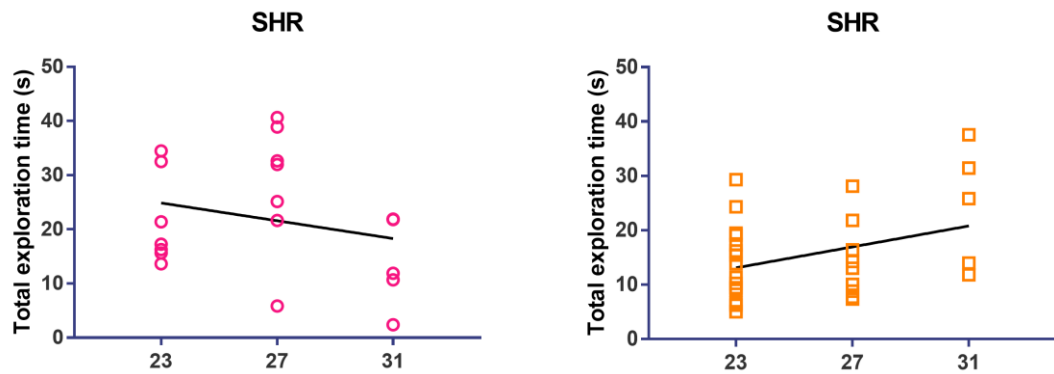


Figure 47. Trend analysis for total exploration time of SHRs and Wistar control group rats from week 23 to 31.

3.3. 3D imaging and Visualization of Microcirculation

In maximum projection and 3D reconstructed 3DISCO images, we can see that T1DM animals have lesser amounts of smaller vessels, which suggests a decline in microcirculatory vessels (Figure 48).

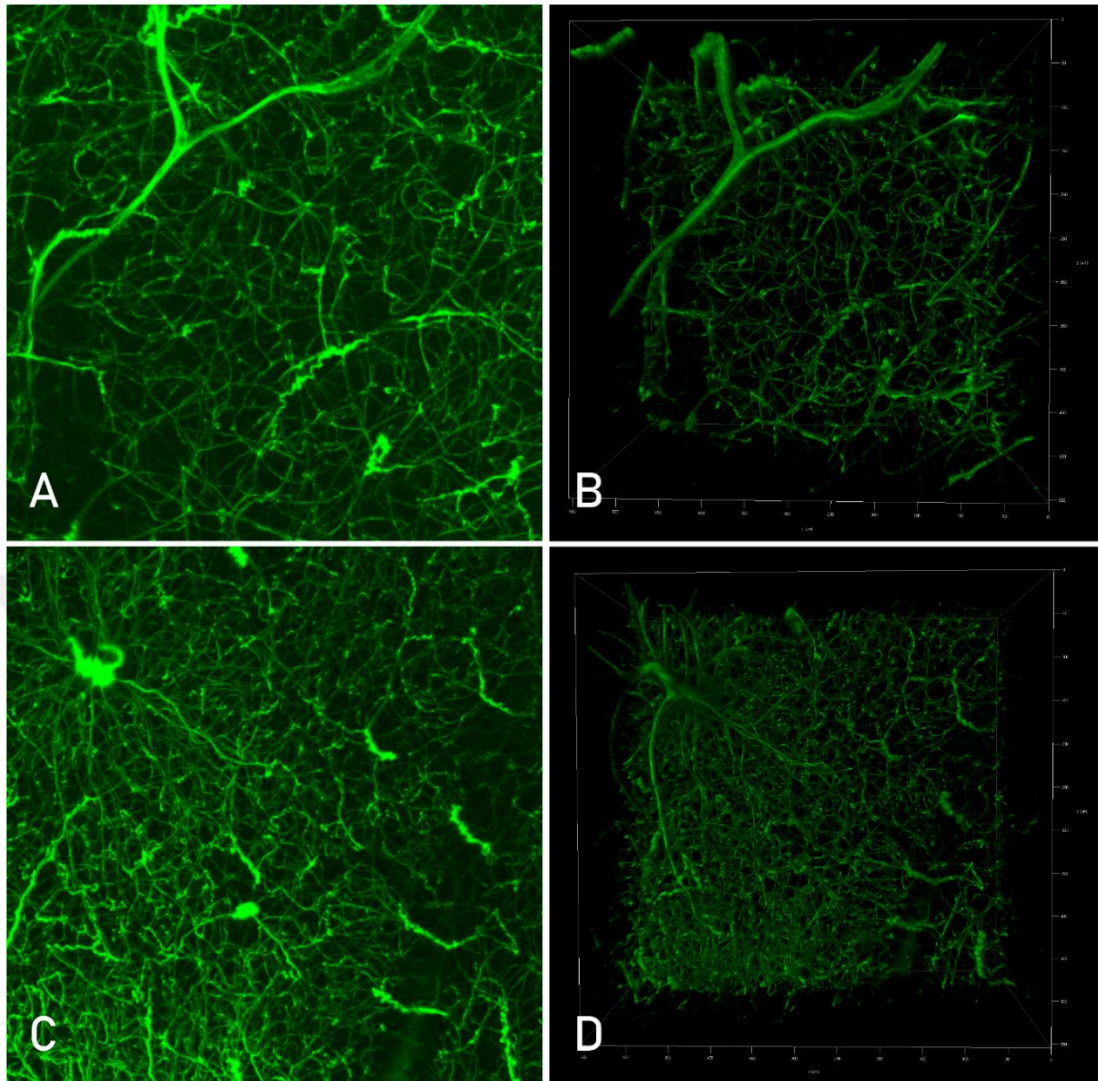


Figure 48. T1DM animal group maximum projection and 3D reconstruction 3DISCO images, respectively. Images A and B show the microcirculation of STZ induced T1DM animal, while images C and D show microcirculation of a control group animal.

In maximum projection and 3D reconstructed 3DISCO images, we can see that HFHS fed animal have decreased amounts of microcirculatory vessels, while LF fed animal's microcirculation density does not seem to be dramatically different from the NC fed control group animal's (Figure 49).

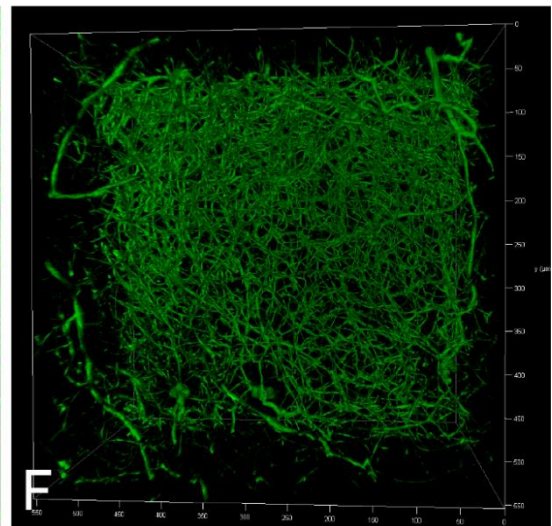
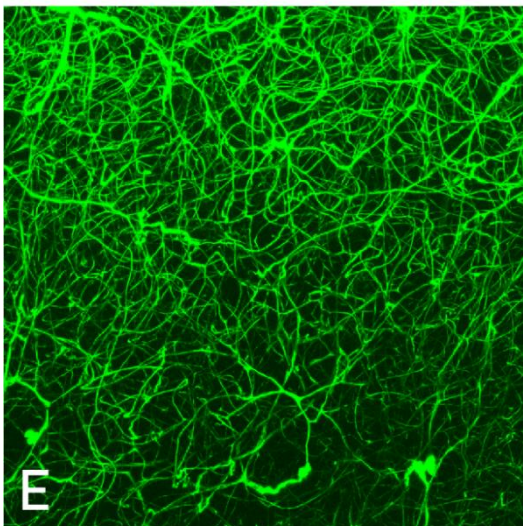
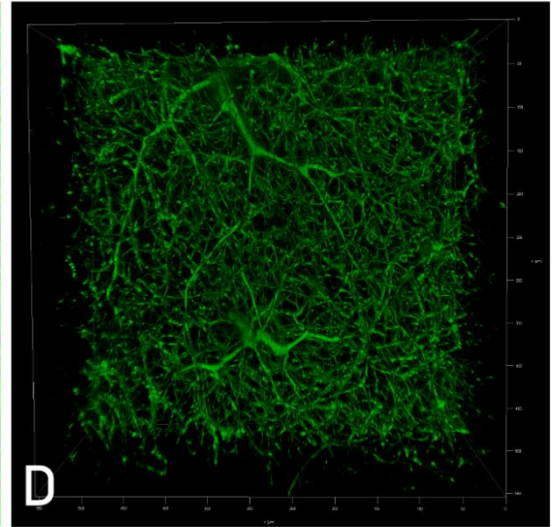
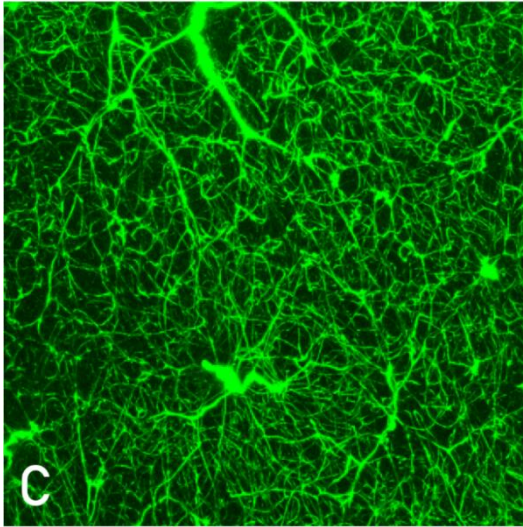
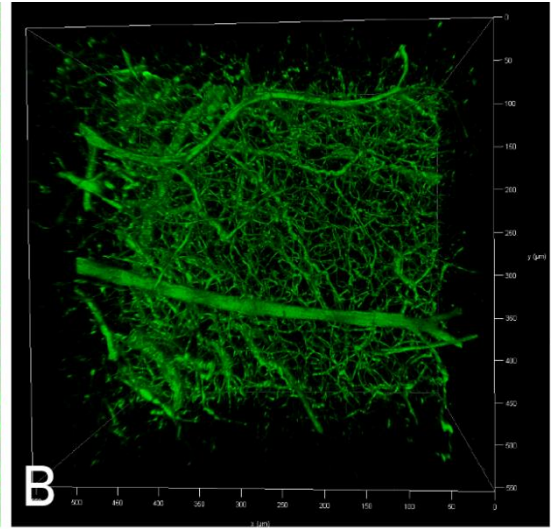
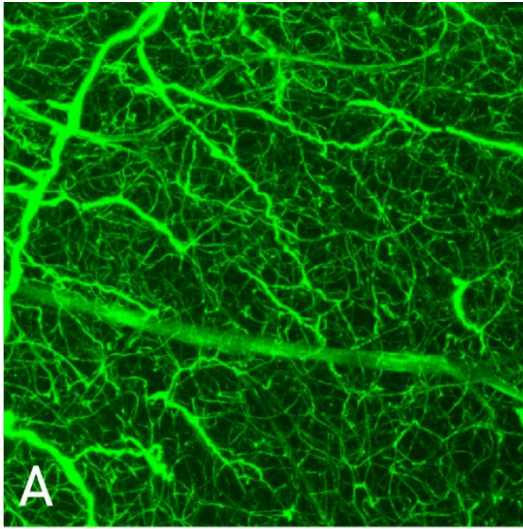


Figure 49. 16-week HFHS animal group maximum projection and 3D reconstruction 3DISCO images, respectively. Images A and B show the microcirculation of a HFHS fed animal; images C and D show the microcirculation of a LF fed animal, and images E and F show the microcirculation of a NC fed control group animal.

3.4. Quantification of capillaries, pericytes and collagen 1 expression levels

3.4.1. Quantification of capillaries

The percentage of isolectin positive areas in parietotemporal cortex were significantly lower in T1DM group compared to its control group ($p=0.0001$), suggesting a probable decline in vascular density (Figure 50). Immunofluorescence staining images are shown in Figure 51.

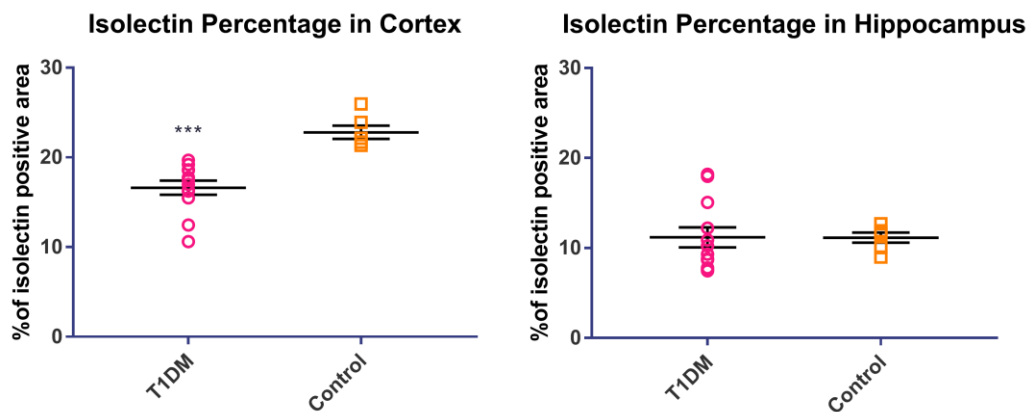


Figure 50. Percentage of isolectin positive areas in parietotemporal cortex and hippocampus for T1DM and control group.

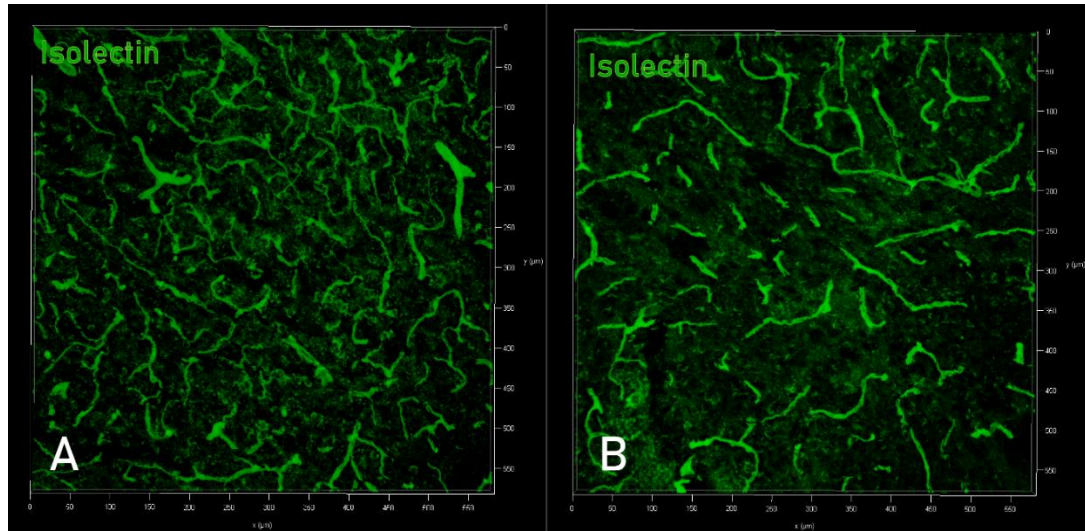


Figure 51. Isolectin B4 immunofluorescence staining of parietotemporal cortex in (A) control and (B) T1DM animals.

The percentage of isolectin positive areas in parietotemporal cortex were significantly higher in HFHS fed group compared to NC control group at both time points ($p < 0.0001$ at week 11, two tailed Student's t-test; $p = 0.0299$ at week 16, Tukey's multiple comparisons test following one-way ANOVA), suggesting endothelial proliferation due to metabolic defects. Additionally, isolectin positive areas in hippocampus were also increased in HFHS group compared to NC fed group ($p = 0.0006$ at week 11, two tailed Student's t-test; $p = 0.0129$ at week 16, Tukey's multiple comparisons test following one-way ANOVA), whereas the LF fed group at week 16 showed highest ratio of isolectin positivity ($p = 0.0003$, Tukey's multiple comparisons test following one-way ANOVA) (Figure 52). The hippocampal isolectin positivity rates show similar patterns to the outcomes of Y maze spontaneous alternation test results, further suggesting the decline in working memory due to hippocampal vascular changes. Immunofluorescence staining images are shown in Figure 53.

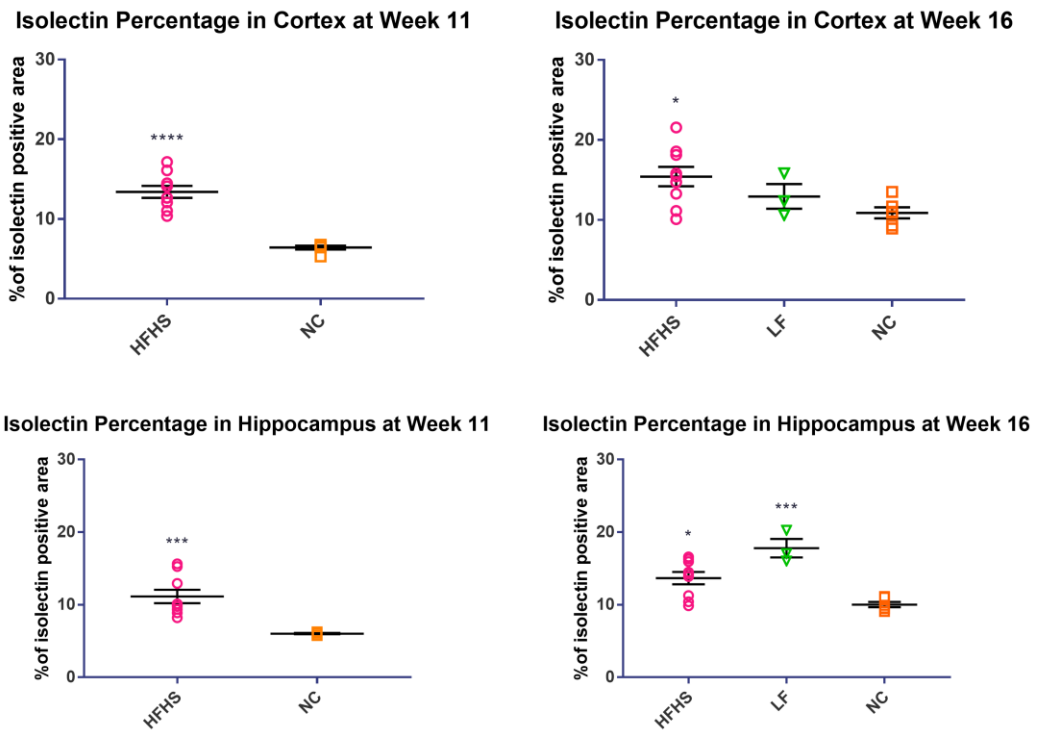


Figure 52. Percentage of isolectin positive areas in parietotemporal cortex and hippocampus for HFHS, LF, and NC fed groups at week 11 and week 16.

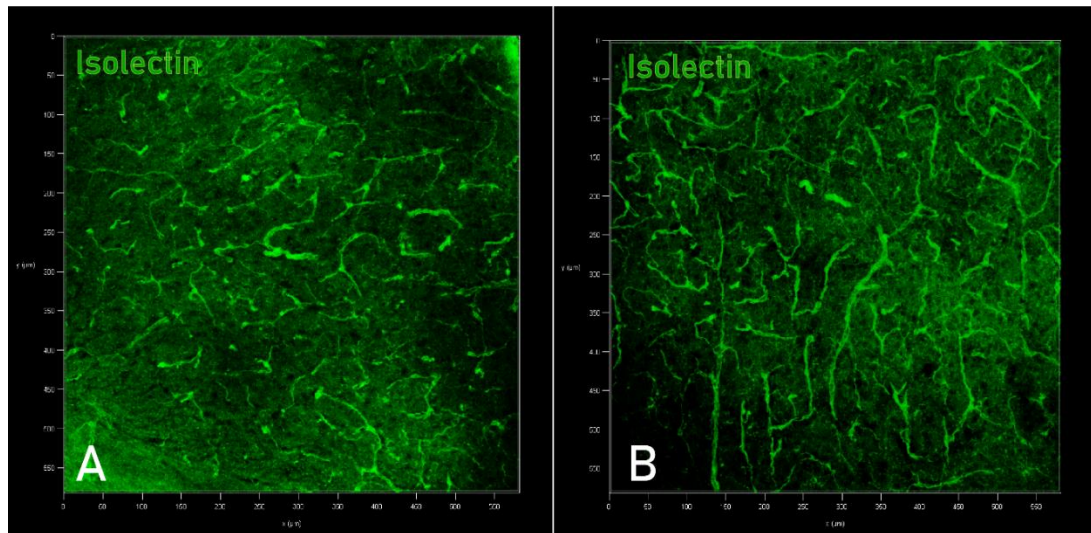


Figure 53. Isolectin B4 immunofluorescence staining of parietotemporal cortex in (A) NC fed and (B) HFHS fed animals.

While there is a decline in the isolectin positive vessel percentage in

hippocampus at week 23 ($p=0.0496$, two tailed Student's t-test) and an increase in week 31 ($p=0.0496$, two tailed Student's t-test), there are no significant changes in isolectin positivity in SHRs in cortical and hippocampal regions (Figure 54).

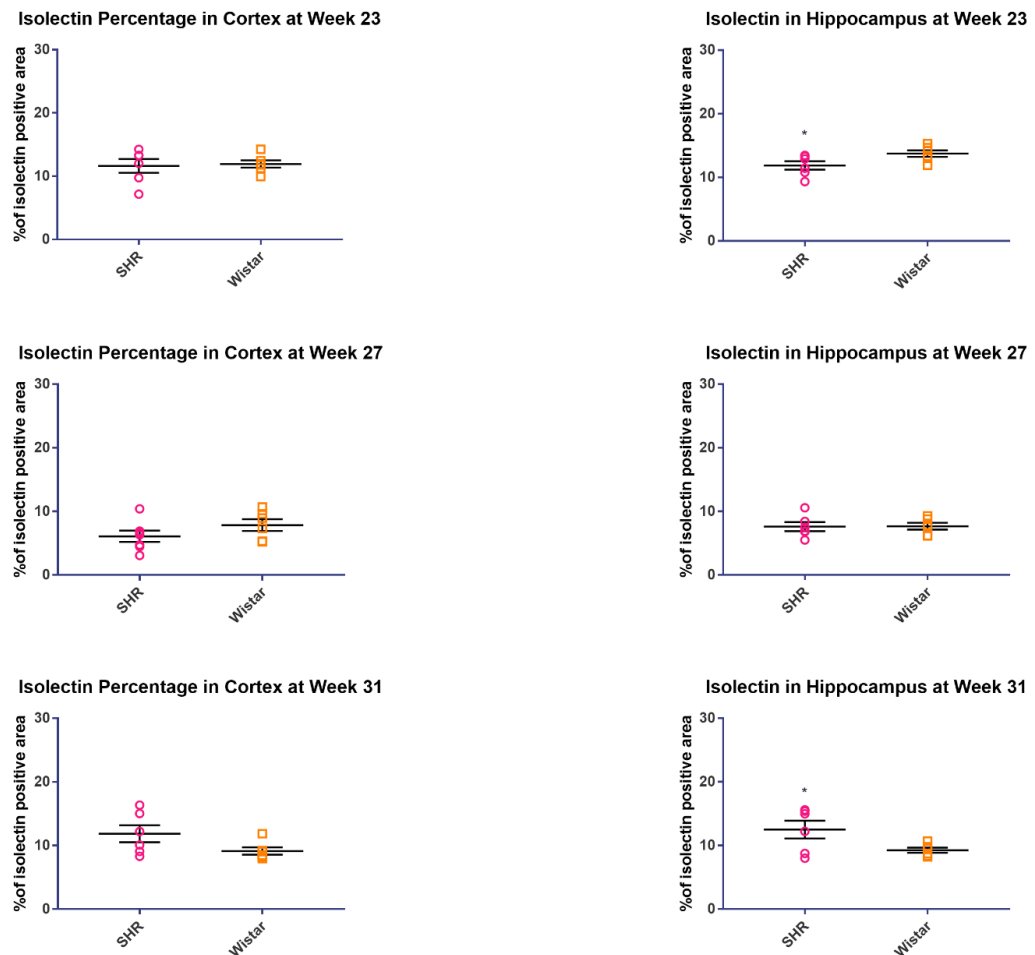


Figure 54. Percentage of isolectin positive areas in parietotemporal cortex and hippocampus for SHRs and Wistar control groups at weeks 23, 27, and 31.

However, when trend analysis is performed, there is a significant decrease in isolectin positive area percentage in both hippocampus ($p<0.0001$, trend analysis following one-way ANOVA) and parietotemporal cortex ($p=0.0145$, trend analysis following one-way ANOVA) of Wistar control groups from week 23 to week 31 (Figure 55).

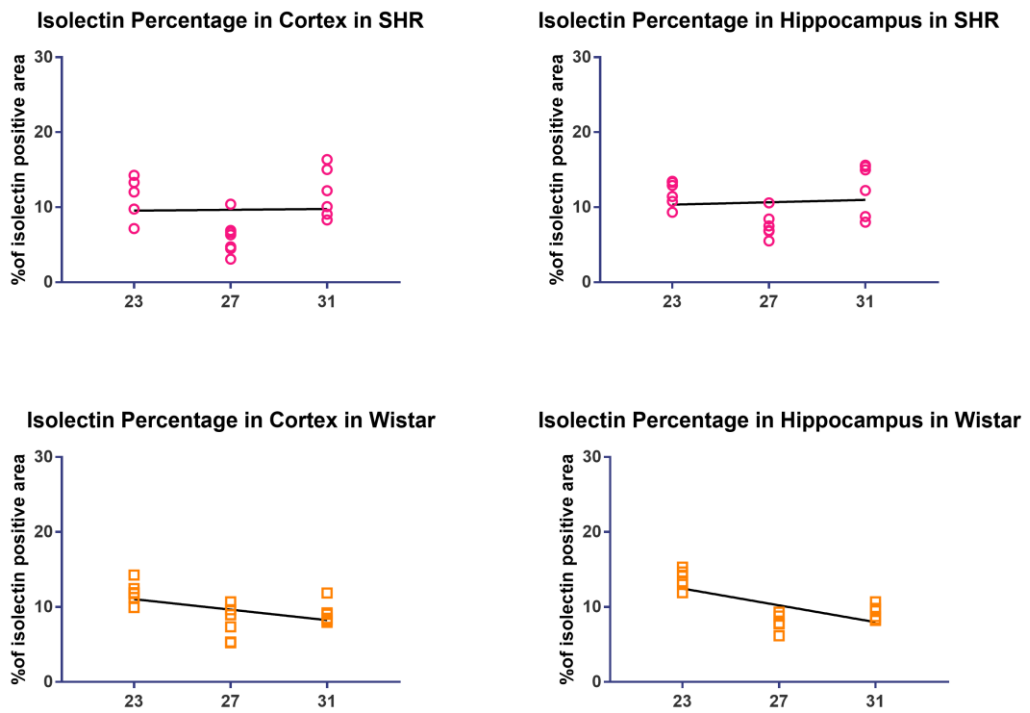


Figure 55. Trend analysis of isolectin positive area percentage in SHRs and Wistar rats from week 23 to 31.

Immunofluorescence staining images are shown in Figure 56.

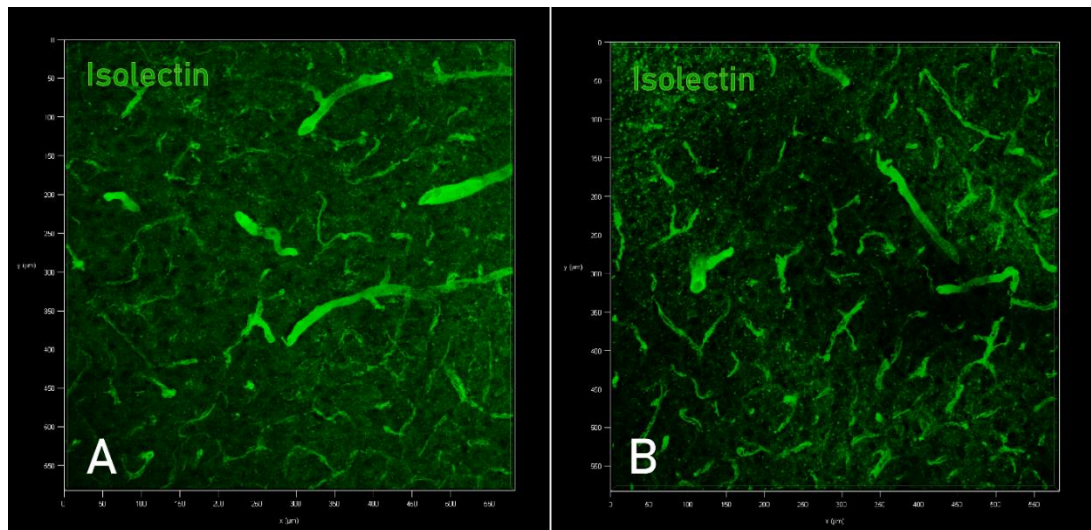


Figure 56. Isolectin B4 immunofluorescence staining of parietotemporal cortex in 23-week-old (A) Wistar control group and (B) SHR animals.

Two-way ANOVA results revealed a significant difference in isolectin percentages between weeks in both parietotemporal cortex and hippocampus. However, no significant difference was observed between experimental groups (Figure 57).

Isolectin Percentage In Cortex		
Source of Variation	% of total variation	P value
Interaction	8.92	0.0665
Week	42.85	<0,0001
Group	0.1138	0.7852

Isolectin Percentage In Hippocampus		
Source of Variation	% of total variation	P value
Interaction	12.87	0.0086
Week	52.12	<0,0001
Group	0.563	0.4892

Figure 57. Two-way ANOVA results of isolectin percentages in SHR and Wistar rats.

3.4.2. Quantification of total numbers of pericytes and pericytes around vessels

Total number of pericytes in T1DM group is significantly increased compared to its control group ($p < 0.0001$, two tailed Student's t-test), whereas the percentage of pericytes around vessels is significantly decreased ($p < 0.0001$, two tailed Student's t-test) (Figure 58).

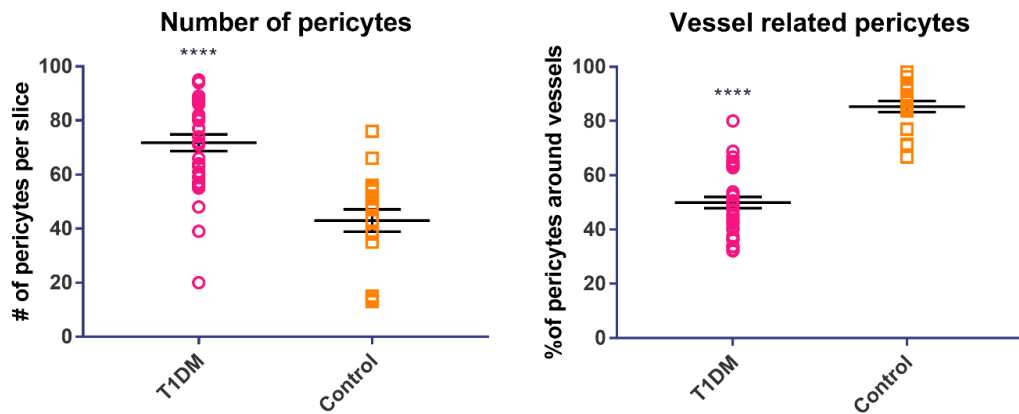


Figure 58. Pericyte count and location in T1DM and control group.

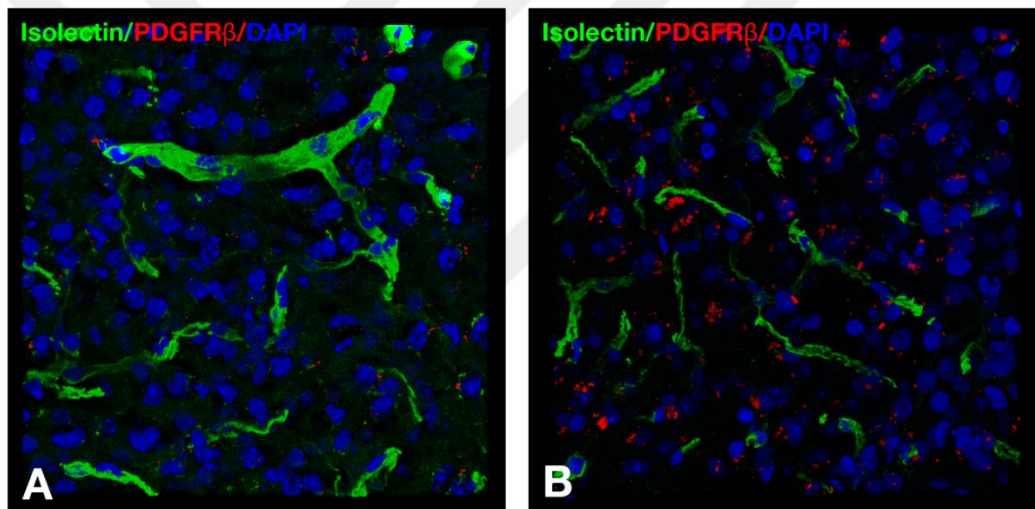


Figure 59. Double immunofluorescent staining showing PDGFR β and isolectin B4 expression in parietotemporal cortex of (A) control (B) T1DM animal group.

While total number of pericytes in HFHS group is not significantly different compared to NC fed control group at both time points ($p=0.1516$ at week 11, two tailed Student's t-test; $p=0.0589$ at week 16, Tukey's multiple comparisons test following one-way ANOVA), there is an increase in total pericyte count of LF fed animals in week 16 ($p=0.0472$, Tukey's multiple comparisons test following one-way ANOVA). On the other hand, the percentage of pericytes around vessels is significantly decreased in HFHS animals at week 11

($p=0.0016$, two tailed Student's t-test). However, the percentage of pericytes around vessels is significantly higher at week 16 for both HFHS ($p=0.0144$, Tukey's multiple comparisons test following one-way ANOVA) and LF ($p=0.0018$, Tukey's multiple comparisons test following one-way ANOVA) fed groups compared to NC animals (Figure 60).

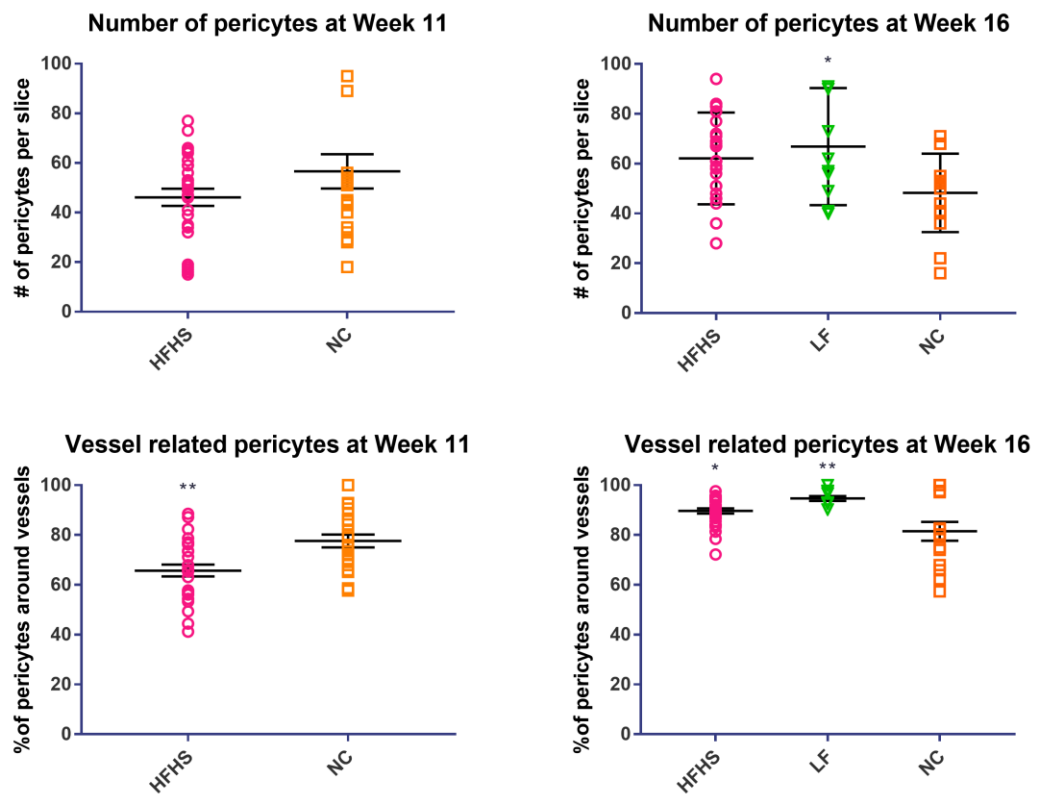


Figure 60. Pericyte count and location in HFHS, LF, and NC fed groups at weeks 11 and 16.

Total number of pericytes are increased in SHR on both week 23 ($p=0.03$, two tailed Student's t-test) and week 27 ($p=0.0006$, two tailed Student's t-test), while the difference is insignificant on week 31 ($p=0.1291$, two tailed Student's t-test). On the other hand, the percentage of vessel related pericytes were significantly decreased on weeks 23 ($p<0.0001$, two tailed Student's t-test) and 31 ($p<0.0001$, two tailed Student's t-test). (Figure 61).

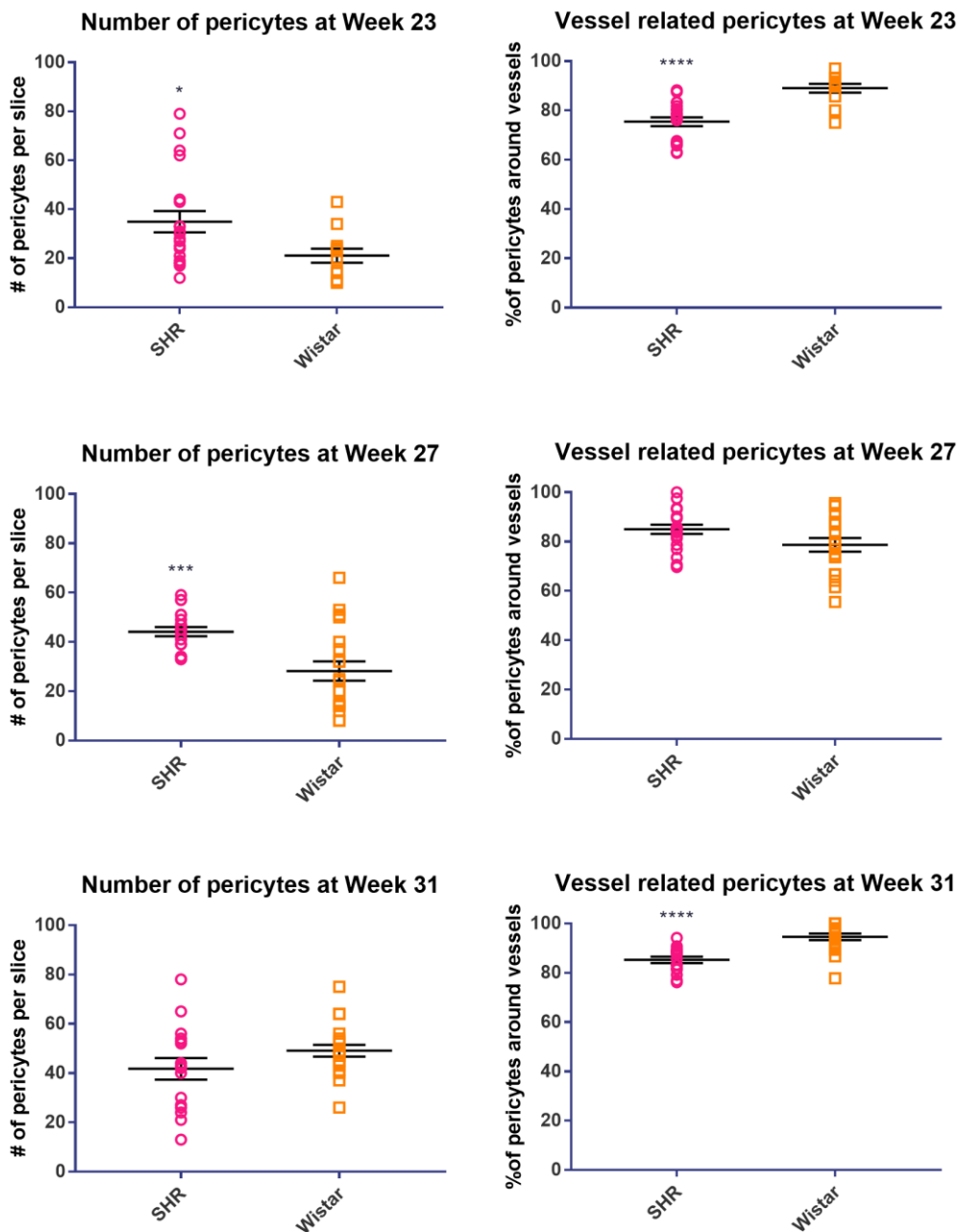


Figure 61. Pericyte count and location in SHR and Wistar control groups at weeks 23, 27 and 31.

3.4.3. Quantification of Collagen 1 expression levels by measuring mean pixel intensity

While there is an increase in average intensity of Col1 in T1DM mice, the difference is not statistically significant ($p = 0.1459$, two tailed Student's t-test)

(Figure 62).

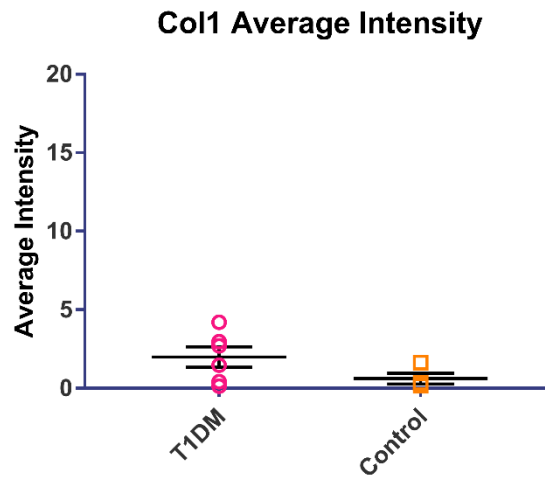


Figure 62. Collagen 1 (Col1) average pixel intensity in T1DM and control groups.

We also calculated the percentage of collagen 1 stained area to the total imaged area to support the intensity measurements. Although the trends in both graphics are quite similar, the percentage of col1 positive area is not significantly different between T1DM animals and their control group, supporting the average intensity data (Figure 63).

Col1 Percentage

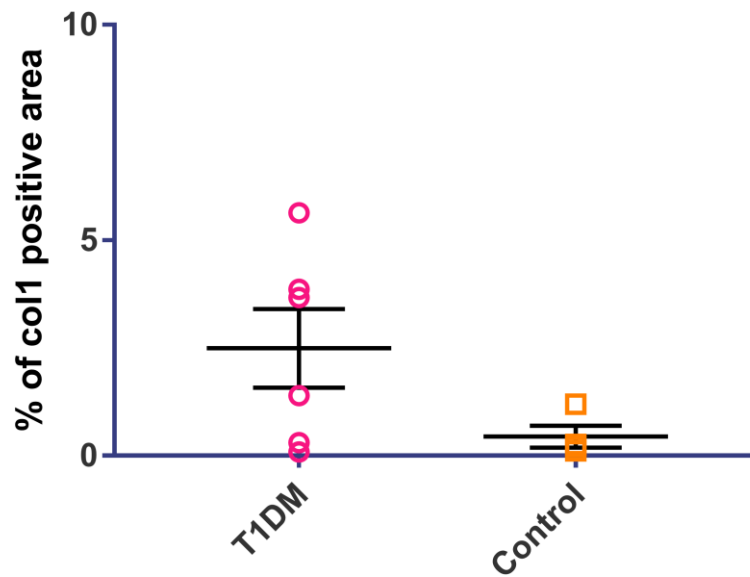


Figure 63. Percentage of collagen 1 positive area in T1DM animals and their control group

The average intensity of Col1 in HFHS fed animals are significantly less than those of the NC fed group ($p = 0.0228$, two tailed Student's t-test), suggesting decreased Col1 levels in HFHS fed animals. However, HFHS group exhibited significantly higher average intensity of Col1 in week 16 when compared to NC fed group ($p = 0.0021$, Tukey's multiple comparisons test following one-way ANOVA) (Figure 64).

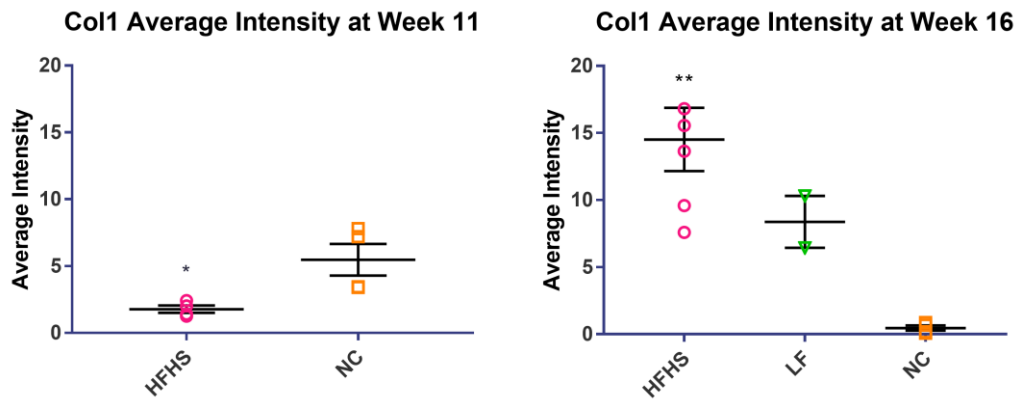


Figure 64. Collagen 1 (Col1) average pixel intensity in HFHS, LF, and NC fed animals in week 11 and 16.

We also calculated the percentage of collagen 1 stained area to the total imaged area to support the intensity measurements. The results are quite similar to the average intensity data. Percentage of col1 positive area of HFHS fed group is significantly lower than the NC fed group at week 11 ($p = 0.0389$, two tailed t-test), while in week 16 as though the trend is the same with average intensity data, the results are not statistically significant (Figure 65).

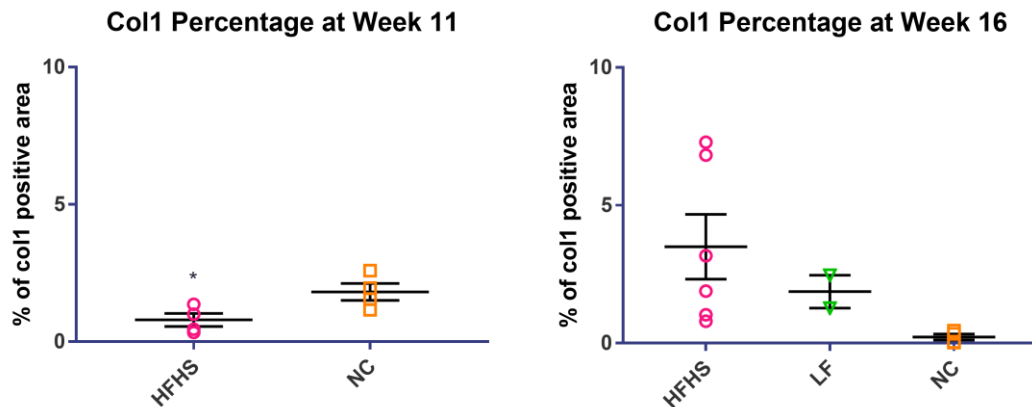


Figure 65. Percentage of collagen 1 positive area in HFHS, LF, and NC fed animals in week 11 and 16

The average intensities of Col1 in SHR are significantly higher than the Wistar control group at week 23. ($p = 0.0386$, two tailed Student's t-test).

Furthermore, the average intensity of Col1 in SHR are also higher when all weeks were combined ($p = 0.0120$, two tailed Student's t-test) (Figure 66).

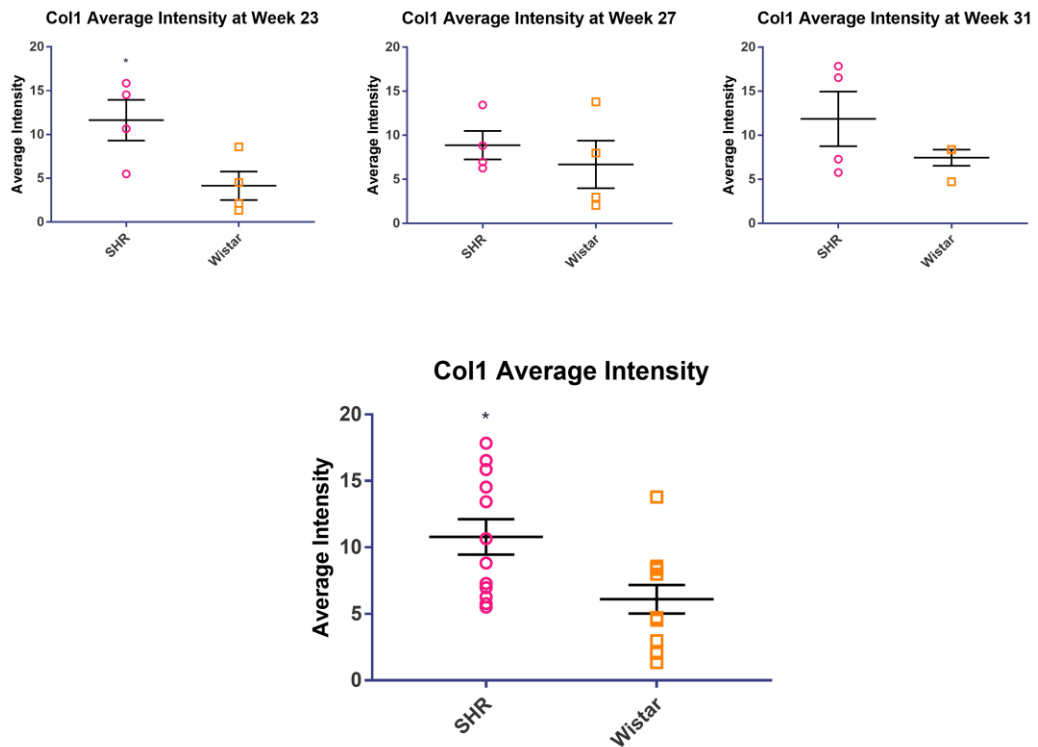


Figure 66. Collagen 1 (Col1) average pixel intensity in SHR and Wistar control groups at weeks 23, 27 and 31.

To assess if there is a trend in Col1 average pixel intensity data between weeks trend analysis was performed, and there were no significant changes in SHR or Wistar group (Figure 67).

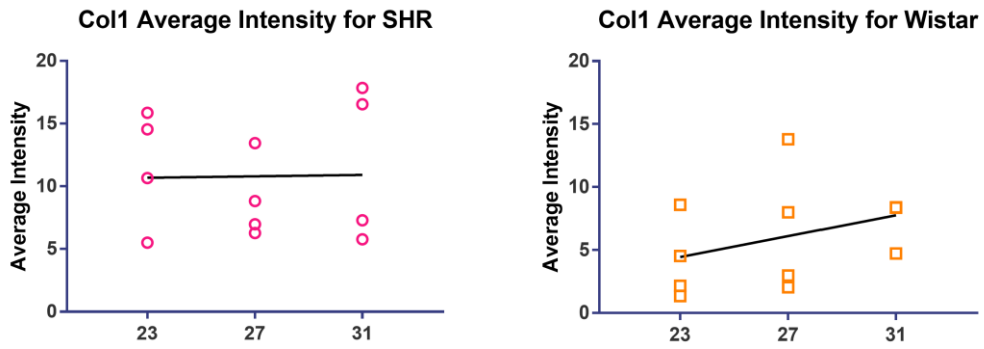


Figure 67. Trend analysis of Col1 Average Pixel Intensity in SHRs and Wistar rats from week 23 to 31.

The percentage of collagen 1 stained area to the total imaged area did not exhibit statistically significant difference in any of the three time points observed (Figure 68).

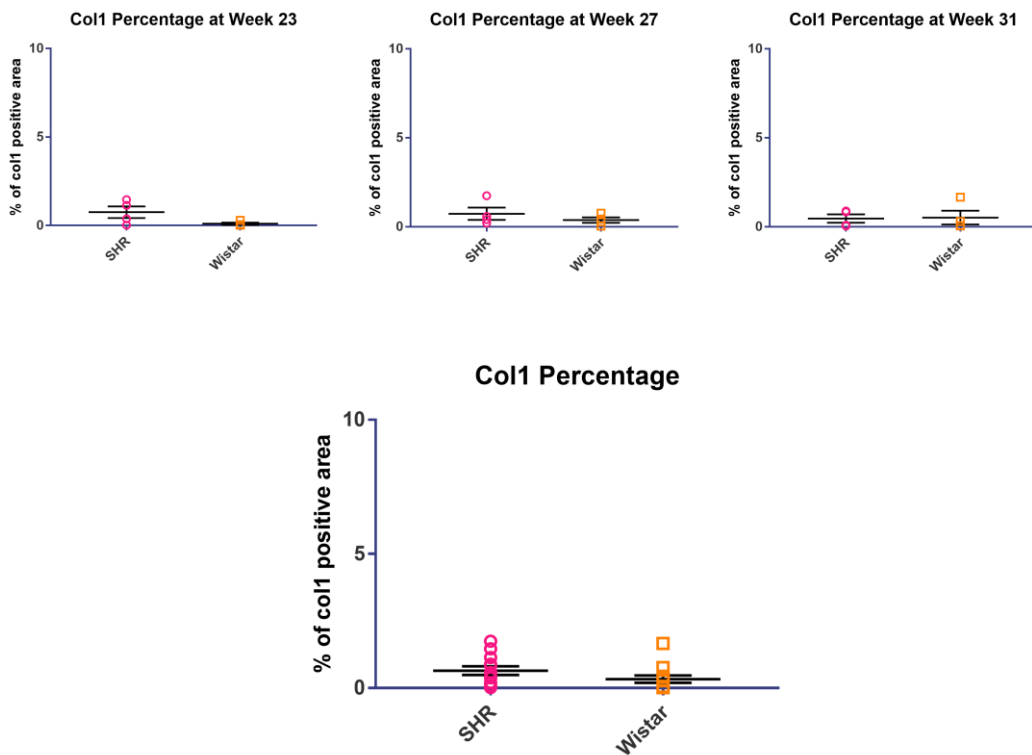


Figure 68. Percentage of collagen 1 positive area in SHRs and Wistar control groups in week 23, 27 and 31.

Immunofluorescence staining images of Col1 and isolectin are shown in Figure 69.

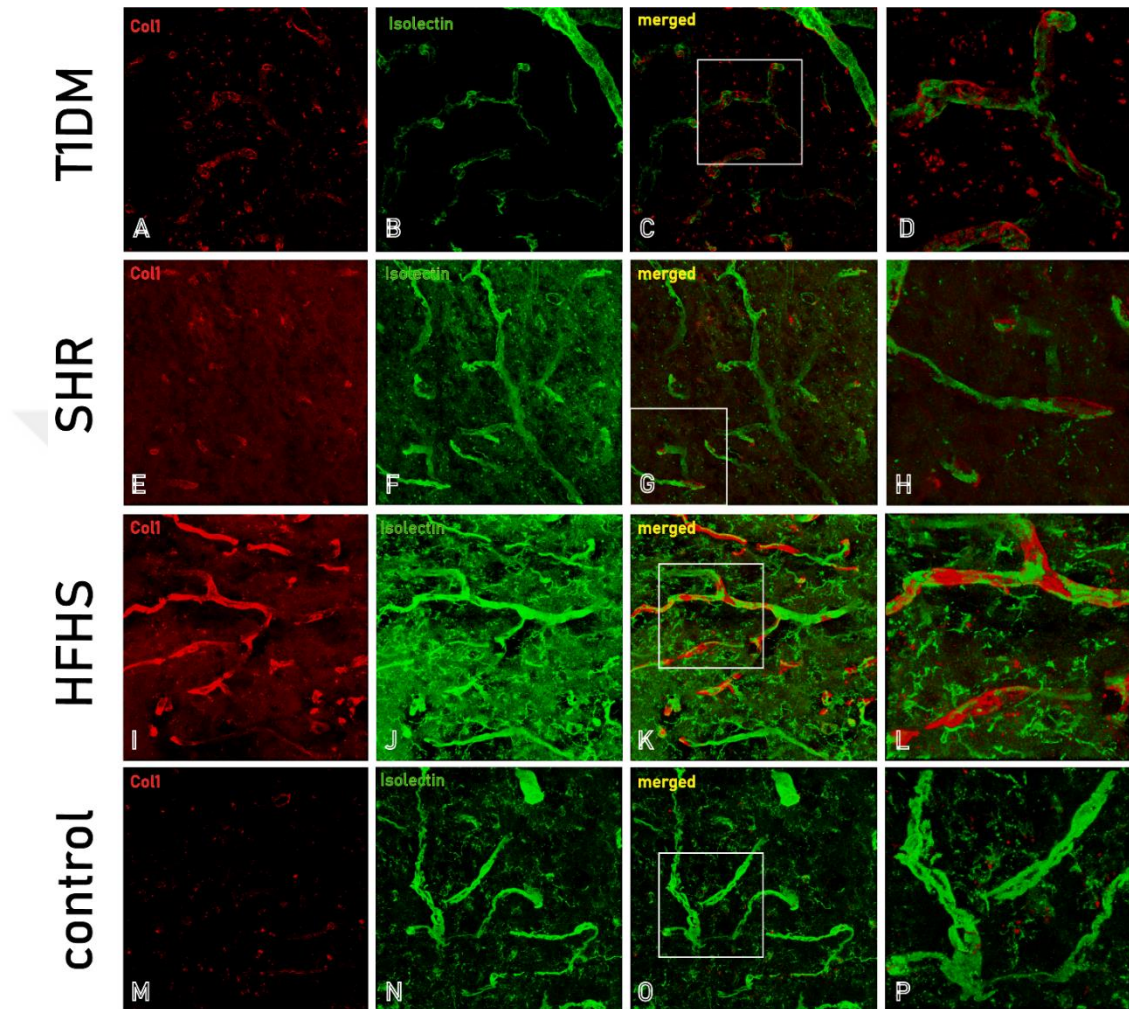


Figure 69. Immunofluorescence staining of Col1 and isolectin in the parietotemporal cortex of T1DM (A-D), SHR (E-H), HFHS fed animals (I-L) and control group (M-P) is shown above. Images D, H, L, and P are zoomed from the previous images.

3.4.4. Quantification of tortuosity

While the numbers of tortuous vessels were elevated in mice with T1DM, the difference between the groups is non-significant (Figure 70).

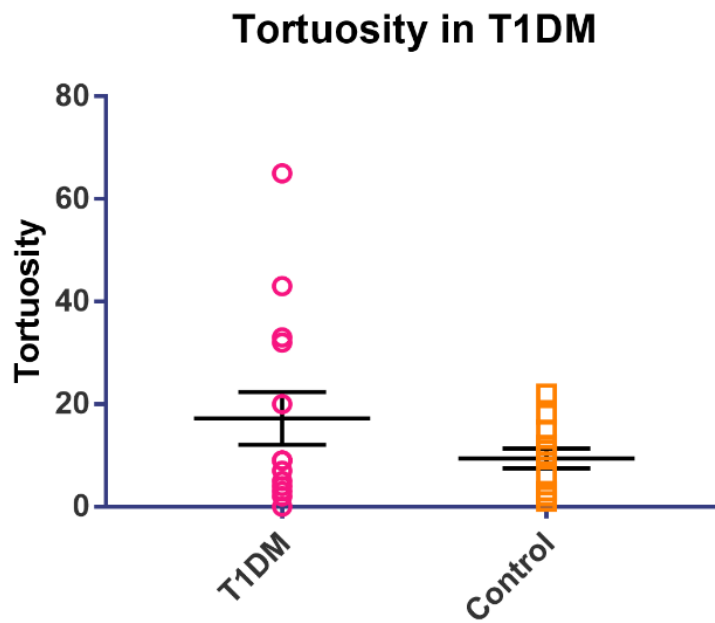


Figure 70. Number of tortuous vessels in T1DM mice and control group

There was no statistically significant difference in tortuous vessel numbers between groups in both week 11 and week 16 (Figure 71).

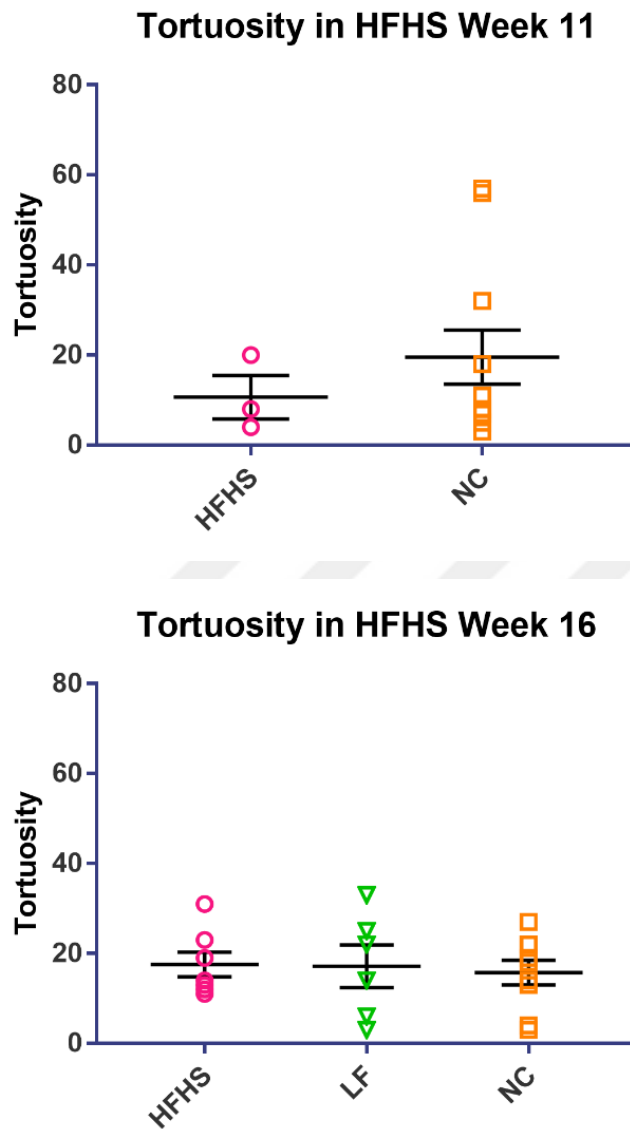


Figure 71. Number of tortuous vessels in HFHS, low-fat and normal chow fed animals

3.4.5. Quantification of pial arteriole exit point narrowing

The number of obstructed vessels were higher in mice with T1DM compared to the control group ($p = 0.0236$, two tailed Student's t-test) (Figure 72).

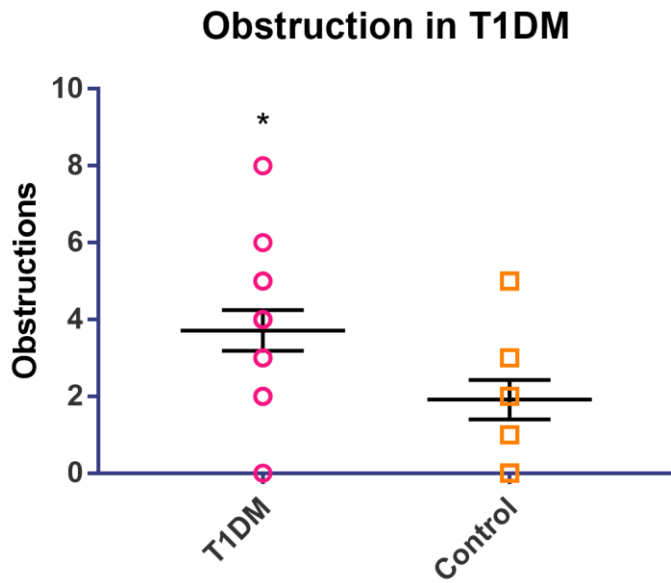


Figure 72. Number of obstructed vessels in T1DM mice and control group

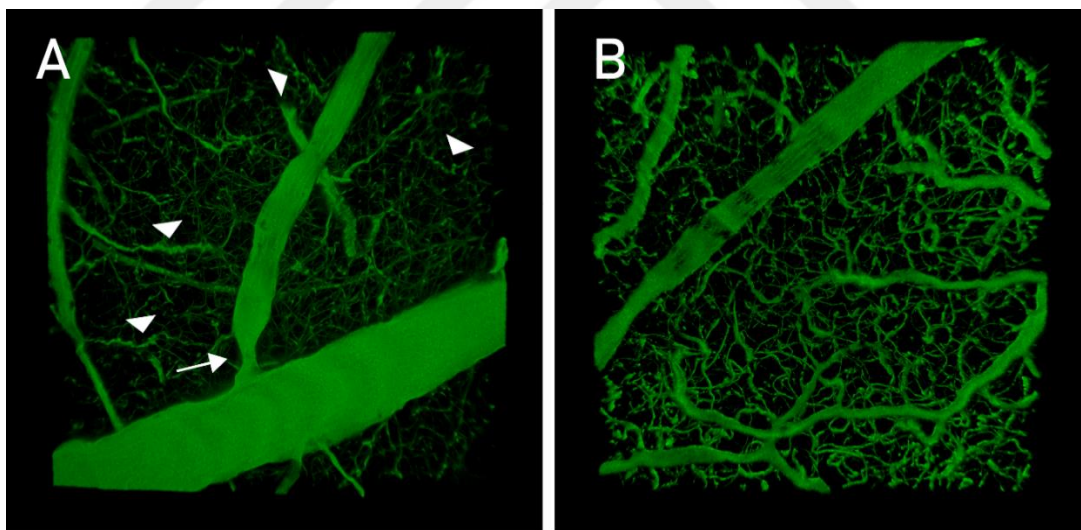


Figure 73. Maximum projection 3DISCO images of (A) T1DM (B) control group. Arrow indicates pial arteriole exit point obstruction point, while arrowheads indicate tortuous vessels.

There has been no statistically significant difference between HFHS-fed, LF-fed and normal chow fed mice groups in both week 11 and week 16 (Figure 74).

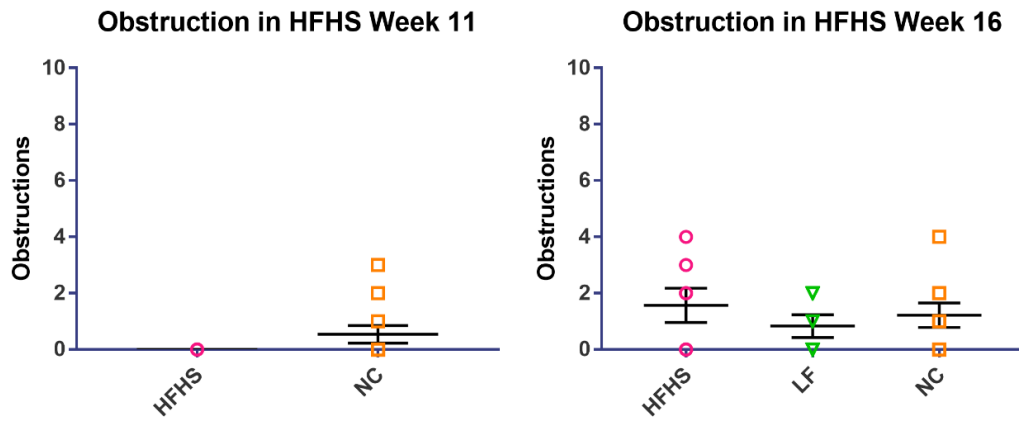


Figure 74. Number of obstructed vessels in HFHS, low-fat and normal chow fed animals

4. DISCUSSION

We herein established three different animal models to visualize the effects on cognition and cerebral microcirculation. In HFHS animal model, HFHS fed animals gained weight and weighed 2 times as the NC fed control group at the end of the study. We saw that in HFHS fed animals, fasting glucose and insulin levels were not statistically different from LF or NC fed groups. However, in IPGTT their blood glucose and blood insulin levels were significantly higher after administrating a certain amount of glucose. HFHS fed group also had higher HOMA-IR scores, which suggested a glucose intolerance and peripheral insulin resistance. Numerous rodent studies showed a high sucrose diet induces insulin resistance and hypertriglyceridemia. High fat diet induces insulin resistance, obesity and increases the tendency to develop atherosclerotic lesions. In our experiment, HFHS fed animal group manifested prominent insulin resistance and obesity in both week 11 and 16. We also observed a significant increase in ALT and AST levels in week 16, which suggested the development of nonalcoholic fatty liver disease. The HFHS fed animals also had a significant increase in total cholesterol, LDL and HDL levels in both weeks, but no significant changes in triglyceride levels. Blood pressure measurements at week 16 showed no statistically significant changes. HFHS diet we used is comprised of 36% fat derived-calories ((9% corn oil and 27% butter), and 43.2% carbohydrate-derived calories with sucrose (30% sucrose-derived calories)) and is therefore different in terms of fat constitution when compared to commercial high fat diets, which can have 20-60% fat derived-calories (Buettner, Schölmerich, & Bollheimer, 2007; Frederich et al., 1995; Pendyala, Walker, & Holt, 2012; Weisberg et al., 2006) and also different from commercial high sucrose diets, which have 30-50% (Maekawa et al., 2017; Sakamoto et al., 2012) sucrose-derived calories. Unexpected blood lipid panel changes such as low triglyceride and high HDL levels might be explained with the dietary difference in fatty acids between the conventional HF diets and the one we used. And as the LF diet consists of 11% fat-derived calories (9% corn oil and 2.5% butter), it also has 67.7% carbohydrate-derived calories without sugar, which

suggests the missing calorie gap was closed by carbohydrates. Although there are many other metabolic changes, our HFHS animal group can be called as a 'glucose intolerance' animal model but might not be named as T2DM or MetS animal model.

To establish the metabolic changes seen in animal model to a full extent, we kept their mobility minimal, so we chose the behavioral tests accordingly. We did not do Morris Water Maze test because it required high amount of swimming movement and might have compromised the metabolic derangements. We chose open field test (OFT) to assess their anxiety, Y maze spontaneous alternation test to assess their spatial working memory, and novel object recognition test (NORT) to assess their visual recognition memory. Both LF and HFHS fed animals exhibited lower levels of anxiety when compared to NC fed group. This result is compatible with existing studies on the effects of high fat diet on anxiety (Zemdegs et al., 2016). Furthermore, LF fed group had higher spontaneous alternation rates, suggesting higher functioning spatial working memory than the control group. HFHS fed group had no significant changes in their spontaneous alternation rates when compared to NC fed control group. When we compared the same animal's spontaneous alternation scores, we saw a significant decrease in LF fed group, which suggested a decrease in working memory performance between weeks 11 and 16. HFHS and LF fed animal group had no significant differences between their novel object recognition test scores when compared to NC fed animals, which suggested no impairment in visual recognition memory. However, LF fed animals had a significant increase in the total exploration time, which suggested even though they explored the objects more, they found it hard to remember which one is novel and which one is old, therefore this might suggest an impairment in learning abilities or attention. When we analyzed the novel object recognition scores of the same animals between week 11 and 16, we saw significant decline in both HFHS and LF animals but not in NC fed group. When we analyzed the percentage of time spent exploring the novel object, LF fed animals had a significantly higher score on week 11 but not in week 16. Later we analyzed the percentage of

time spent exploring the novel object data of the same animals, we observed a significant decline in LF fed group from week 11 to week 16, which supports the data obtained by comparing same animals novel object recognition test scores suggesting a decline in visual recognition memory in both HFHS and LF fed animals.

To assess endothelial proliferation in the cerebral microcirculation of these animals, we stained the brain slices with isolectin and quantified it by thresholding as it was described in the methods section. There was a significant increase in isolectin positive area percentage at both parietotemporal cortex and hippocampal areas of HFHS fed group when compared to NC fed group in both week 11 and 16. Week 16 hippocampal isolectin data shows significantly higher isolectin percentage in LF fed group as well as the HFHS fed group when compared to NC fed group. This data suggests both LF and HFHS diet cause endothelial proliferation in hippocampus, but only HFHS diet causes endothelial proliferation in parietotemporal cortex, as the data shows no significant differences between LF and NC fed groups in week 16. The decline seen in the visual recognition memories of the HFHS and LF fed animals might be the result of this hippocampal endothelial proliferation as the proliferated endothelia might not be forming fully functional microvessels. Whether these proliferated endothelia form functional microvessels or not should be further investigated. In HFHS animal group, there were no significant changes in number of pericytes in the parietotemporal cortex, but the vessel related pericyte percentage was significantly decreased at week 11. LF fed group had significantly higher numbers of pericytes when compared to NC fed group at week 16, but they were significantly related with vessels. Vessel related pericyte percentage was significantly decreased in HFHS fed animals at week 11, but at week 16 it was significantly increased, which might suggest the proliferating endothelia might be recruiting pericytes around newly formed vessels in week 16, and therefore increase its functionality.

To assess the arteriolar stiffening that is created by the accumulation of extracellular membrane proteins, we used collagen-1, as it also is a prominent

factor in fibrotic conditions. We used Col-1 average pixel intensity values to compare the Col-1 amounts around microvessels between HFHS, LF and NC fed animals. Although there was no major difference between HFHS and NC fed animals. Although there was no major difference between HFHS and NC fed group in week 11, there was a significant increase in HFHS fed group's average col-1 pixel intensity values in week 16 when compared to NC fed group. This data suggests increased microcirculatory stiffening in HFHS fed animals, and it should be further verified by western blot and PCR analysis.

As the vessel tortuosity and pial arteriolar point obstructions were seen in the samples, we counted and measured the differences between those parameters. We could not find any significant differences in between experimental animal groups.

In T1DM group, we observed significant weight loss after the weeks following intraperitoneal STZ injection, which was compatible with the other studies using STZ induced T1DM animal models (Howarth, Jacobson, Shafiullah, & Adeghate, 2005). T1DM animals exhibited much higher fasting blood glucose levels when compared to HFHS animal group. The slight ALT increase that is seen in the blood biochemical parameters might be because of the STZ injection itself, but there was no other difference in other parameters. As there are some studies that show STZ might increase blood pressure, we measured T1DM animal group's blood pressure non-invasively, and found no significant changes.

In the T1DM animal group, we did not observe any significant behavioral changes regarding anxiety, visual recognition, or spatial working memory. Total distance travelled was significantly lower in T1DM group, and this might suggest reluctance to explore new areas. The lack of cognitive impairment might be because of the relatively late onset of T1DM, as the studies mostly show cognitive deficits and brain structural changes observed in T1DM are related to early-onset T1DM.

However, the percentage of isolectin positive area in T1DM group showed a significant decline in parietotemporal cortex, whereas it did not show a significant change in hippocampal area. As there is an increase in the isolectin percentage in the parietotemporal cortex of the HFHS fed animals, and a

decrease in T1DM animals, this might suggest the endothelial proliferation at the cortical level might be related to hyperinsulinemia.

Number of pericytes in the parietotemporal cortex was significantly increased in T1DM animals, while the percentages of pericytes around vessels were significantly decreased. This data suggests an increased amount of pericytes in the brain parenchyma, which are not related to capillaries. This might be causing the endothelial decrease, as it is the pericytes that maintain endothelial robustness in microcirculatory level. STZ is also known for its neurotoxic effects, and it might be toxic to other cells, such as endothelia and pericytes. Therefore, whether the microcirculatory differences seen are results of T1DM or the effects of STZ should further be investigated.

The collagen1 average pixel intensity measurement showed no significant changes in T1DM animal group, which suggested no arteriolar stiffness.

When we analyzed 3DISCO images for tortuosity and pial arteriole exit point obstructions, we could show no significance in tortuosity in both HFHS and T1DM animal groups. However, the number of pial arteriole exit point obstruction was significantly higher in T1DM animals when compared to its control group. This might suggest a higher order response to the metabolic derangements in T1DM group, which might be due to smooth muscle cell rigor or just atherosclerosis.

In the hypertension group, we noninvasively measured systolic, diastolic, and mean blood pressures in SHR and their same aged Wistar control groups. Spontaneously hypertensive rats exhibited significantly higher systolic, diastolic, and mean blood pressures in all three time points. We designed the experiment in three separate timelines to see progression of the changes that would be observed in cerebral microcirculation. When we measured blood biochemical parameters, we observed significantly higher ALT, AST, total cholesterol, LDL, HDL levels in SHR in almost every time point. We hypothesized that the changes seen in SHR might be due to the end-organ damage that is caused by very high systolic blood pressure, as the SHR exhibit systolic blood pressures higher than 160 mmHg from five weeks of age, which means the youngest animal in the total group was chronic

hypertensive for at least 18 weeks. The blood lipid panel changes we saw in SHR animals were also established by other scientists (Swislocki & Tsuzuki, 1993). As a limitation, we did not measure fasting glucose and insulin levels in these animals, although it is a fairly controversial subject, there are several studies that demonstrate adult SHRs have insulin resistance without being obese (Potenza et al., 2005; Swislocki & Tsuzuki, 1993). Therefore, the results cannot be solely attributed to hypertension, but might be the effect of insulin resistance and hypertension combined. It is known that there are certain hormones that regulate food intake, such as leptin and ghrelin. Leptin is an anorexigenic hormone, which suppresses the food intake in long term and results with weight loss. It is produced by mature adipocytes and its amount is positively correlated with the mass of adipose tissue. On the other hand, ghrelin is an orexigenic hormone, which initiates food consumption, and results with weight gain (Klok, Jakobsdottir, & Drent, 2007). Obese patients have increased leptin and decreased ghrelin levels (Labayen et al., 2011). As an advantage, SHRs were not obese; in fact, they were leaner than their same aged Wistar control groups, so their ghrelin and leptin levels were not expected to change. Therefore, we could observe the effect of hypertension and insulin resistance itself, without the effects of ghrelin and leptin.

SHRs exhibited significantly lower anxiety in weeks 27 and 31, but no difference was seen at week 23. This data is consistent with the other anxiety studies in SHRs (Calzavara, Lopez, Abílio, Silva, & Frussa-Filho, 2004). Numerous human studies show increased anxiety levels in hypertension and T2DM (Ali et al., 2006; Kahl et al., 2015; Pan et al., 2015; Scalco et al., 2005), but it is not known if it is the cause or the result of the diseases. Our data might suggest that the increased anxiety levels seen in these patients might be the result of the life style changes. It might also suggest that rodent experiments regarding anxiety in these two metabolic conditions might not be translated to humans. From another aspect, SHRs are also used as a model for ADHD, as they show increased locomotion, impulsivity and attention deficits. The behavioral changes seen in these animals might be due to increased impulsivity which originates from the changes in frontal cortex and

dopaminergic activity instead of anxiety, which was not investigated in this study (Sagvolden, Pettersen, & Larsen, 1993).

SHRs also had lower spontaneous alternation rates, but it was not significant in any time point. However, when we excluded the age effect, we observed a significant decline in the spontaneously alternation rates of SHRs, suggesting a decline in working and spatial memory. Although SHRs had slightly higher scores in all three time points, their novel object recognition test scores were not significantly different from the control group, suggesting an intact visual recognition memory. These findings also add to the knowledge that the effect of hypertension could be on frontal area rather than hippocampus.

In the hypertension animal group, there was no significant changes in the isolectin positive area percentage in parietotemporal cortex in all three time points, while in the hippocampal area there was a decrease in week 23, and an increase in week 31 and no significant changes in week 27. When we performed trend analysis following one-way ANOVA, we saw a significant decrease in isolectin positive area percentage in both hippocampus and parietotemporal cortex in Wistar control groups from week 23 to 31. We concluded that this might be related to the normal aging process. However, it should be noted that there are genetic differences between SHRs and Wistar control groups which might affect the neurodevelopmental processes of these animals (Zhang-James, Middleton, & Faraone, 2013). The neurodevelopmental effects of these genetic differences should also be considered as a potential reason for these results, alongside the hypertension observed in these animals.

In the hypertension group, the number of pericytes was significantly higher in SHRs when compared to same age Wistar control groups in weeks 23 and 27, while week 31 showed no significant changes. Vessel related pericyte percentages were lower in SHRs when compared to same age Wistar control groups in weeks 23 and 31, and there were no significant changes in week 27. This suggested that hypertension might cause a proliferated state in pericytes, while impairing their functions as they detach from the vessel wall. Although the SHR animals exhibited higher values of col1 average intensity in

all 3 weeks when compared to their Wistar control groups, it was only significant in week 23. When we excluded the age effect, we saw that there was a significant increase in col1 intensity in SHR animals. Increased collagen 1 data suggests increased vessel stiffness due to the accumulation of col1 around vessels.



5. CONCLUSION AND FUTURE PERSPECTIVES

- HFHS diet caused obesity, glucose intolerance, increased ALT, AST, total cholesterol, LDL and HDL levels, whereas it had no effects in blood pressure, triglyceride, fasting blood glucose and insulin levels when compared to NC fed control group.
- HFHS diet fed animals spent significantly more time in the central area in the OFT test, suggesting a decline in anxiety levels.
- LF diet fed animals had better spontaneous alternation rates in both weeks, but they had a significant decline from week 11 to week 16, which suggests a decline in working and spatial memory performance.
- LF diet fed animals explored the objects more in novel object recognition test, but the attention they show to the novel object is lower, and this might suggest an impairment in their learning abilities or attention, which needs further investigation.
- There was a decline in both the novel object test scores and the percentage of time spent exploring the novel object of the same animals in the LF fed group from week 11 to week 16, which suggests a decline in the visual recognition memory of LF fed animals. HFHS fed animals also had a decline in their novel object recognition scores between weeks 11 and 16. However, there was no decline in the novel object recognition scores of normal chow fed animals between weeks 11 and 16.
- Leptin and ghrelin levels are also potentially relevant factors in the behavioral and cognitive changes of these animal groups, and should be further investigated.
- Both LF and HFHS diet cause endothelial proliferation in hippocampus, but only HFHS diet causes endothelial proliferation in parietotemporal cortex. The decline seen in the visual recognition memories of the HFHS and LF fed animals might be the result of this hippocampal endothelial proliferation as the proliferated endothelia might not be forming fully functional microvessels.

- LF fed group had significantly higher numbers of pericytes when compared to NC fed group at week 16, but they were significantly related with vessels. Vessel related pericyte percentage was significantly decreased in HFHS fed animals at week 11, but at week 16 it was significantly increased, which might suggest the proliferating endothelia might be recruiting pericytes around newly formed vessels in week 16, and therefore increase its functionality.
- Col-1 accumulation of HFHS fed animals is significantly increased in week 16. Stiffening at the microcirculatory level might be guided by col-1 build up around the vessels of HFHS fed animals, and this might be leading to energy-demand mismatch at the cellular level, followed by conditional hypoxia, and increased neuroinflammation. The increase should be further verified by Western Blot and PCR analysis.
- In the T1DM animal group, we did not observe any significant behavioral changes regarding anxiety, visual recognition or working and spatial memory. The lack of cognitive impairment might be because of the relatively late onset of T1DM, as the studies mostly show cognitive deficits and brain structural changes observed in T1DM are related to early-onset T1DM.
- We observed significant decline in isolectin positive area percentage at the parietotemporal cortex of T1DM animals, whereas there was not a significant change in hippocampal area. As there is an increase in the isolectin percentage in the parietotemporal cortex of the HFHS fed animals, and a decrease in T1DM animals, this might suggest the endothelial proliferation at the cortical level might be related to hyperinsulinemia.
- Number of pericytes in the parietotemporal cortex was significantly increased in T1DM animals, while the percentage of pericytes around vessels was significantly decreased. This data suggests an increased amount of pericytes in the brain parenchyma, which are not related to capillaries. This might be causing the endothelial decrease, as it is the pericytes that maintain endothelial robustness in microcirculatory level.

STZ is also known for its neurotoxic effects, and it might be toxic to other cells, such as endothelia and pericytes. Therefore, whether the microcirculatory differences seen are results of T1DM or the effects of STZ should further be investigated.

- The number of pial arteriole exit point obstruction was significantly higher in T1DM animals when compared to its control group. This might suggest a higher order response to the metabolic derangements in T1DM group, which might be due to smooth muscle cell rigor or just atherosclerosis.
- SHRs exhibited significantly lower anxiety in weeks 27 and 31, but no difference was seen at week 23, same as the HFHS fed animal group. Numerous human studies show increased anxiety levels in hypertension and T2DM, but it is not known if it is the cause or the result of the diseases. Our data might suggest that the increased anxiety levels seen in these patients might be the result of the life style changes. It might also suggest that rodent experiments regarding anxiety in these two metabolic conditions might not be translated to humans.
- SHRs had lower spontaneous alternation rates, but it was not significant in any time point. However, when we excluded the age effect, we observed a significant decline in the spontaneously alternation rates of SHRs, suggesting a decline in working and spatial memory. A larger sample size might be required to reveal the effects of hypertension on working and spatial memory further.
- Although SHRs had slightly higher scores in all three time points, their novel object recognition test scores were not significantly different from the control group, suggesting an intact visual recognition memory.
- The number of pericytes in the parietotemporal cortex was significantly higher in SHRs when compared to same age Wistar control groups in weeks 23 and 27, while week 31 showed no significant changes. Vessel related pericyte percentages were lower in SHRs when compared to same age Wistar control groups in weeks 23 and 31, and

there were no significant changes in week 27. This suggested that hypertension might cause a proliferated state in pericytes, while impairing their functions as they detach from the vessel wall.

- Although the SHR animals exhibited higher values of col1 average intensity in all 3 weeks when compared to their Wistar control groups, it was only significant in week 23. When we excluded the age effect, we saw that there was a significant increase in col1 intensity in SHR animals. Increased collagen 1 data suggests increased vessel stiffness due to the accumulation of col1 around vessels. A larger sample size might be required to reveal the collagen-1 accumulation in the vessel walls of hypertensive animals further.

6. REFERENCES

- Alarcon-Martinez, L., Yilmaz-Ozcan, S., Yemisci, M., Schallek, J., Kılıç, K., Can, A., ... Dalkara, T. (2018). Capillary pericytes express α -smooth muscle actin, which requires prevention of filamentous-actin depolymerization for detection. *eLife*, 7. <http://doi.org/10.7554/eLife.34861>
- Ali, S., Stone, M. A., Peters, J. L., Davies, M. J., & Khunti, K. (2006). The prevalence of co-morbid depression in adults with Type 2 diabetes: a systematic review and meta-analysis. *Diabetic Medicine*, 23(11), 1165–1173. <http://doi.org/10.1111/j.1464-5491.2006.01943.x>
- Antunes, M., & Biala, G. (2012). The novel object recognition memory: neurobiology, test procedure, and its modifications. *Cognitive Processing*, 13(2), 93–110. <http://doi.org/10.1007/s10339-011-0430-z>
- Armulik, A., Abramsson, A., & Betsholtz, C. (2005). Endothelial/pericyte interactions. *Circulation Research*, 97(6), 512–523. <http://doi.org/10.1161/01.RES.0000182903.16652.d7>
- Armulik, A., Genové, G., & Betsholtz, C. (2011). Pericytes: Developmental, Physiological, and Pathological Perspectives, Problems, and Promises. *Developmental Cell*, 21(2), 193–215. <http://doi.org/10.1016/j.devcel.2011.07.001>
- Armulik, A., Genové, G., Mäe, M., Nisancioglu, M. H., Wallgard, E., Niaudet, C., ... Betsholtz, C. (2010). Pericytes regulate the blood-brain barrier. *Nature*, 468(7323), 557–561. <http://doi.org/10.1038/nature09522>
- Attwell, D., Mishra, A., Hall, C. N., Farrell, F. M. O., & Dalkara, T. (2016). What is a pericyte ?, 6–10. <http://doi.org/10.1177/0271678X15610340>
- Augustin, R. (2010). The protein family of glucose transport facilitators: It's not only about glucose after all. *IUBMB Life*, 62(5), NA-NA. <http://doi.org/10.1002/iub.315>
- Barnes, D. E., & Yaffe, K. (2011). The projected effect of risk factor reduction on Alzheimer's disease prevalence. *The Lancet Neurology*, 10(9), 819–828. [http://doi.org/10.1016/S1474-4422\(11\)70072-2](http://doi.org/10.1016/S1474-4422(11)70072-2)
- Baskin, D. G., Sipols, A. J., Schwartz, M. W., & White, M. F. (1993).

- Immunocytochemical detection of insulin receptor substrate-1 (IRS-1) in rat brain: colocalization with phosphotyrosine. *Regulatory Peptides*, 48(1–2), 257–66.
- Bell, R. D., Winkler, E. A., Sagare, A. P., Singh, I., LaRue, B., Deane, R., & Zlokovic, B. V. (2010). Pericytes Control Key Neurovascular Functions and Neuronal Phenotype in the Adult Brain and during Brain Aging. *Neuron*, 68(3), 409–427. <http://doi.org/10.1016/j.neuron.2010.09.043>
- Berger, M., Bergers, G., Arnold, B., Hämmerling, G. J., & Ganss, R. (2005). Regulator of G-protein signaling-5 induction in pericytes coincides with active vessel remodeling during neovascularization. *Blood*, 105(3), 1094–1101. <http://doi.org/10.1182/blood-2004-06-2315>
- Bevins, R. A., & Besheer, J. (2006). Object recognition in rats and mice: A one-trial non-matching-to-sample learning task to study “recognition memory.” *Nature Protocols*, 1(3), 1306–1311. <http://doi.org/10.1038/nprot.2006.205>
- Biessels, G. J., Staekenborg, S., Brunner, E., Brayne, C., & Scheltens, P. (2006). Risk of dementia in diabetes mellitus: a systematic review. *Lancet Neurology*, 5(1), 64–74. [http://doi.org/10.1016/S1474-4422\(05\)70284-2](http://doi.org/10.1016/S1474-4422(05)70284-2)
- Bondjers, C., Kalén, M., Hellström, M., Scheidl, S. J., Abramsson, A., Renner, O., ... Betsholtz, C. (2003). Transcription profiling of platelet-derived growth factor-B-deficient mouse embryos identifies RGS5 as a novel marker for pericytes and vascular smooth muscle cells. *American Journal of Pathology*, 162(3), 721–729. [http://doi.org/10.1016/S0002-9440\(10\)63868-0](http://doi.org/10.1016/S0002-9440(10)63868-0)
- Buettner, R., Schölmerich, J., & Bollheimer, L. C. (2007). High-fat Diets: Modeling the Metabolic Disorders of Human Obesity in Rodents*. *Obesity*, 15(4), 798–808. <http://doi.org/10.1038/oby.2007.608>
- Burns, J. M., Donnelly, J. E., Anderson, H. S., Mayo, M. S., Spencer-Gardner, L., Thomas, G., ... Brooks, W. M. (2007). Peripheral insulin and brain structure in early Alzheimer disease. *Neurology*, 69(11), 1094–1104. <http://doi.org/10.1212/01.wnl.0000276952.91704.af>
- Calzavara, M. B., Lopez, G. B., Abílio, V. C., Silva, R. H., & Frussa-Filho, R.

- (2004). Role of anxiety levels in memory performance of spontaneously hypertensive rats. *Behavioural Pharmacology*, 15(8), 545–53.
- Carmeliet, P., & Jain, R. K. (2011). Molecular mechanisms and clinical applications of angiogenesis. *Nature*, 473(7347), 298–307. <http://doi.org/10.1038/nature10144>
- Carroll, D., Phillips, A. C., Thomas, G. N., Gale, C. R., Deary, I., & Batty, G. D. (2009). Generalized Anxiety Disorder Is Associated with Metabolic Syndrome in the Vietnam Experience Study. *Biological Psychiatry*, 66(1), 91–93. <http://doi.org/10.1016/j.biopsych.2009.02.020>
- Carruthers, A., DeZutter, J., Ganguly, A., & Devaskar, S. U. (2009). Will the original glucose transporter isoform please stand up! *American Journal of Physiology-Endocrinology and Metabolism*, 297(4), E836–E848. <http://doi.org/10.1152/ajpendo.00496.2009>
- Chatterjee, S., Peters, S. A. E., Woodward, M., Arango, S. M., Batty, G. D., Beckett, N., ... Huxley, R. R. (2016). Type 2 diabetes as a risk factor for dementia in women compared with men: A pooled analysis of 2.3 million people comprising more than 100,000 cases of dementia. *Diabetes Care*, 39(2), 300–307. <http://doi.org/10.2337/dc15-1588>
- Chen, G.-J., Xu, J., Lahousse, S. A., Caggiano, N. L., & de la Monte, S. M. (2003). Transient hypoxia causes Alzheimer-type molecular and biochemical abnormalities in cortical neurons: potential strategies for neuroprotection. *Journal of Alzheimer's Disease : JAD*, 5(3), 209–28.
- Cheung, C. Y. -I., Ikram, M. K., Sabanayagam, C., & Wong, T. Y. (2012). Retinal Microvasculature as a Model to Study the Manifestations of Hypertension. *Hypertension*, 60(5), 1094–1103. <http://doi.org/10.1161/HYPERTENSIONAHA.111.189142>
- Cheung, C. Y.-L., Lamoureux, E., Ikram, M. K., Sasongko, M. B., Ding, J., Zheng, Y., ... Wong, T. Y. (2012). Retinal Vascular Geometry in Asian Persons with Diabetes and Retinopathy. *Journal of Diabetes Science and Technology*, 6(3), 595–605. <http://doi.org/10.1177/193229681200600315>
- Cheung, N., Mitchell, P., & Wong, T. Y. (2010). Diabetic retinopathy. *The*

- Lancet*, 376(9735), 124–136. [http://doi.org/10.1016/S0140-6736\(09\)62124-3](http://doi.org/10.1016/S0140-6736(09)62124-3)
- Clarke, D. W., Mudd, L., Boyd, F. T., Fields, M., & Raizada, M. K. (2006). Insulin Is Released from Rat Brain Neuronal Cells in Culture. *Journal of Neurochemistry*, 47(3), 831–836. <http://doi.org/10.1111/j.1471-4159.1986.tb00686.x>
- cognition | Definition of cognition in English by Oxford Dictionaries. (n.d.). Retrieved July 18, 2018, from <https://en.oxforddictionaries.com/definition/cognition>
- Collins, M. M., Corcoran, P., & Perry, I. J. (2009). Anxiety and depression symptoms in patients with diabetes. *Diabetic Medicine*, 26(2), 153–161. <http://doi.org/10.1111/j.1464-5491.2008.02648.x>
- Conejo, R., & Lorenzo, M. (2001). Insulin signaling leading to proliferation, survival, and membrane ruffling in C2C12 myoblasts. *Journal of Cellular Physiology*, 187(1), 96–108. [http://doi.org/10.1002/1097-4652\(2001\)9999:9999<::AID-JCP1058>3.0.CO;2-V](http://doi.org/10.1002/1097-4652(2001)9999:9999<::AID-JCP1058>3.0.CO;2-V)
- Cowan, N. (2008). What are the differences between long-term, short-term, and working memory? *Progress in Brain Research*, 169, 323–38. [http://doi.org/10.1016/S0079-6123\(07\)00020-9](http://doi.org/10.1016/S0079-6123(07)00020-9)
- Crowder, R. J., & Freeman, R. S. (2000). Glycogen Synthase Kinase-3 β Activity Is Critical for Neuronal Death Caused by Inhibiting Phosphatidylinositol 3-Kinase or Akt but Not for Death Caused by Nerve Growth Factor Withdrawal. *Journal of Biological Chemistry*, 275(44), 34266–34271. <http://doi.org/10.1074/jbc.M006160200>
- de la Monte, S. M. (2012). Contributions of Brain Insulin Resistance and Deficiency in Amyloid-Related Neurodegeneration in Alzheimer's Disease. *Drugs*, 72(1), 49–66. <http://doi.org/10.2165/11597760-000000000-00000>
- de Leeuw, F.-E., de Groot, J. C., Oudkerk, M., Witteman, J. C. M., Hofman, A., van Gijn, J., & Breteler, M. M. B. (2002). Hypertension and cerebral white matter lesions in a prospective cohort study. *Brain: A Journal of Neurology*, 125(Pt 4), 765–772. <http://doi.org/10.1093/brain/awf077>

- de Souza, L. E. B., Malta, T. M., Kashima Haddad, S., & Covas, D. T. (2016). Mesenchymal Stem Cells and Pericytes: To What Extent Are They Related? *Stem Cells and Development*, 25(24), 1843–1852. <http://doi.org/10.1089/scd.2016.0109>
- dementia | Definition of dementia in English by Oxford Dictionaries. (n.d.). Retrieved July 18, 2018, from <https://en.oxforddictionaries.com/definition/dementia>
- Desmond, D. W., Moroney, J. T., Paik, M. C., Sano, M., Mohr, J. P., Aboumatar, S., ... Stern, Y. (2000). Frequency and clinical determinants of dementia after ischemic stroke. *Neurology*, 54(5), 1124–31.
- Díaz-Flores, L., Gutiérrez, R., Madrid, J. F., Varela, H., Valladares, F., Acosta, E., ... Díaz-Flores, J. (2009). Pericytes. Morphofunction, interactions and pathology in a quiescent and activated mesenchymal cell niche. *Histology and Histopathology*, 24(7), 909–969. <http://doi.org/10.14670/HH-24.909>
- Ding, J., Wai, K. L., McGeechan, K., Ikram, M. K., Kawasaki, R., Xie, J., ... Meta-Eye Study Group, for the M.-E. S. (2014). Retinal vascular caliber and the development of hypertension: a meta-analysis of individual participant data. *Journal of Hypertension*, 32(2), 207–15. <http://doi.org/10.1097/HJH.0b013e32836586f4>
- Duelli, R., Maurer, M. H., Staudt, R., Heiland, S., Duembgen, L., & Kuschinsky, W. (2000). Increased cerebral glucose utilization and decreased glucose transporter Glut1 during chronic hyperglycemia in rat brain. *Brain Research*, 858(2), 338–47.
- Ejaz, S., Chekarova, I., Ejaz, A., Sohail, A., & Lim, C. W. (2007). Importance of pericytes and mechanisms of pericyte loss during diabetes retinopathy. *Diabetes, Obesity and Metabolism*, 0(0), 071018044430008–???. <http://doi.org/10.1111/j.1463-1326.2007.00795.x>
- Ertürk, A., Becker, K., Jährling, N., Mauch, C. P., Hojer, C. D., Egen, J. G., ... Dodt, H. U. (2012). Three-dimensional imaging of solvent-cleared organs using 3DISCO. *Nature Protocols*, 7(11), 1983–1995. <http://doi.org/10.1038/nprot.2012.119>
- Escudero, C. A., Herlitz, K., Troncoso, F., Guevara, K., Acurio, J., Aguayo, C.,

- ... González, M. (2017). Pro-angiogenic Role of Insulin: From Physiology to Pathology. *Frontiers in Physiology*, 8, 204. <http://doi.org/10.3389/fphys.2017.00204>
- Faraco, G., & Iadecola, C. (2013). Hypertension: A harbinger of stroke and dementia. *Hypertension*. <http://doi.org/10.1161/HYPERTENSIONAHA.113.01063>
- Ferguson, S. C., Blane, A., Perros, P., McCrimmon, R. J., Best, J. J. K., Wardlaw, J., ... Frier, B. M. (2003). Cognitive ability and brain structure in type 1 diabetes: Relation to microangiopathy and preceding severe hypoglycemia. *Diabetes*, 52(1), 149–156. <http://doi.org/10.2337/diabetes.52.1.149>
- Fernandez-Klett, F., Offenhauser, N., Dirnagl, U., Priller, J., & Lindauer, U. (2010). Pericytes in capillaries are contractile in vivo, but arterioles mediate functional hyperemia in the mouse brain. *Proceedings of the National Academy of Sciences*, 107(51), 22290–22295. <http://doi.org/10.1073/pnas.1011321108>
- Fisher, L., Skaff, M. M., Mullan, J. T., Arean, P., Glasgow, R., & Masharani, U. (2008). A longitudinal study of affective and anxiety disorders, depressive affect and diabetes distress in adults with Type 2 diabetes. *Diabetic Medicine*, 25(9), 1096–1101. <http://doi.org/10.1111/j.1464-5491.2008.02533.x>
- Frederich, R. C., Hamann, A., Anderson, S., Löllmann, B., Lowell, B. B., & Flier, J. S. (1995). Leptin levels reflect body lipid content in mice: Evidence for diet-induced resistance to leptin action. *Nature Medicine*, 1(12), 1311–1314. <http://doi.org/10.1038/nm1295-1311>
- Freret, T., Bouet, V., Quiedeville, A., Nee, G., Dallemagne, P., Rochais, C., & Boulouard, M. (2012). Synergistic effect of acetylcholinesterase inhibition (donepezil) and 5-HT 4 receptor activation (RS67333) on object recognition in mice. *Behavioural Brain Research*, 230(1), 304–308. <http://doi.org/10.1016/j.bbr.2012.02.012>
- Furman, B. L. (2015). Streptozotocin-Induced Diabetic Models in Mice and Rats. In *Current Protocols in Pharmacology* (Vol. 70, p. 5.47.1-5.47.20).

Hoboken, NJ, USA: John Wiley & Sons, Inc.
<http://doi.org/10.1002/0471141755.ph0547s70>

- Ganss, R., Ryschich, E., Klar, E., Arnold, B., & Hammerling, G. J. (2002). Combination of T-cell therapy and trigger of inflammation induces remodeling of the vasculature and tumor eradication. *Cancer Research*, *62*(5), 1462–70.
- Geiger, P. C., Wright, D. C., Han, D.-H., & Holloszy, J. O. (2005). Activation of p38 MAP kinase enhances sensitivity of muscle glucose transport to insulin. *American Journal of Physiology-Endocrinology and Metabolism*, *288*(4), E782–E788. <http://doi.org/10.1152/ajpendo.00477.2004>
- Grillo, C. A., Piroli, G. G., Kaigler, K. F., Wilson, S. P., Wilson, M. A., & Reagan, L. P. (2011). Downregulation of hypothalamic insulin receptor expression elicits depressive-like behaviors in rats. *Behavioural Brain Research*, *222*(1), 230–235. <http://doi.org/10.1016/j.bbr.2011.03.052>
- Grillo, C. A., Piroli, G. G., Lawrence, R. C., Wrighten, S. A., Green, A. J., Wilson, S. P., ... Reagan, L. P. (2015). Hippocampal Insulin Resistance Impairs Spatial Learning and Synaptic Plasticity. *Diabetes*, *64*(11), 3927–3936. <http://doi.org/10.2337/db15-0596>
- Guimarães-Camboa, N., Cattaneo, P., Sun, Y., Moore-Morris, T., Gu, Y., Dalton, N. D., ... Evans, S. M. (2017). Pericytes of Multiple Organs Do Not Behave as Mesenchymal Stem Cells In Vivo. *Cell Stem Cell*, *20*(3), 345–359.e5. <http://doi.org/10.1016/j.stem.2016.12.006>
- Gursoy-Ozdemir, Y., & Cetin Tas, Y. (2017). Anatomy and Physiology of the Blood-Brain Barrier. In *Nanotechnology Methods for Neurological Diseases and Brain Tumors* (pp. 3–13). <http://doi.org/10.1016/B978-0-323-01830-2.50077-8>
- Hall, C. N., Reynell, C., Gesslein, B., Hamilton, N. B., Mishra, A., Sutherland, B. A., ... Attwell, D. (2014). Capillary pericytes regulate cerebral blood flow in health and disease. *Nature*, *508*(7494), 55–60. <http://doi.org/10.1038/nature13165>
- Hellström, M., Gerhardt, H., Kalén, M., Li, X., Eriksson, U., Wolburg, H., & Betsholtz, C. (2001). Lack of pericytes leads to endothelial hyperplasia

- and abnormal vascular morphogenesis. *Journal of Cell Biology*, 152(3), 543–553. <http://doi.org/10.1083/jcb.153.3.543>
- Hellström, M., Kalén, M., Lindahl, P., Abramsson, A., & Betsholtz, C. (1999). Role of PDGF-B and PDGFR-beta in recruitment of vascular smooth muscle cells and pericytes during embryonic blood vessel formation in the mouse. *Development (Cambridge, England)*, 126(14), 3047–3055.
- Hill, R. A., Tong, L., Yuan, P., Murikinati, S., Gupta, S., & Grutzendler, J. (2015). Regional Blood Flow in the Normal and Ischemic Brain Is Controlled by Arteriolar Smooth Muscle Cell Contractility and Not by Capillary Pericytes. *Neuron*, 87(1), 95–110. <http://doi.org/10.1016/j.neuron.2015.06.001>
- Holman, R. R., Paul, S. K., Bethel, A. M., Matthews, D. R., & Neil, H. A. W. (2008). 10-Year Follow-up of Intensive Glucose Control in Type 2 Diabetes. *The New England Journal of Medicine*, 1577–1589.
- Howarth, F. C., Jacobson, M., Shafiullah, M., & Adeghate, E. (2005). Long-term effects of streptozotocin-induced diabetes on the electrocardiogram, physical activity and body temperature in rats. *Experimental Physiology*, 90(6), 827–835. <http://doi.org/10.1113/expphysiol.2005.031252>
- Hoyer, S. (2003). Memory Function and Brain Glucose Metabolism. *Pharmacopsychiatry*, 36, 62–67. <http://doi.org/10.1055/s-2003-40452>
- Hughes, R. N. (2004). The value of spontaneous alternation behavior (SAB) as a test of retention in pharmacological investigations of memory. *Neuroscience and Biobehavioral Reviews*, 28(5), 497–505. <http://doi.org/10.1016/j.neubiorev.2004.06.006>
- Ikram, M. K., Janssen, J. A. M. J. L., Roos, A. M. E., Rietveld, I., Witteman, J. C. M., Breteler, M. M. B., ... de Jong, P. T. V. M. (2006). Retinal vessel diameters and risk of impaired fasting glucose or diabetes: the Rotterdam study. *Diabetes*, 55(2), 506–10.
- Ivan, C. S., Seshadri, S., Beiser, A., Au, R., Kase, C. S., Kelly-Hayes, M., & Wolf, P. A. (2004). Dementia After Stroke: The Framingham Study. *Stroke*, 35(6), 1264–1268. <http://doi.org/10.1161/01.STR.0000127810.92616.78>

- Jiang, Z. Y., He, Z., King, B. L., Kuroki, T., Opland, D. M., Suzuma, K., ... King, G. L. (2003). Characterization of Multiple Signaling Pathways of Insulin in the Regulation of Vascular Endothelial Growth Factor Expression in Vascular Cells and Angiogenesis. *Journal of Biological Chemistry*, 278(34), 31964–31971. <http://doi.org/10.1074/jbc.M303314200>
- Kahl, K. G., Schweiger, U., Correll, C., Müller, C., Busch, M.-L., Bauer, M., & Schwarz, P. (2015). Depression, anxiety disorders, and metabolic syndrome in a population at risk for type 2 diabetes mellitus. *Brain and Behavior*, 5(3), n/a-n/a. <http://doi.org/10.1002/brb3.306>
- Kandel, E. R., Dudai, Y., & Mayford, M. R. (2014). The Molecular and Systems Biology of Memory. *Cell*, 157(1), 163–186. <http://doi.org/10.1016/J.CELL.2014.03.001>
- Keaney, J., & Campbell, M. (2015). The dynamic blood-brain barrier. *FEBS Journal*, 282(21), 4067–4079. <http://doi.org/10.1111/febs.13412>
- Kennelly, S. P., Lawlor, B. A., & Kenny, R. A. (2009). Blood pressure and dementia - a comprehensive review. *Therapeutic Advances in Neurological Disorders*, 2(4), 241–260. <http://doi.org/10.1177/1756285609103483>
- King, G. L., Buzney, S. M., Kahn, C. R., Hetu, N., Buchwald, S., Macdonald, S. G., & Rand, L. I. (1983). Differential responsiveness to insulin of endothelial and support cells from micro- and macrovessels. *The Journal of Clinical Investigation*, 71(4), 974–9. <http://doi.org/10.1172/JCI110852>
- Klok, M. D., Jakobsdottir, S., & Drent, M. L. (2007). The role of leptin and ghrelin in the regulation of food intake and body weight in humans: a review. *Obesity Reviews*, 8(1), 21–34. <http://doi.org/10.1111/j.1467-789X.2006.00270.x>
- Kloppenborg, R., van der Berg, E., Kappelle, L. J., & Biessels, G. J. (2008). Diabetes and other vascular risk factors for dementia: Which factor matters most? A systematic review.
- Kodl, C. T., Franc, D. T., Rao, J. P., Anderson, F. S., Thomas, W., Mueller, B. A., ... Seaquist, E. R. (2008). Diffusion tensor imaging identifies deficits

- in white matter microstructure in subjects with type 1 diabetes that correlate with reduced neurocognitive function. *Diabetes*, 57(11), 3083–3089. <http://doi.org/10.2337/db08-0724>
- Kokmen, E., Whisnant, J. P., O'Fallon, W. M., Chu, C. P., & Beard, C. M. (1996). Dementia after ischemic stroke: a population-based study in Rochester, Minnesota (1960-1984). *Neurology*, 46(1), 154–9.
- Kong, S. H., Park, Y. J., Lee, J.-Y., Cho, N. H., & Moon, M. K. (2018). Insulin Resistance is Associated with Cognitive Decline Among Older Koreans with Normal Baseline Cognitive Function: A Prospective Community-Based Cohort Study. *Scientific Reports*, 8(1), 650. <http://doi.org/10.1038/s41598-017-18998-0>
- Konrad, D., Somwar, R., Sweeney, G., Yaworsky, K., Hayashi, M., Ramlal, T., & Klip, A. (2001). The antihyperglycemic drug alpha-lipoic acid stimulates glucose uptake via both GLUT4 translocation and GLUT4 activation: potential role of p38 mitogen-activated protein kinase in GLUT4 activation. *Diabetes*, 50(6), 1464–71.
- Kornfield, T. E., & Newman, E. A. (2014). Regulation of Blood Flow in the Retinal Trilaminar Vascular Network. *Journal of Neuroscience*, 34(34), 11504–11513. <http://doi.org/10.1523/JNEUROSCI.1971-14.2014>
- Kumagai, A. K., Kang, Y. S., Boado, R. J., & Pardridge, W. M. (1995). Upregulation of blood-brain barrier GLUT1 glucose transporter protein and mRNA in experimental chronic hypoglycemia. *Diabetes*, 44(12), 1399–404.
- Kumar, A., Souza, S. S. D., Moskvina, O. V, Guo, L., Thomson, J. A., Slukvin, I. I., ... Swanson, S. (2017). Specification and Diversification of Pericytes and Smooth Muscle Cells from Mesenchymoangioblasts Article Specification and Diversification of Pericytes and Smooth Muscle Cells from Mesenchymoangioblasts. *CellReports*, 19(9), 1902–1916. <http://doi.org/10.1016/j.celrep.2017.05.019>
- Labayen, I., Ortega, F. B., Ruiz, J. R., Lasa, A., Simón, E., & Margareto, J. (2011). Role of Baseline Leptin and Ghrelin Levels on Body Weight and Fat Mass Changes after an Energy-Restricted Diet Intervention in Obese

- Women: Effects on Energy Metabolism. *The Journal of Clinical Endocrinology & Metabolism*, 96(6), E996–E1000.
<http://doi.org/10.1210/jc.2010-3006>
- Lawes, C. M. M., Bennett, D. A., Feigin, V. L., & Rodgers, A. (2004). Blood pressure and stroke: an overview of published reviews. *Stroke*, 35(4), 1024.
- Leger, M., Quiedeville, A., Bouet, V., Haelewyn, B., Boulouard, M., Schumann-Bard, P., & Freret, T. (2013). Object recognition test in mice. *Nature Protocols*, 8(12), 2531–2537.
<http://doi.org/10.1038/nprot.2013.155>
- Leney, S. E., & Tavaré, J. M. (2009). The molecular basis of insulin-stimulated glucose uptake: signalling, trafficking and potential drug targets. *Journal of Endocrinology*, 203(1), 1–18. <http://doi.org/10.1677/JOE-09-0037>
- Lesort, M., & Johnson, G. V. (2000). Insulin-like growth factor-1 and insulin mediate transient site-selective increases in tau phosphorylation in primary cortical neurons. *Neuroscience*, 99(2), 305–16.
- Lesort, M., Jope, R. S., & Johnson, G. V. (1999). Insulin transiently increases tau phosphorylation: involvement of glycogen synthase kinase-3 β and Fyn tyrosine kinase. *Journal of Neurochemistry*, 72(2), 576–84.
- Li, W., Huang, E., & Gao, S. (2017). Type 1 Diabetes Mellitus and Cognitive Impairments: A Systematic Review. *Journal of Alzheimer's Disease*, 57(1), 29–36. <http://doi.org/10.3233/JAD-161250>
- Liao, D., Cooper, L., Cai, J., Toole, J. F., Bryan, N. R., Hutchinson, R. G., & Tyroler, H. A. (1996). Presence and severity of cerebral white matter lesions and hypertension, its treatment, and its control. The ARIC Study. Atherosclerosis Risk in Communities Study. *Stroke*, 27(12), 2262–2270.
<http://doi.org/10.1161/01.STR.27.12.2262>
- Lindahl, P., Johansson, B. R., Levéen, P., & Betsholtz, C. (1997). Pericyte loss and microaneurysm formation in PDGF-B-deficient mice. *Science*, 277(5323), 242–245. <http://doi.org/10.1126/science.277.5323.242>
- Lindblom, P., Gerhardt, H., Liebner, S., Abramsson, A., Enge, M., Hellström, M., ... Betsholtz, C. (2003). Endothelial PDGF-B retention is required for

- proper investment of pericytes in the microvessel wall. *Genes and Development*, 17(15), 1835–1840. <http://doi.org/10.1101/gad.266803>
- Liu, Y., Petreaca, M., & Martins-Green, M. (2009). Cell and molecular mechanisms of insulin-induced angiogenesis. *Journal of Cellular and Molecular Medicine*, 13(11–12), 4492–504. <http://doi.org/10.1111/j.1582-4934.2008.00555.x>
- Long, J., Duan, G., Tian, W., Wang, L., Su, P., Zhang, W., ... Zhang, H. (2015). Hypertension and risk of depression in the elderly: a meta-analysis of prospective cohort studies. *Journal of Human Hypertension*, 29(8), 478–482. <http://doi.org/10.1038/jhh.2014.112>
- Luchsinger, J. A. (2012). Type 2 diabetes and cognitive impairment: Linking mechanisms. *Journal of Alzheimer's Disease*, 30(SUPPL.2). <http://doi.org/10.3233/JAD-2012-111433>
- Lugo-Hernandez, E., Squire, A., Hagemann, N., Brenzel, A., Sardari, M., Schlechter, J., ... Hermann, D. M. (2017). 3D visualization and quantification of microvessels in the whole ischemic mouse brain using solvent-based clearing and light sheet microscopy. *Journal of Cerebral Blood Flow and Metabolism*, 37(10), 3355–3367. <http://doi.org/10.1177/0271678X17698970>
- Lutski, M., Weinstein, G., Goldbourt, U., & Tanne, D. (2017). Insulin Resistance and Future Cognitive Performance and Cognitive Decline in Elderly Patients with Cardiovascular Disease. *Journal of Alzheimer's Disease: JAD*, 57(2), 633–643. <http://doi.org/10.3233/JAD-161016>
- Maekawa, R., Seino, Y., Ogata, H., Murase, M., Iida, A., Hosokawa, K., ... Arima, H. (2017). Chronic high-sucrose diet increases fibroblast growth factor 21 production and energy expenditure in mice. *The Journal of Nutritional Biochemistry*, 49, 71–79. <http://doi.org/10.1016/j.jnutbio.2017.07.010>
- Mak, E., Gabel, S., Mirette, H., Su, L., Williams, G. B., Waldman, A., ... O'Brien, J. (2017). Structural neuroimaging in preclinical dementia: From microstructural deficits and grey matter atrophy to macroscale connectomic changes. *Ageing Research Reviews*, 35, 250–264.

<http://doi.org/10.1016/j.arr.2016.10.001>

- Manschot, S. M., Brands, A. M. A., Van Der Grond, J., Kessels, R. P. C., Algra, A., Kappelle, L. J., & Biessels, G. J. (2006). Brain magnetic resonance imaging correlates of impaired cognition in patients with type 2 diabetes. *Diabetes*, 55(4), 1106–1113. <http://doi.org/10.2337/diabetes.55.04.06.db05-1323>
- Marzelli, M. J., Mazaika, P. K., Barnea-Goraly, N., Hershey, T., Tsalikian, E., Tamborlane, W., ... Reiss, A. L. (2014). Neuroanatomical correlates of dysglycemia in young children with type 1 diabetes. *Diabetes*, 63(1), 343–353. <http://doi.org/10.2337/db13-0179>
- Mies, G., & Paschen, W. (1984). Regional changes of blood flow, glucose, and ATP content determined on brain sections during a single passage of spreading depression in rat brain cortex. *Experimental Neurology*, 84(2), 249–258. [http://doi.org/10.1016/0014-4886\(84\)90222-X](http://doi.org/10.1016/0014-4886(84)90222-X)
- Mitchell, P., Cheung, N., De Haseth, K., Taylor, B., Rohtchina, E., Islam, F. M. A., ... Wong, T. Y. (2007). Blood pressure and retinal arteriolar narrowing in children. *Hypertension*, 49(5), 1156–1162. <http://doi.org/10.1161/HYPERTENSIONAHA.106.085910>
- Moloney, A. M., Griffin, R. J., Timmons, S., O'Connor, R., Ravid, R., & O'Neill, C. (2010). Defects in IGF-1 receptor, insulin receptor and IRS-1/2 in Alzheimer's disease indicate possible resistance to IGF-1 and insulin signalling. *Neurobiology of Aging*, 31(2), 224–243. <http://doi.org/10.1016/j.neurobiolaging.2008.04.002>
- Monzell, S. (1981). Representations, processes, memory mechanisms: The basic components of cognition. *Journal of the American Society for Information Science*, 32(5), 378–390. <http://doi.org/10.1002/asi.4630320518>
- Moreira, P. I., Duarte, A. I., Santos, M. S., Rego, A. C., & Oliveira, C. R. (2009). An Integrative View of the Role of Oxidative Stress, Mitochondria and Insulin in Alzheimer's Disease. *Journal of Alzheimer's Disease*, 16(4), 741–761. <http://doi.org/10.3233/JAD-2009-0972>
- Mullins, R. J., Diehl, T. C., Chia, C. W., & Kapogiannis, D. (2017). Insulin

- Resistance as a Link between Amyloid-Beta and Tau Pathologies in Alzheimer's Disease. *Frontiers in Aging Neuroscience*, 9, 118. <http://doi.org/10.3389/fnagi.2017.00118>
- Murakami, N., Ohtsubo, T., Kansui, Y., Goto, K., Noguchi, H., Haga, Y., ... Kitazono, T. (2014). Mice heterozygous for the xanthine oxidoreductase gene facilitate lipid accumulation in adipocytes. *Arteriosclerosis, Thrombosis, and Vascular Biology*, 34(1), 44–51. <http://doi.org/10.1161/ATVBAHA.113.302214>
- Murata, T., Nagai, R., Ishibashi, T., Inomuta, H., Ikeda, K., & Horiuchi, S. (1997). The relationship between accumulation of advanced glycation end products and expression of vascular endothelial growth factor in human diabetic retinas. *Diabetologia*, 40(7), 764–9.
- Norton, S., Matthews, F. E., Barnes, D. E., Yaffe, K., & Brayne, C. (2014). Potential for primary prevention of Alzheimer's disease: An analysis of population-based data. *The Lancet Neurology*, 13(8), 788–794. [http://doi.org/10.1016/S1474-4422\(14\)70136-X](http://doi.org/10.1016/S1474-4422(14)70136-X)
- Nunley, K. A., Rosano, C., Ryan, C. M., Jennings, J. R., Aizenstein, H. J., Zgibor, J. C., ... Saxton, J. A. (2015). Clinically relevant cognitive impairment in Middle-Aged adults with childhood-onset type 1 diabetes. *Diabetes Care*, 38(9), 1768–1776. <http://doi.org/10.2337/dc15-0041>
- Nunley, K., Ryan, C. ., Orchard, T. J., Aizenstein, H. J., Jennings, J. R., Ryan, J., ... Rosano, C. (2015). White matter hyperintensities in middle-aged adults with childhood-onset type 1 diabetes. *Neurology*, 84(20), 2062–2069. <http://doi.org/10.2337/db14-0723>
- Pan, Y., Cai, W., Cheng, Q., Dong, W., An, T., & Yan, J. (2015). Association between anxiety and hypertension: a systematic review and meta-analysis of epidemiological studies. *Neuropsychiatric Disease and Treatment*, 11, 1121–30. <http://doi.org/10.2147/NDT.S77710>
- Pantoni, L. (2010). Cerebral small vessel disease: from pathogenesis and clinical characteristics to therapeutic challenges. *The Lancet Neurology*, 9(7), 689–701. [http://doi.org/10.1016/S1474-4422\(10\)70104-6](http://doi.org/10.1016/S1474-4422(10)70104-6)
- Pap, M., & Cooper, G. M. (1998). Role of glycogen synthase kinase-3 in the

- phosphatidylinositol 3-Kinase/Akt cell survival pathway. *The Journal of Biological Chemistry*, 273(32), 19929–32.
- Patching, S. G. (2017). Glucose Transporters at the Blood-Brain Barrier: Function, Regulation and Gateways for Drug Delivery. *Molecular Neurobiology*, 54(2), 1046–1077. <http://doi.org/10.1007/s12035-015-9672-6>
- Pendyala, S., Walker, J. M., & Holt, P. R. (2012). A High-Fat Diet Is Associated With Endotoxemia That Originates From the Gut. *Gastroenterology*, 142(5), 1100–1101.e2. <http://doi.org/10.1053/j.gastro.2012.01.034>
- Peppiatt, C. M., Howarth, C., Mobbs, P., & Attwell, D. (2006). Bidirectional control of CNS capillary diameter by pericytes. *Nature*, 443(7112), 700–704. <http://doi.org/10.1038/nature05193>
- Pohjasvaara, T., Erkinjuntti, T., Vataja, R., & Kaste, M. (1997). Dementia three months after stroke. Baseline frequency and effect of different definitions of dementia in the Helsinki Stroke Aging Memory Study (SAM) cohort. *Stroke*, 28(4), 785–92.
- Potenza, M. A., Marasciulo, F. L., Chieppa, D. M., Brigiani, G. S., Formoso, G., Quon, M. J., & Montagnani, M. (2005). Insulin resistance in spontaneously hypertensive rats is associated with endothelial dysfunction characterized by imbalance between NO and ET-1 production. *American Journal of Physiology-Heart and Circulatory Physiology*, 289(2), H813–H822. <http://doi.org/10.1152/ajpheart.00092.2005>
- Prince, M., Bryce, R., Albanese, E., Wimo, A., Ribeiro, W., & Ferri, C. P. (2013). The global prevalence of dementia: A systematic review and metaanalysis. *Alzheimer's and Dementia*, 9(1), 63–75. <http://doi.org/10.1016/j.jalz.2012.11.007>
- Prince, M., Wimo, A., Guerchet, M., Ali, G.-C., Wu, Y.-T., & Prina, M. (2015). World Alzheimer Report 2015 The Global Impact of Dementia.
- Purnell, C., & Gao, S. (2009). Cardiovascular risk factors and incident Alzheimer disease: a systematic review of the literature. *Alzheimer Disease and ...*, 23(1), 1–10.

- <http://doi.org/10.1097/WAD.0b013e318187541c>. Cardiovascular
- Reijmer, Y. D., Brundel, M., De Bresser, J., Kappelle, L. J., Leemans, A., & Biessels, G. J. (2013). Microstructural white matter abnormalities and cognitive functioning in type 2 diabetes: A diffusion tensor imaging study. *Diabetes Care*, *36*(1), 137–144. <http://doi.org/10.2337/dc12-0493>
- Reynolds, K. A., & Helgeson, V. S. (2011). Children with Diabetes Compared to Peers: Depressed? Distressed? *Annals of Behavioral Medicine*, *42*(1), 29–41. <http://doi.org/10.1007/s12160-011-9262-4>
- Richards, O. C., Raines, S. M., & Attie, A. D. (2010). The Role of Blood Vessels, Endothelial Cells, and Vascular Pericytes in Insulin Secretion and Peripheral Insulin Action. *Endocrine Reviews*, *31*(3), 343–363. <http://doi.org/10.1210/er.2009-0035>
- Roser, M. (2018). Life expectancy. Retrieved June 2, 2018, from <https://ourworldindata.org/life-expectancy>
- Roy, S., Kim, N., Desai, A., Komaragiri, M., Baxi, N., Jassil, N., ... Hunter, K. (2015). Cognitive function and control of type 2 diabetes mellitus in young adults. *North American Journal of Medical Sciences*, *7*(5), 220–226. <http://doi.org/10.4103/1947-2714.157627>
- Rubin, K., Hansson, G. K., Rönstrand, L., Claesson-Welsh, L., Fellström, B., Tingström, A., ... Terracio, L. (1988). Induction of B-Type Receptors for Platelet-Derived Growth Factor in Vascular Inflammation: Possible Implications for Development of Vascular Proliferative Lesions. *The Lancet*, *331*(8599), 1353–1356. [http://doi.org/10.1016/S0140-6736\(88\)92177-0](http://doi.org/10.1016/S0140-6736(88)92177-0)
- Sagvolden, T., Pettersen, M. B., & Larsen, M. C. (1993). Spontaneously hypertensive rats (SHR) as a putative animal model of childhood hyperkinesis: SHR behavior compared to four other rat strains. *Physiology & Behavior*, *54*(6), 1047–55.
- Sakamoto, E., Seino, Y., Fukami, A., Mizutani, N., Tsunekawa, S., Ishikawa, K., ... Ozaki, N. (2012). Ingestion of a moderate high-sucrose diet results in glucose intolerance with reduced liver glucokinase activity and impaired glucagon-like peptide-1 secretion. *Journal of Diabetes*

Investigation, 3(5), 432–40. <http://doi.org/10.1111/j.2040-1124.2012.00208.x>

- Sanchez, J. F., Sniderhan, L. F., Williamson, A. L., Fan, S., Chakraborty-Sett, S., & Maggirwar, S. B. (2003). Glycogen synthase kinase 3 β -mediated apoptosis of primary cortical astrocytes involves inhibition of nuclear factor kappaB signaling. *Molecular and Cellular Biology*, 23(13), 4649–62.
- Sasongko, M. B., Wang, J. J., Donaghue, K. C., Cheung, N., Benitez-Aguirre, P., Jenkins, A., ... Wong, T. Y. (2010). Alterations in Retinal Microvascular Geometry in Young Type 1 Diabetes. *Diabetes Care*, 33(6), 1331–1336. <http://doi.org/10.2337/dc10-0055>
- Sasongko, M. B., Wong, T. Y., Nguyen, T. T., Cheung, C. Y., Shaw, J. E., & Wang, J. J. (2011). Retinal vascular tortuosity in persons with diabetes and diabetic retinopathy. *Diabetologia*, 54(9), 2409–2416. <http://doi.org/10.1007/s00125-011-2200-y>
- Scalco, A. Z., Scalco, M. Z., Azul, J. B. S., & Lotufo Neto, F. (2005). Hypertension and depression. *Clinics*, 60(3), 241–250. <http://doi.org/10.1590/S1807-59322005000300010>
- Schechter, R., Whitmire, J., Holtzclaw, L., George, M., Harlow, R., & Devaskar, S. U. (1992). Developmental regulation of insulin in the mammalian central nervous system. *Brain Research*, 582(1), 27–37. [http://doi.org/10.1016/0006-8993\(92\)90313-X](http://doi.org/10.1016/0006-8993(92)90313-X)
- Schulingkamp, R. ., Pagano, T. ., Hung, D., & Raffa, R. . (2000). Insulin receptors and insulin action in the brain: review and clinical implications. *Neuroscience & Biobehavioral Reviews*, 24(8), 855–872. [http://doi.org/10.1016/S0149-7634\(00\)00040-3](http://doi.org/10.1016/S0149-7634(00)00040-3)
- Shrader, C. D., Bailey, K. M., Konat, G. W., Cilento, E. V., & Reilly, F. D. (2009). Insulin enhances proliferation and viability of human umbilical vein endothelial cells. *Archives of Dermatological Research*, 301(2), 159–166. <http://doi.org/10.1007/s00403-008-0921-7>
- Şik, A., Van Nieuwehuyzen, P., Prickaerts, J., & Blokland, A. (2003). Performance of different mouse strains in an object recognition task.

- Behavioural Brain Research*, 147(1–2), 49–54.
[http://doi.org/10.1016/S0166-4328\(03\)00117-7](http://doi.org/10.1016/S0166-4328(03)00117-7)
- Simpson, I. A., Appel, N. M., Hokari, M., Oki, J., Holman, G. D., Maher, F., ... Smith, Q. R. (1999). Blood-brain barrier glucose transporter: effects of hypo- and hyperglycemia revisited. *Journal of Neurochemistry*, 72(1), 238–47.
- Skilton, M. R., Moulin, P., Terra, J.-L., & Bonnet, F. (2007). Associations Between Anxiety, Depression, and the Metabolic Syndrome. *Biological Psychiatry*, 62(11), 1251–1257.
<http://doi.org/10.1016/j.biopsych.2007.01.012>
- Steen, E., Terry, B. M., Rivera, E. J., Cannon, J. L., Neely, T. R., Tavares, R., ... de la Monte, S. M. (2005). Impaired insulin and insulin-like growth factor expression and signaling mechanisms in Alzheimer's disease--is this type 3 diabetes? *Journal of Alzheimer's Disease : JAD*, 7(1), 63–80.
- Stout, R. W. (1991). Insulin as a mitogenic factor: Role in the pathogenesis of cardiovascular disease. *The American Journal of Medicine*, 90(2), S62–S65. [http://doi.org/10.1016/0002-9343\(91\)90041-U](http://doi.org/10.1016/0002-9343(91)90041-U)
- Strachan, M. W., Deary, I. J., Ewing, F. M., & Frier, B. M. (1997). Is type II diabetes associated with an increased risk of cognitive dysfunction? A critical review of published studies. *Diabetes Care*, 20(3), 438–45.
<http://doi.org/10.2337/diacare.20.3.438>
- Sun, C., Wang, J. J., Mackey, D. A., & Wong, T. Y. (2009). Retinal Vascular Caliber: Systemic, Environmental, and Genetic Associations. *Survey of Ophthalmology*, 54(1), 74–95.
<http://doi.org/10.1016/j.survophthal.2008.10.003>
- Sweatt, J. D. (2010). *Mechanisms of memory*. Academic.
- Swislocki, A., & Tsuzuki, A. (1993). Insulin resistance and hypertension: glucose intolerance, hyperinsulinemia, and elevated free fatty acids in the lean spontaneously hypertensive rat. *The American Journal of the Medical Sciences*, 306(5), 282–6.
- Tangvarasittichai, S. (2015). Oxidative stress, insulin resistance, dyslipidemia and type 2 diabetes mellitus. *World Journal of Diabetes*, 6(3), 456–80.

<http://doi.org/10.4239/wjd.v6.i3.456>

- Tatemichi, T. K., Paik, M., Bagiella, E., Desmond, D. W., Stern, Y., Sano, M., ... Mayeux, R. (1994). Risk of dementia after stroke in a hospitalized cohort: results of a longitudinal study. *Neurology*, *44*(10), 1885–91.
- Tian, X., Brookes, O., & Battaglia, G. (2017). Pericytes from Mesenchymal Stem Cells as a model for the blood-brain barrier. *Scientific Reports*, *7*, 3–9. <http://doi.org/10.1038/srep39676>
- Tiehuis, A. M., van der Graaf, Y., Visseren, F. L., Vincken, K. L., Biessels, G. J., Appelman, A. P. A., ... Mali, W. P. T. M. (2008). Diabetes increases atrophy and vascular lesions on brain MRI in patients with symptomatic arterial disease. *Stroke; a Journal of Cerebral Circulation*, *39*(5), 1600–1603. <http://doi.org/10.1161/STROKEAHA.107.506089>
- Timothy J Lyons, J. Y. Y., & Lyons, T. J. (2013). Modified Lipoproteins in Diabetic Retinopathy: A Local Action in the Retina. *Journal of Clinical & Experimental Ophthalmology*, *4*(6), 1–8. <http://doi.org/10.4172/2155-9570.1000314>
- Tonoli, C., Heyman, E., Roelands, B., Pattyn, N., Buyse, L., Piacentini, M. F., ... Meeusen, R. (2014). Type 1 diabetes-associated cognitive decline: A meta-analysis and update of the current literature. *Journal of Diabetes*, *6*(6), 499–513. <http://doi.org/10.1111/1753-0407.12193>
- Trost, A., Lange, S., Schroedl, F., Bruckner, D., Motloch, K. A., Bogner, B., ... Reitsamer, H. A. (2016). Brain and Retinal Pericytes: Origin, Function and Role. *Frontiers in Cellular Neuroscience*, *10*(February), 1–13. <http://doi.org/10.3389/fncel.2016.00020>
- Unger, J. W., Moss, A. M., & Livingston, J. N. (1991). Immunohistochemical localization of insulin receptors and phosphotyrosine in the brainstem of the adult rat. *Neuroscience*, *42*(3), 853–61.
- van der Heide, L. P., Ramakers, G. M. J., & Smidt, M. P. (2006). Insulin signaling in the central nervous system: Learning to survive. *Progress in Neurobiology*, *79*(4), 205–221. <http://doi.org/10.1016/j.pneurobio.2006.06.003>
- van Dijk, E. J., Breteler, M. M. B., Schmidt, R., Berger, K., Nilsson, L.-G.,

- Oudkerk, M., ... Hofman, A. (2004). The association between blood pressure, hypertension, and cerebral white matter lesions: cardiovascular determinants of dementia study. *Hypertension*, *44*(5), 625–30. <http://doi.org/10.1161/01.HYP.0000145857.98904.20>
- van Harten, B., Oosterman, J. M., Potter van Loon, B.-J., Scheltens, P., & Weinstein, H. C. (2007). Brain lesions on MRI in elderly patients with type 2 diabetes mellitus. *European Neurology*, *57*(2), 70–4. <http://doi.org/10.1159/000098054>
- van Harten, B., Oosterman, J., Muslimovic, D., van Loon, B.-J. P., Scheltens, P., & Weinstein, H. C. (2007). Cognitive impairment and MRI correlates in the elderly patients with type 2 diabetes mellitus. *Age and Ageing*, *36*(2), 164–70. <http://doi.org/10.1093/ageing/afl180>
- van Swieten, J. C., Geyskes, G. G., Derix, M. M., Peeck, B. M., Ramos, L. M., van Latum, J. C., & van Gijn, J. (1991). Hypertension in the elderly is associated with white matter lesions and cognitive decline. *Annals of Neurology*, *30*(6), 825–830. <http://doi.org/10.1002/ana.410300612>
- Wada, A., Yokoo, H., Yanagita, T., & Kobayashi, H. (2005). New twist on neuronal insulin receptor signaling in health, disease, and therapeutics. *Journal of Pharmacological Sciences*, *99*(2), 128–43.
- Wallow, I. H. L., Bindley, C. D., Reboussin, D. M., Gange, S. J., & Fisher, M. R. (1993). Systemic hypertension produces pericyte changes in retinal capillaries. *Investigative Ophthalmology and Visual Science*, *34*(2), 420–430.
- Watson, G. S., Peskind, E. R., Asthana, S., Purganan, K., Wait, C., Chapman, D., ... Craft, S. (2003). Insulin increases CSF Abeta42 levels in normal older adults. *Neurology*, *60*(12), 1899–903.
- Weinger, K., Jacobson, A. M., Musen, G., Lyoo, I. K., Ryan, C. M., Jimerson, D. C., & Renshaw, P. F. (2008). The effects of type 1 diabetes on cerebral white matter. *Diabetologia*, *51*(3), 417–425. <http://doi.org/10.1007/s00125-007-0904-9>
- Weisberg, S. P., Hunter, D., Huber, R., Lemieux, J., Slaymaker, S., Vaddi, K., ... Ferrante, A. W. (2006). CCR2 modulates inflammatory and metabolic

- effects of high-fat feeding. *The Journal of Clinical Investigation*, 116(1), 115–24. <http://doi.org/10.1172/JCI24335>
- Wessels, A. M., Rombouts, S. A. R. B., Remijnse, P. L., Boom, Y., Scheltens, P., Barkhof, F., ... Snoek, F. J. (2007). Cognitive performance in type 1 diabetes patients is associated with cerebral white matter volume. *Diabetologia*, 50(8), 1763–1769. <http://doi.org/10.1007/s00125-007-0714-0>
- Winkler, E. A., Bell, R. D., & Zlokovic, B. V. (2011). Central nervous system pericytes in health and disease. *Nature Neuroscience*, 14(11), 1398–1405. <http://doi.org/10.1038/nn.2946>
- Wong, T. Y., Klein, R., Sharrett, A. R., Schmidt, M. I., Pankow, J. S., Couper, D. J., ... ARIC Investigators. (2002). Retinal arteriolar narrowing and risk of diabetes mellitus in middle-aged persons. *JAMA*, 287(19), 2528–33.
- Wong, T. Y., Shankar, A., Klein, R., Klein, B. E. K., & Hubbard, L. D. (2005). Retinal Arteriolar Narrowing, Hypertension, and Subsequent Risk of Diabetes Mellitus. *Archives of Internal Medicine*, 165(9), 1060. <http://doi.org/10.1001/archinte.165.9.1060>
- Yamagishi, S., Kawakami, T., Fujimori, H., Yonekura, H., Tanaka, N., Yamamoto, Y., ... Yamamoto, H. (1999). Insulin Stimulates the Growth and Tube Formation of Human Microvascular Endothelial Cells through Autocrine Vascular Endothelial Growth Factor. *Microvascular Research*, 57(3), 329–339. <http://doi.org/10.1006/MVRE.1999.2145>
- Yamamoto, N., Matsubara, T., Sobue, K., Tanida, M., Kasahara, R., Naruse, K., ... Suzuki, K. (2012). Brain insulin resistance accelerates A β fibrillogenesis by inducing GM1 ganglioside clustering in the presynaptic membranes. *Journal of Neurochemistry*, 121(4), 619–628. <http://doi.org/10.1111/j.1471-4159.2012.07668.x>
- Yang, Z. H., Miyahara, H., Takeo, J., & Katayama, M. (2012). Diet high in fat and sucrose induces rapid onset of obesity-related metabolic syndrome partly through rapid response of genes involved in lipogenesis, insulin signalling and inflammation in mice. *Diabetology and Metabolic Syndrome*, 4(1), 1–10. <http://doi.org/10.1186/1758-5996-4-32>

- Yates, K., Sweat, V., Yau, P., Turchiano, M., & Convit, A. (2012). Impact of metabolic syndrome on cognition and Brain: A selected review of the Litterature. *Arteriosler Tromb. and Vascular Biology*, 32(9), 2060–2067. <http://doi.org/10.1161/ATVBAHA.112.252759>.Impact
- Zemdegs, J., Quesseveur, G., Jarriault, D., Pénicaud, L., Fioramonti, X., & Guiard, B. P. (2016). High-fat diet-induced metabolic disorders impairs 5-HT function and anxiety-like behavior in mice. *British Journal of Pharmacology*. <http://doi.org/10.1111/bph.13343>
- Zhang-James, Y., Middleton, F. A., & Faraone, S. V. (2013). Genetic architecture of Wistar-Kyoto rat and spontaneously hypertensive rat substrains from different sources. *Physiological Genomics*, 45(13), 528–538. <http://doi.org/10.1152/physiolgenomics.00002.2013>
- Zherdiova, N. M., Med, C. S., Medvedovska, N. V, Med, S., Makeev, S. K., Med, S., ... Med, S. (2018). Relationship between diabetic retinopathy and cerebral perfusion in type 2 diabetes mellitus. *Journal of Ophthalmology (Ukraine)*, 1(1), 49–53.
- Zhou, N., Rungta, R. L., Malik, A., Han, H., Wu, D. C., & MacVicar, B. A. (2013). Regenerative Glutamate Release by Presynaptic NMDA Receptors Contributes to Spreading Depression. *Journal of Cerebral Blood Flow & Metabolism*, 33(10), 1582–1594. <http://doi.org/10.1038/jcbfm.2013.113>
- Zlokovic, B. V. (2011). Neurovascular pathways to neurodegeneration in Alzheimer's disease and other disorders. *Nature Reviews Neuroscience*, 12(12), 723–738. <http://doi.org/10.1038/nrn3114>